Compositional variations of garnets in eclogitized rocks, Kokchetav Massif, Kazakhstan: Implications to the origin and crustal processes

BSc in Geology

C-Thesis Project

Ilyas Saduov

Supervisor: Dr. George Paul Mathews

May 3, 2023

Abstract

Mineral chemistry is widely used in the past three decades to understand original setting and the source composition of rocks, thereby unravelling crustal processes. A good example is chrome spinel. The trace element composition of garnet is also in use to study the composition of protolith in metamorphic rocks since early 2000. The objective of this thesis is to see the plausibility of using garnet major element chemistry to understand about the protolith composition and the crustal processes. The samples used in this study were collected from Kokchetav massif, located around the city of Kokchetav, northern Kazakhstan. This region widely studied and is known worldwide for subduction related high-pressure metamorphism happened ca. 500 Ma ago, during the formation of the Central Asian Orogenic Belt. The Kokchetav massif is also famous for the occurrence of diamond bearing meta-sedimentary rocks. Several garnet bearing rocks samples were collected from the region that includes eclogite, gabbro, garnet amphibolite and pelitic schist along with non-garnetiferous granite, amphibolite and granitic gneiss. Thin- sections of all 15 samples collected were made for petrography; out of which garnet bearing samples were selected for detailed study and analyses. The petrography revealed eclogite has a mineral assemblage - Grt+Omph+Rt+Qtz±Amph; gabbro- Grt+Omph+Amph+Qtz±Plg; garnet amphibolite– Grt+Amph+Qtz with minor inclusions of omphacite and pelitic schist- Grt+Phe+Qz; exhibiting granoblastic-ameboid granoblastic to porphyroblastic textures. The major element chemistry of garnet were determined using SEM-EDS technique. The mineral chemistry shows similar composition for Si and Al composition but variations in Mg, Ca and the Fe contents. Compositionally all garnets are of almandine variety. The *X*Fe= Fe/(Fe+Mg) values of eclogite, gabbro and garnet amphibolite are in the range 0.654-0.799; 0.656-0.665; 0.817-0.865 respectively. However, for the pelitic schist *X*Fe falls between 0.876-0.922, indicating a sharp change in the composition. Since all of the rocks included in this study have experienced regional high-pressure metamorphism, in can be postulated that they are all affected by similar physical conditions i.e., pressure, temperature, although, depth of metamorphism can affect the mineral composition due to changes in geothermal gradient. The thesis argue that a drastic change of Fe content in these rocks esp. the pelitic schist is a reflection of the protolith composition. While, eclogite, gabbro and the garnet amphibolite probably can have common protolith-i.e., Fe rich basalt indicating a fractionated source with crustal inputs; the high Fe content in the pelitic schist shows it has more crustal input, also because of the presence of K, Al bearing phengite mica in its assemblage. Crustal inputs in various levels points towards a mixed source that can occur due to crust-mantle interaction. The most efficient processes where crust interacts with mantle is the due to subduction, as also reported in several previous studies from this region. Hence, the results from this study is a proof that major element composition of garnet can be a good proxy to understand stand petrogenesis and related crustal processes esp.in the metamorphic rocks.

Table of Contents

Acknowledgment

I am grateful to all SMG faculty for their incredible efforts and dedication which helped me to acquire a lot of knowledge during my bachelor studies and helped me to improve my study and research skills. I would like to express my sincere gratitude to my supervisor, Assistant Professor George Mathews, who guided and supported me throughout my senior year and assisted in writing my bachelor's thesis work. No a separate note, I want to thank my parents and classmates, who always helped and supported me. Lastly, not the least I want to thank the reviewers of this thesis Prof. Emil Bayramov and Prof. Kamal Regmi who have kindly agreed to go evaluate this work.

1. Introduction

Petrogenesis is the key to unravel crustal processes. Although, the whole rock chemistry is widely used in understanding the original setting, mineral composition also is a very useful indicator on magma source and the formation. For instance, the chrome-spinel chemistry is used to understand the original setting of several ophiolite sequences worldwide. The logic behind the usage of mineral chemistry is that, composition of a mineral is depended on the physico-chemical conditions prevailing during its occurrence. The changes in the conditions are brought about by various crustal processes in operation in corresponding tectonic regimes. This thesis is an attempt to use major element chemistry of garnet to unravel the source and thereby understanding the crustal processes. The trace element chemistry of garnet is a widely utilized esp. in metamorphic rocks to understand crustal processes, in the past two decades. The samples used in this study are from the Kokchetav massif, northern Kazakhstan. This region is widely known for the occurrence of high-pressure rocks in the form of eclogite, gabbro, garnet amphibolite and micro-diamond bearing phengite schist (white schist) as well as marble. Previous studies reports the Kokchetav massif to have formed because of subduction ca. 500 Ma ago. All the samples in this study are metamorphosed garnet bearing samples. The aim is to look at the major element chemistry of each of the sample and to compare them to reason out if there are any variations in their composition.

1.1. Research statement

The composition variation in the mineral is an indicator of the original setting. Garnet is a common mineral found in metamorphic rocks and hence is a good proxy to understand the metamorphic process and thereby the crustal processes. The Kokchetav massif in northern Kazakhstan is a well-studied region for high-pressure metamorphism due to subduction and is also known for occurrence of diamond bearing rocks. Although there are various studies from this region high-pressure metamorphism and occurrences of eclogite, there are no attempts so far in my knowledge to compare the composition variations of garnet among the garnet bearing rocks. The results on the compositional variations of garnet from various rock type is expected to bring insights to rock formation and the crustal processes.

1.2.Scope of the study

This study primarily does not have any direct commercial or industrial application, as it attempts to answer a fundamental question in Earth science such as crustal processes. However, in a geological perspective it is significant as the garnet chemistry (or mineral chemistry) is still an emerging proxy to understand the crustal processes. It is also significant in a regional perspective of the Kokchetav massif as no previous attempt have been made to compare the composition of garnet bearing rocks.

1.3. Objectives

Objectives of the thesis project are to:

- Obtain rock samples during the field work in the Kokchetav massif
- Select garnet bearing rock samples.
- Perform petrographic analysis of the samples to understand mineral assemblage and textural relations
- Analyze the mineral compositions of various rock types including garnet
- Compare the composition of garnets within the selected samples to understand the garnet formation processes and thereby the crustal process

2. Literature review

2.1. Introduction

The process of metamorphism transforms the existing rocks into rocks with a different mineral composition and/or texture as a result of exposure to high pressure and/or temperature. The Kokchetav UHP-HP metamorphic belt in northern Kazakhstan, also known as the Kokchetav massif, is situated in the western part of the Central Asian Orogenic Belt. The Kokchetav massif is famous for being a location where microdiamonds were first discovered within metamorphic rocks, which served as an important push for its detailed study (Sobolev & Shatsky, 1990). This region has undergone intense metamorphism and therefore contains slices of high pressure (HP) and ultra-high pressure (UHP) metamorphic rocks (Kaneko et al., 2000). One of them is eclogite, which transforms from basalt at moderate to high temperatures and high pressures. While some eclogites may be either 80% garnet or clinopyroxene, eclogites generally have similar proportions of the two minerals (Clarke et al., 2013). Garnet is usually considered to be a significant carrier of primary mineral inclusions and has been used to obtain the evolutionary history of metamorphic

rocks (Schertl & Sobolev, 2013). Consequently, garnet chemistry is key in order to understand the metamorphism.

2.2. Central Asian Orogenic Belt

One of the largest accretionary orogens in the world, the ancestral Central Asian Orogenic Belt (CAOB), developed during the late Precambrian and Palaeozoic era and the closing of the Palaeo-Asian Ocean (PAO) (e.g. Dobretsov et al., 2003; Windley et al., 2007). This consolidation included several types of terranes such as island arcs, accretionary complexes, and microcontinental fragments originating from Gondwana (e.g. Buslov et al., 2004; Buslov, 2011; Glorie et al., 2011a). During the Ediacaran – Cambrian, the oceanic crust of the PAO subducted under the Precambrian Kokchetav microcontinent. The supracrustal rocks at the margin of the Kokchetav microcontinent were drawn into the subduction zone in the Early-Middle Cambrian, which led to UHP metamorphism. By the end of the Cambrian, deeply subducted supracrustal rocks were exhumed into the upper crustal layers, resulting in the formation of the UHP-HP metamorphic belt of the KSCZ. Subduction stopped in the Ordovician, when the Kokchetav microcontinent finally collided with the Stepnyak island arc.

2.3. Kokchetav massif

2.3.1. Introduction

The Kokchetav UHP-HP metamorphic belt of north Kazakhstan, also known as the Kokchetav massif. This region is located in the north of Kazakhstan, southwest of the city of Kokshetau (Fig. 1). It is made up of ultrahigh pressure (UHP) and high pressure (HP) units, and stretches at least 80 km along a NW-SE axis with a width of about 17 km (Dobretsov et al., 1995). The Early Cambrian metamorphic units of the Kokchetav complex are remnants of what was initially a sequence that initially shared a smooth and continuous pressure-temperature (P-T) temporal path, but extreme post-metamorphic deformation produced a chaotically mixed sequence. Some of the mapped blocks with various P-T conditions demonstrate paragenesis of the fragmented HP/UHP rocks (Dobretsov et al., 1995; Ernst et al., 1995). Due to their restricted exposure and low topography, the Kokchetav UHP-HP rocks have poorly documented structural detail, making tectonic interpretation difficult (Kaneko et al., 2000).

The core of the massif, where diamond-bearing rocks were described by Sobolev and Shatsky (1990), is composed of crystalline schist, gneiss, eclogite, garnet peridotite, quartzite, marble, and associated rocks of the amphibolite-granulite facies. In carbonate rocks that contain pyroxene and

garnet as well as garnet-biotite gneiss and schist, diamond can be found as small inclusions in garnet and zircon.

It is still unclear where the microdiamond in these rocks came from. Diamond inclusions in garnet, zircon, and pyroxene formed within the diamond stability field at pressure (P) > 40 kbar and temperature (T) from 900 to 1000°C according to Sobolev and Shatsky (1987, 1990) and Zhang et al. (1997). However, it has been hypothesized that microdiamond formed metastably at low pressures as a result of dynamic stress, condensation from a reduced mantle fluid along shear zones, or solid-state flow (Letnikov, 1983; Lavrova, 1991; Ekimova et al., 1992; Lavrova et al., 1995).

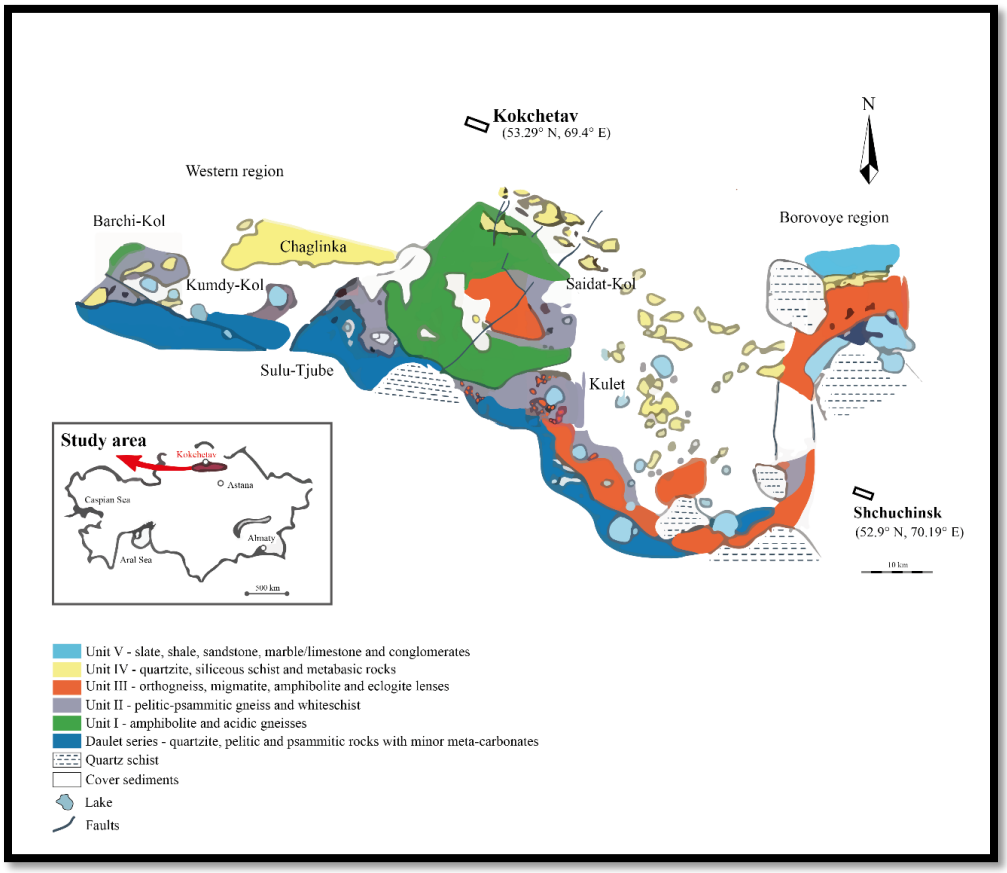

Figure 1. Simplified geologic map of Kokchetav metamorphic belt showing the major tectonostratigraphic divisions, (after Kaneko et al., 2000).

2.3.2. Outline of geology

The Devonian volcanic molasse, Carboniferous and Triassic shallow water and lacustrine deposits, Cambrian-Ordovician volcanic and sedimentary strata, and Precambrian protoliths make up the Kokchetav UHP and HP metamorphic belt. The UHP and HP rocks underwent a number of

orogenic events and were intruded by Silurian to Early Devonian syn-tectonic granites as well as by postcollisional granites, syenites, and granite porphyries from the Late Devonian to Carboniferous periods (Dobretsov et al., 1995). The limited topographic relief makes it difficult to identify the structural contacts between the various units in the field. The UHP–HP unit is structurally overlain by a low-grade metamorphic unit on top, and is underlain by the low-P facies series of the Daulet Suite. These two primary tectonic boundaries are subhorizontal, and additional high-angle normal faults have locally altered them (Maruyama et al., 1997; Ishikawa et al., 1998; Kaneko et al., 1998). Postorogenic and post-metamorphic intrusions of Devonian granitoid are located in the southern part of the area. Postorogenic deformation is indicated by a group of high-angle strike-slip faults with NE-SW and NW-SE trends. Sm-Nd and U-Pb ages between 520 and 540 Ma show that the metamorphism of the diamond-bearing paragneisses, schists, and associated tectonic rocks occurred in the Middle Cambrian (Jagoutz et al., 1990; Claoue-Long et al., 1991). According to Claoue-Long et al. (1991), the UHP metamorphism occurred at 530 ± 7 Ma based on analysis of metamorphic zircons, which agrees with the Sm-Nd isochron ages of 533 ± 7 and 505 ± 43 Ma for eclogite, biotite gneiss, and diamondiferous rocks (Shatsky et al., 1993).

23.3 Ultrahigh pressure (UHP) and high pressure (HP) units

The following variations in lithofacies resulted in the division of the Kokchetav UHP-HP metamorphic belt into four units Fig. 2 (Kaneko et al., 2000):

- Unit I is composed mainly of alternating siliceous schist (leptite) and amphibolite;
- Unit II is composed mainly of pelitic–psammitic gneiss with locally abundant eclogite boudins and whiteschist;
- Unit III consists of alternating orthogneiss and amphibolite, with locally abundant large eclogite blocks;
- Unit IV consists mainly of quartzite and siliceous schist.

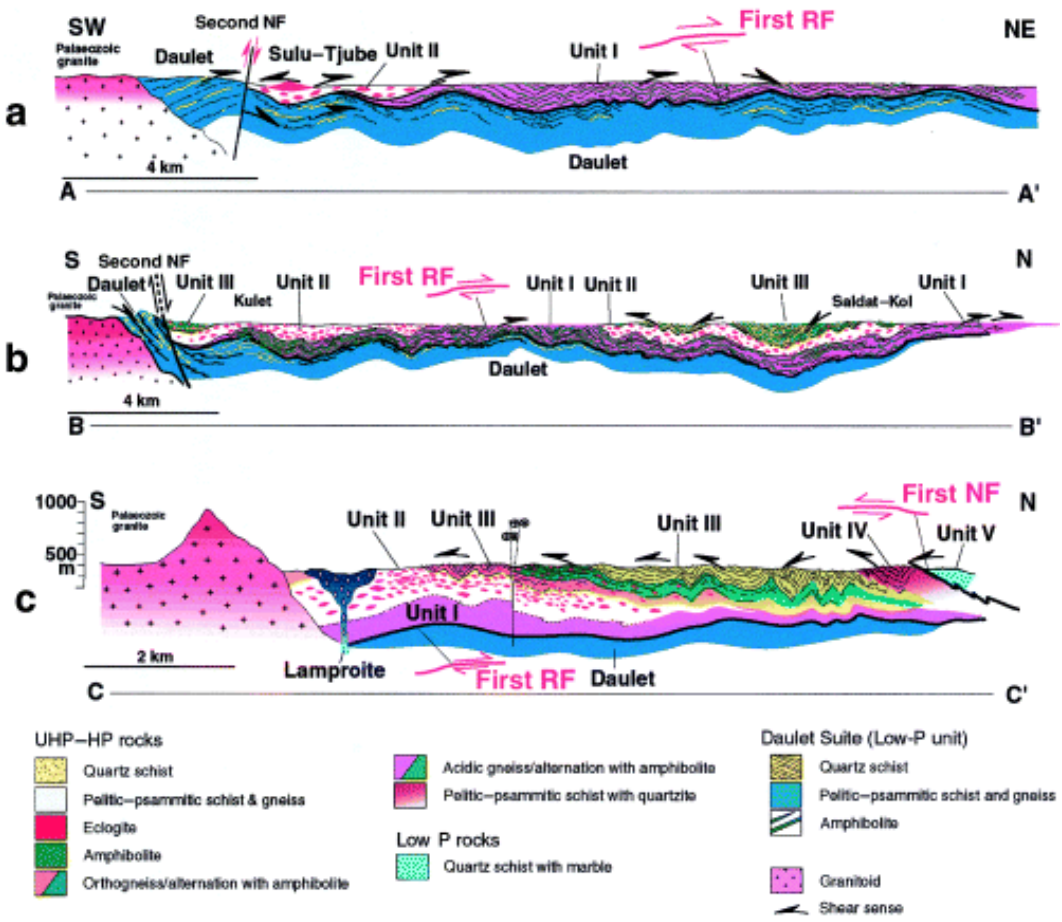

Figure 2. Cross-section of Fig. 1 (a) A-A'; (b) B-B'. (c) C-C', (Kaneko et al., 2000)

Unit I

The majority of Unit I is made up of amphibolite (as massive bodies or thin layers) and acidic gneiss (leptite) mixed with a small amount of pelitic schist and orthogneiss, which are found as lenses or layers of varied sizes. Only a window (25 km × 10 km) along the WNW-ESE axis of an antiformal fold in the western portion exposes this structurally the lowest metamorphic unit (Figs. 1, 3), which is tectonically overlain by the UHP rocks of Unit II. Geologic cross-sections of this unit indicate that the host surface is subhorizontal (Fig. 2a, b) (Kaneko et al., 2000).

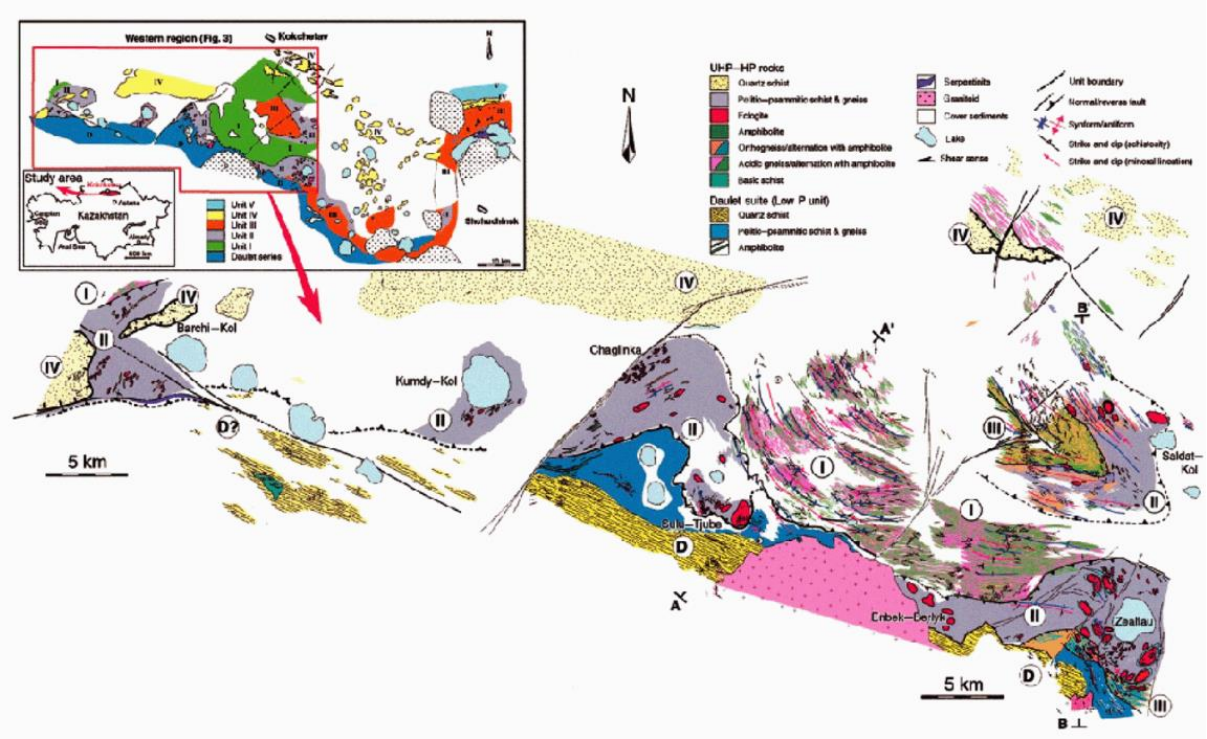

Figure 3. Geologic map of the Western region (Kaneko et al., 2000).

The constituent minerals of the amphibolite are: Hbl + Pl + Qtz + Ep + Ilm ± Grt. Pelitic schist is strongly foliated and often microfolded. The constituent minerals are: Bt + Qtz + Pl + Ms ± Grt ± Sil ± Tur ± Ap ± Ep. Mineral assemblages of the coarse-grained orthogneiss are: Pl + Qtz + Kfs + Ms + Bt + Sil ± Rt ± Ilm ± Tur and Pl + Qtz + Kfs + Ms + Bt ± Rt ± Ilm ± Tur (Kaneko et al., 2000).

Unit II

Whiteschist and pelitic-psammitic gneiss, which contain blocks of eclogite, make up the majority of Unit II (Figs. 2, 3). There are low volumes of orthogneiss, peridotite, and metacarbonate. Muscovite, biotite, quartz, and plagioclase are the most frequent minerals found in paragneiss, along with various amounts of garnet, kyanite, sillimanite, K-feldspar, and rutile. Whiteschist and pelitic schist, which sometimes contain huge garnet porphyroblasts, are surrounded by lenticular eclogite blocks, which are typically a few hundred meters across (Kaneko et al., 2000). These eclogite block formations can be found in a number of places, including Barchi-Kol, Kumdy-Kol, Chaglinka, Sulu-Tube, Kulet, and Soldat-Kol in the west of the mapped area, and also extend to the north of Borovoye in the east (Fig. 1). According to their main mineral assemblages, these eclogites are categorized as: (i) amphibole eclogite (dark eclogite); (ii) zoisite eclogite (pale eclogite); or (iii) dry eclogite (without hydrous minerals). Diamonds are found in pelitic gneiss, whiteschist, and marble in Kumdy-Kol as inclusions in garnet and zircon (Figs. 1, 4).

Eclogite in the Barchi–Kol area

This region has hundreds of lenticular bodies, layers, and pods of eclogite that range in size from a few decimeters to several tens of meters (Fig. 4). The alternation of garnet-quartz (± zoisite) and omphacite (± amphibole) zones, which are typically parallel to the elongated contacts of the lenses, defines the millimeter-scale compositional banding in the majority of eclogites (Kaneko et al., 2000).

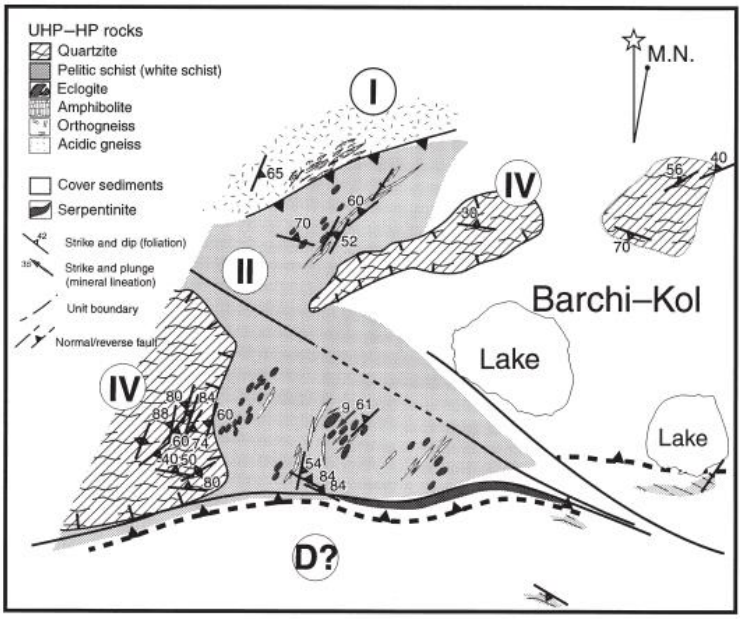

Figure 4. Geologic map of the Barchi–Kol region. (Kaneko et al., 2000).

Eclogite in the Kumdy–Kol area

The Kumdy-Kol region's eclogites are elongated and parallel to the local foliation; their sharp contact with the host gneiss is evident (Fig. 5). Numerous eclogite bodies or lenses exhibit a gradual transformation, starting with an eclogitic core and progressing to garnet amphibolite and then an amphibolite rim. Eclogites of this region display the general dry eclogite assemblage: Grt + Omp + Rt + Coe/Qtz. Exsolution lamellae of quartz or K-feldspar in omphacite that have been recrystallized at 70 kbar and 900–1000 °C make up the core of eclogite bodies in the diamond zone (Okamoto & Maruyama, 1998).

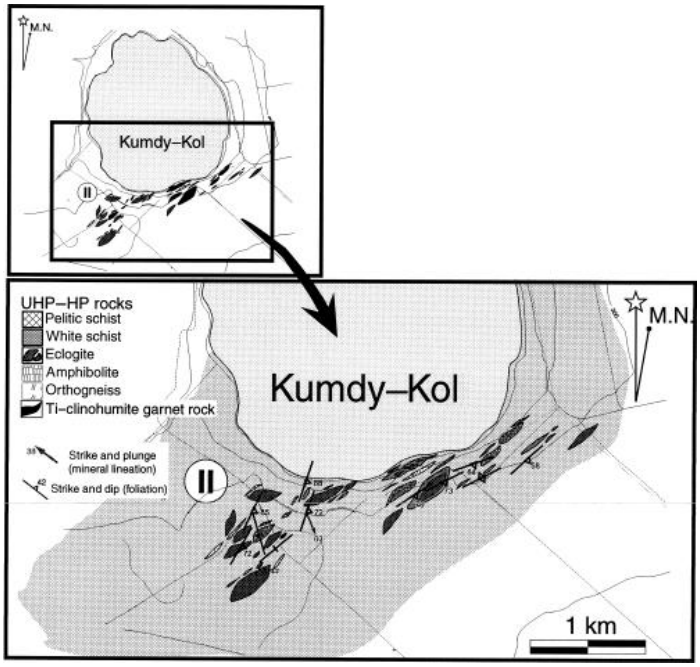

Figure 5. Geologic map of the Kumdy–Kol region. (Kaneko et al., 2000).

Eclogite in the Chaglinka area

More than 50 tiny eclogite bodies in the Chaglinka village that are between a few meters and 100 meters broad are cemented matrix-forming, high-grade pelitic-psammitic gneiss and whiteschist, together with the abundant coarse-grained porphyroblastic garnet. Subhorizontal and NE-trending fold axes characterize it (Fig. 6).

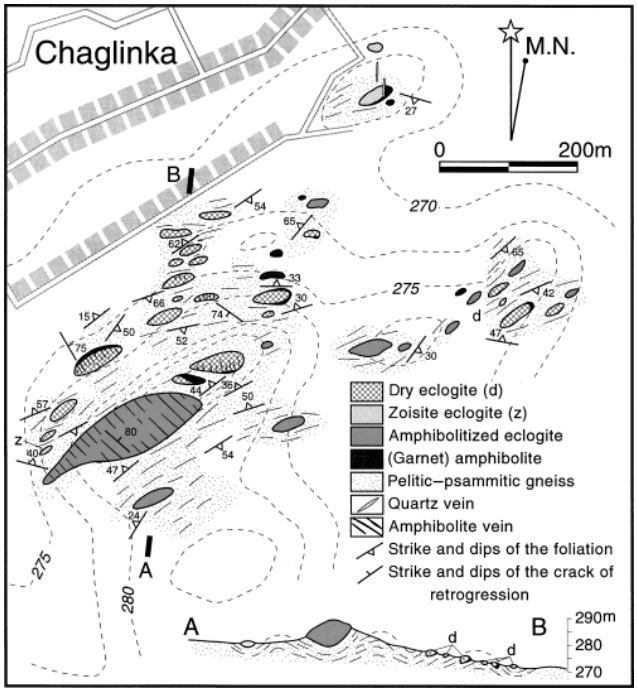

Figure 6. Geologic map and cross-section of the Chaglinka region. (Kaneko et al., 2000).

The host of the eclogite bodies mainly is composed of whiteschist. Small hills or mounds are created from eclogite pieces. Dry eclogites less than 50 m in diameter predominate. A few amphibolitized eclogite blocks, however, are up to 200 m across. Blocks of minor zoisite eclogite are about the same size as blocks of dry eclogite. Phengite, garnet, talc, kyanite, and ancillary minerals are usually found in whiteschist. The principal eclogite facies mineral assemblages are found in the interior of the blocks, where they are alternately replaced and pseudomorphed by greenschist to form amphibolite facies assemblages with a favored orientation. Amphibolized eclogite contains amphibole spots ranging in size from a few millimeters to 1 cm in diameter. The constituent minerals of the amphibolite are: hornblende + plagioclase + quartz + epidote + ilmenite ± garnet (Kaneko et al., 2000).

Eclogite in the Sulu–Tube area

Zoisite-eclogite, amphibolitized eclogite, paragneiss, and pelitic gneiss/schist make up the majority of the rock types in the Sulu-Tube area. One of the biggest eclogite bodies in the UHP unit is the hill of Sulu-Tube (Fig. 7). Usually a few hundred meters long, eclogite emerges as lenticular or pod-shaped masses across 2 sq. km. Eclogite consists of omphacite, garnet, quartz, amphibole, zoisite, rutile, and minor phengite, zircon and apatite. Eclogite in the Sulu–Tube region is mainly zoisite eclogite. Along margins and cracks, amphibolitization has obliterated the primary texture and mineralogy (Kaneko et al., 2000).

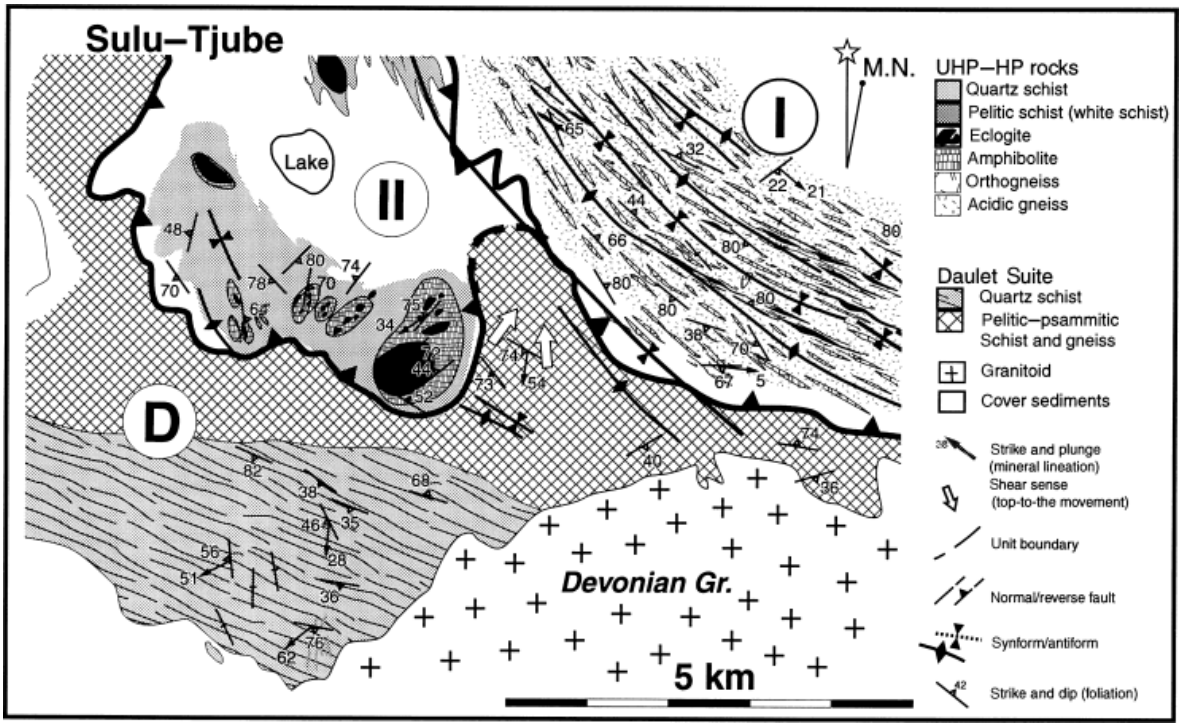

Figure 7. Geologic map of the Sulu–Tube region. (Kaneko et al., 2000).

Eclogites in the north and west of Zealtau Lake (Kulet area)

Unit II is made up of whiteschist, eclogite, amphibolite, and minor quartz schist to the north and west of Zealtau Lake. Individual blocks of eclogite can be found within the whiteschist matrix (Fig. 8). The majority of eclogites are observed in the west and north-west of Zealtau Lake. The distribution of numerous small exposures (each several meters across) in Figure 8 indicates the size of the one eclogite body have pod- or lens-like shapes (Kaneko et al., 2000).

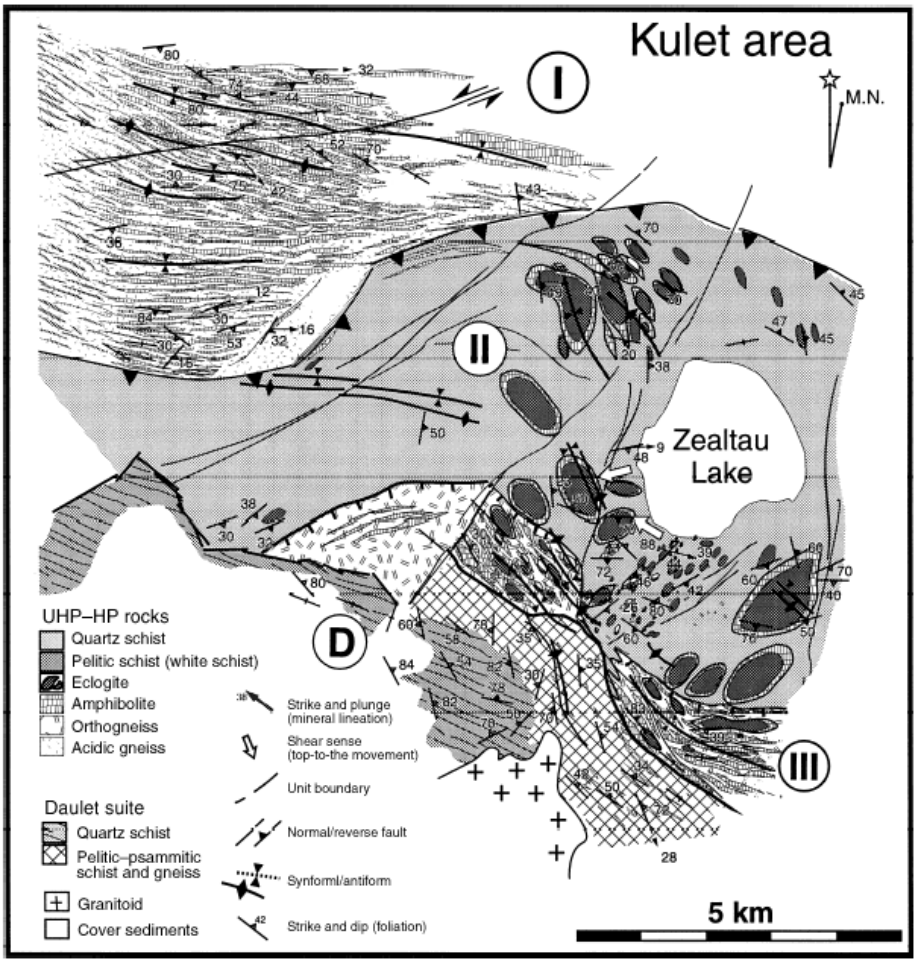

Figure 8. Geologic map of the Kulet region (Kaneko et al., 2000).

Eclogites consist of omphacite + garnet + quartz + rutile + zoisite (or epidote) ± phengite ± zircon ± apatite and omphacite + garnet + quartz + rutile + amphibole ± zircon ± apatite. The texture is generally coarse-grained and equi-dimensional. The eclogite masses are amphibolized to some extent. Eclogite blocks feature garnet amphibolite crusts that range in thickness from a few millimeters to several meters on the outcrop scale. Eclogite is locally pierced by thin amphibolitized zones (up to several centimeters in thickness), and dark-colored veins, which are

1-3 mm thick, occur in the centre of the narrow zones. Whiteschist consists mainly of phengite, quartz, talc, disthene, and garnet. A few millimeters to several centimeters in diameter, garnet is found as porphyroblasts (Kaneko et al., 2000).

Eclogite in the Soldat–Kol area

Unit II in north-western part of Soldat-Kol is made up of whiteschist, eclogite, amphibolite, and a little amount of acidic gneiss. There are eight eclogite pods in the mapped area, with the largest one being to the north of Soldat-Kol and measuring roughly 1500 meters long and 600 meters broad (Fig. 9). The eclogite lenses and pods elongate in a NW-SE direction (Kaneko et al., 2000).

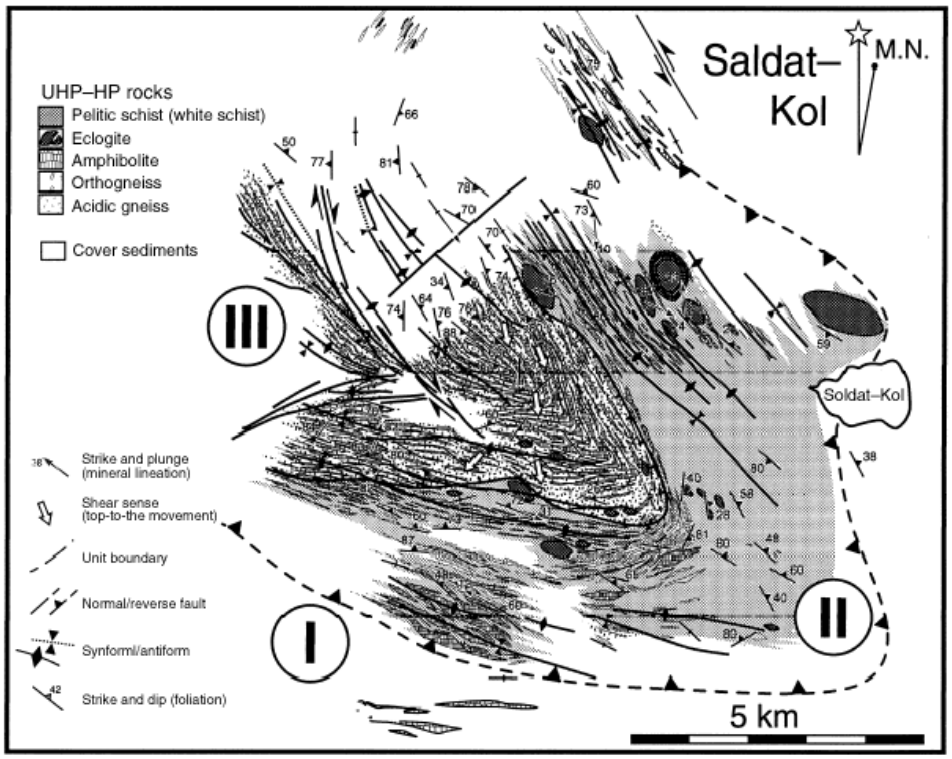

Figure 9. Geologic map of the Soldat–Kol region

Eclogite consists of omphacite, garnet, quartz, rutile, and minor amphibole, zoisite, phengite, zircon and apatite. With the exception of an eclogite pod in Unit II's westernmost region, it is generally coarse-grained and equi-dimensional. The compositional layering of felsic gneiss is characterized by thick quartzo-feldspathic layers (up to 1 m thick) and thin micaceous layers (several millimeters thick), and it frequently contains plagioclase and porphyroblastic quartz. The lenses trend NW-SE and can be up to 70 m wide and at least 400 m long. The characteristic mineral assemblage is: quartz + plagioclase + muscovite ± biotite ± garnet ± K-feldspar ± ilmenite ± tourmaline ± apatite (Kaneko et al., 2000).

Eclogite in the Borovoye area

The northern Bolishoe Chebachye Lake coastline is exposed for Unit II (Fig. 10). Lenticular eclogite blocks here have a north-south to NE-SW trend. Eclogite consists of omphacite, garnet, quartz, rutile, and minor amphibole, zoisite (or epidote), phengite, zircon and apatite (Kaneko et al., 2000).

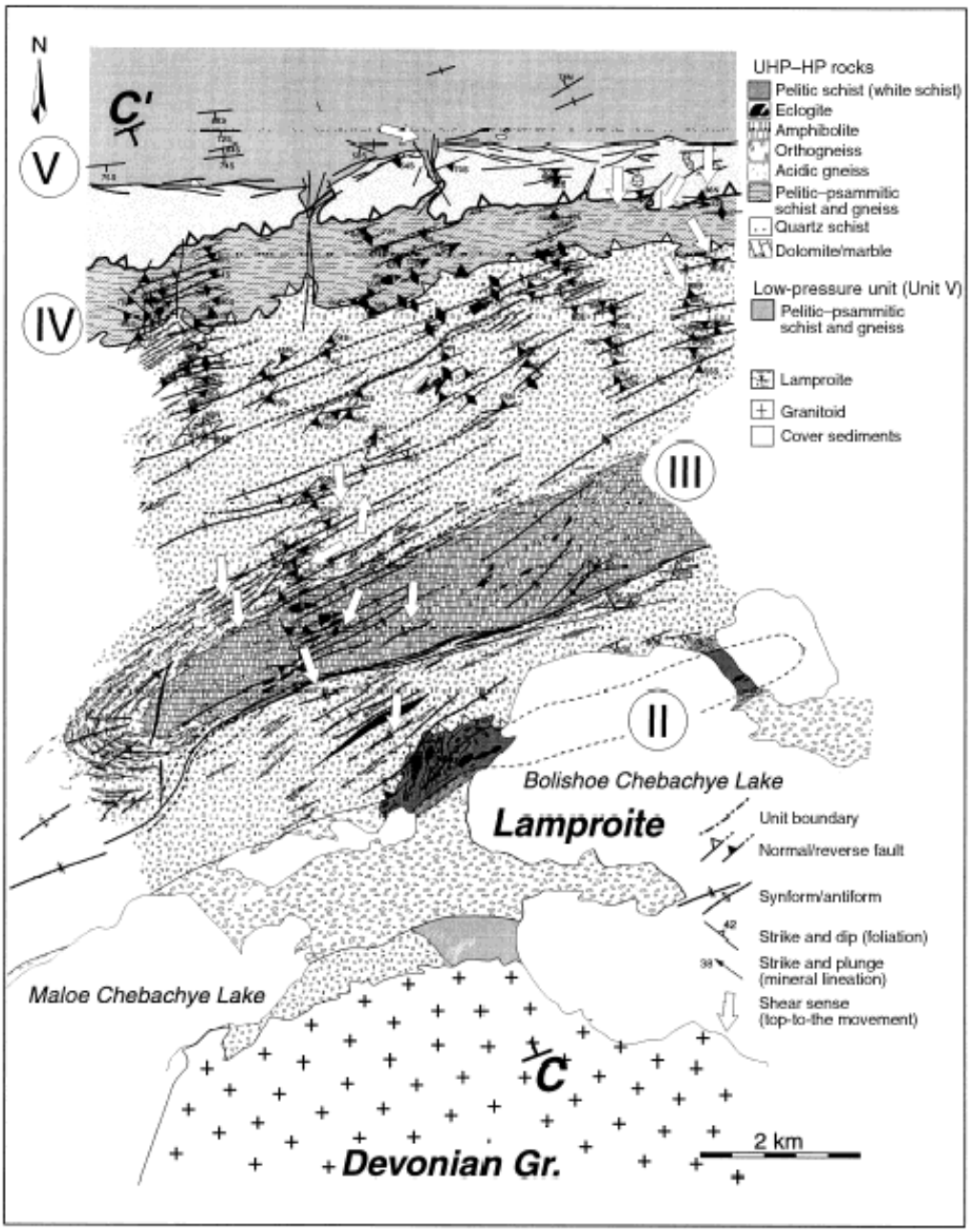

Figure 10. Geologic map of the Borovoyoe region, (Kaneko et al., 2000)

Unit III

Unit III is composed mainly of orthogneisses, migmatites, and amphibolites, as well as small lenses of eclogites. Its main characteristics is the absence of coesite and diamond in eclogite and country rocks. Eclogite lenses have undergone amphibolitization along contacts with host orthogneiss, same as in Unit II (Figs. 1, 2). Eclogite consists of omphacite, garnet, quartz, amphibole, zoisite, rutile, and minor phengite, zircon and apatite. Intense amphibolitization has damaged the primary texture and mineralogy in the majority of eclogite masses. Mineral assemblages in orthogneiss are represented by muscovite, biotite, quartz, plagioclase and K-feldspar with small amounts of garnet and sillimanite. Amphibolite is composed of hornblende + plagioclase + quartz + epidote + ilmenite ± garnet (Kaneko et al., 2000).

To the north of Borovoye, the rocks of Unit III cover a vast region around a central antiformal axis ENE–WSW (Fig. 10). Additionally, distinguishable Unit III rock occurrences can be found to the south and southwest of Zealtau Lake (Fig. 8).

Unit IV

The southern and northern portions of the plotted area are represented by this structurally topmost metamorphic unit in the region, which is tectonically overlain by a low-pressure unit (Unit V) (Figs. 1, 2). Quartzite and siliceous schist make up the bulk of it, but metabasic rocks are also present in some areas. The constituent minerals of amphibolite are: Hbl + Pl + Qtz + Ep + Ilm ± Grt (Kaneko et al., 2000).

Other Units

Low-pressure unit (Unit V)

The weakly metamorphosed rocks of Unit V, which are extensively spread in the northernmost section of the Borovoye area, lie on top of the rocks of Unit IV (Fig. 10). Mainly Unit V consists of slate, shale, quartzite, sandstone, marble/limestone, as well as conglomerates with pebbles 2–5 mm in diameter that are severely elongated/flattened. Sandstone shows graded bedding and cross-laminae (Kaneko et al., 2000).

Low-pressure unit (Daulet suite)

This predominantly pelitic unit of high-grade gneisses is present under Unit I (1-3), belongs to a low-P facies series, and is called the Daulet series (Dobretsov et al., 1995). The P–T conditions of Daulet's metamorphic rocks are 500–650 °C at approximately constant pressure of about 3 kbar (Dobretsov et al., 1995; Shatsky et al., 1995).

2.3.4 Tectonic models on formation of Kokchetav massif

The overall thickness of units I–IV of the UHP-HP metamorphic belt is estimated to be around 2 km. The characteristics of the Kokchetav massif is shown in Figure 11a. Later doming along with

many high-angle normal faults and strike-slip faults that cut all the units altered the tectonics of the metamorphic belt (Fig. 11b) (Kaneko et al., 2000).

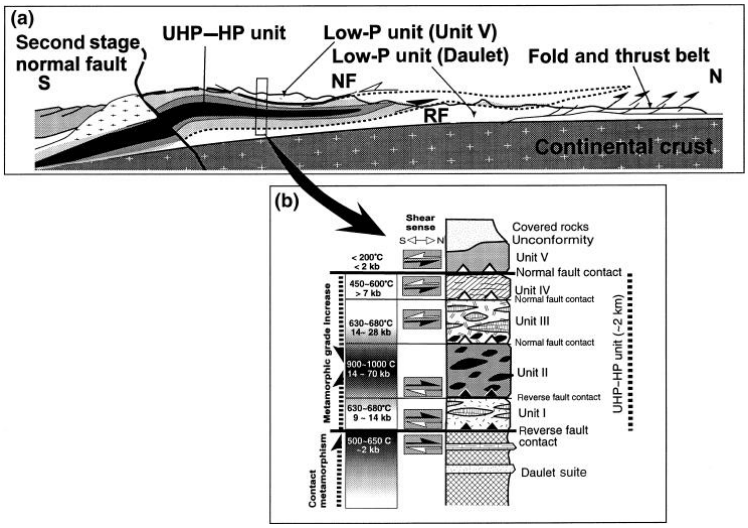

Figure 11. (a) Simplified cross-section of the Kokchetav orogenic belt. (b) Tectonostratigraphic diagram of the Kokchetav metamorphic belt. Pressure–temperature metamorphic conditions showing the metamorphic rocks from Units I–V (Ota et al., 1999) and Daulet Series, (Kaneko et al., 2000)

Figure 12 illustrates a diagram showing the tectonic model for the evolution of the Kokchetav HP-UHP massif. Subhorizontal tectonic extrusion brought the UHP-HP unit from the depths of the upper mantle to the shallower crustal levels (Fig. 12a). The thermal structure of the UHP-HP unit suggests that quartzo-feldspathic materials moved to the surface more quickly than those in the nearby lower-P units because they were more ductile, heated to higher temperatures, and, thus, more buoyant (Kaneko et al., 2000).

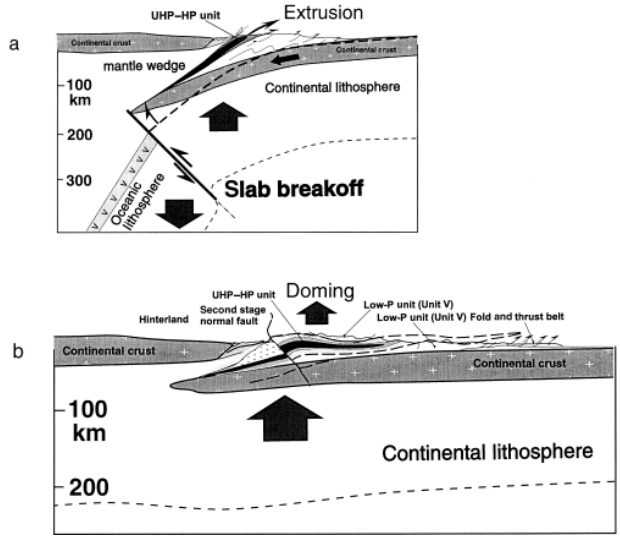

Figure 12. Different exhumation stages of the Kokchetav metamorphic belt. (a) The first stage of exhumation by wedge extrusion. The schematic diagram shows the subduction of the continent at 530–540 Ma. (b) The domal uplift stage (517 Ma); subhorizontal extrusion of the metamorphic belt by synchronous paired normal faulting on the top and reverse faulting at the bottom. Tectonic juxtaposition of these metamorphic units at mid-crustal level, (Kaneko et al., 2000).

The felsic and mafic volcanic-plutonic rocks and sediments of Unit I, overlying pelitic rocks of Unit II, orthogneiss of a Pan–African continent (the rocks of Unit III), together with a descending oceanic plate were subducted to a depth of roughly 200 km in the late Precambrian. After buoyant continental material packed the subduction zone, it cracked, heated up, recrystallized, and then was exhumed. Sialic material started to appear on the surface after the leading part of the high-density oceanic lithosphere was lost owing to "slab breakoff". The metamorphic core of the UHP–HP unit advanced to the mid-crustal level, stopped, and thermally changed the nearby units, including the underlying low-P Daulet. At around 517 Ma, the four stacked and welded units at mid-crustal level began to dome and produce numerous high-angle faults. It is possible to describe the anticline in Unit I as a fault-bend fold (Fig. 12b). This interpretation is connected to late second-stage normal faulting that resulted in block uplift/exhumation (Kaneko et al., 2000).

2.4. Eclogites

2.6.3.1. Eclogites and the Eclogite Facies

Eclogite (Fig. 13) is an extremely dense (3.3-3.5 g/cm3) metamorphic rock consisting mainly of bright green omphacite and red/pinkish garnet with small amounts of quartz (or coesite), kyanite, and rutile. Plagioclase is not found. Amphiboles, hornblende or glaucophane, epidote, lawsonite, phengite, paragonite, talc, carbonate minerals, diamond, and olivine are some additional minor or trace minerals found in eclogites (Tsujimori, 2021).

Eclogite is specifically defined as a "plagioclase-free metamorphic rock composed of >75 vol% of omphacite and garnet, both of which are present as major constituents, the amount of neither of them higher than 70 vol%" by the International Union of Geological Sciences (IUGS) Subcommission on the Systematics of Metamorphic Rocks (SCMR) (Desmons and Smulikowski, 2007). The term "eclogite" was first used to describe the rocks from Saualpe, Austria, in 1822 by French mineralogist René-Just Haüy of the Museum of Natural History in Paris due to the rock's beauty and valuableness (Fig. 1). The name is derived from the Greek word ekloge, and the suffix "-ite," which means "chosen rock."

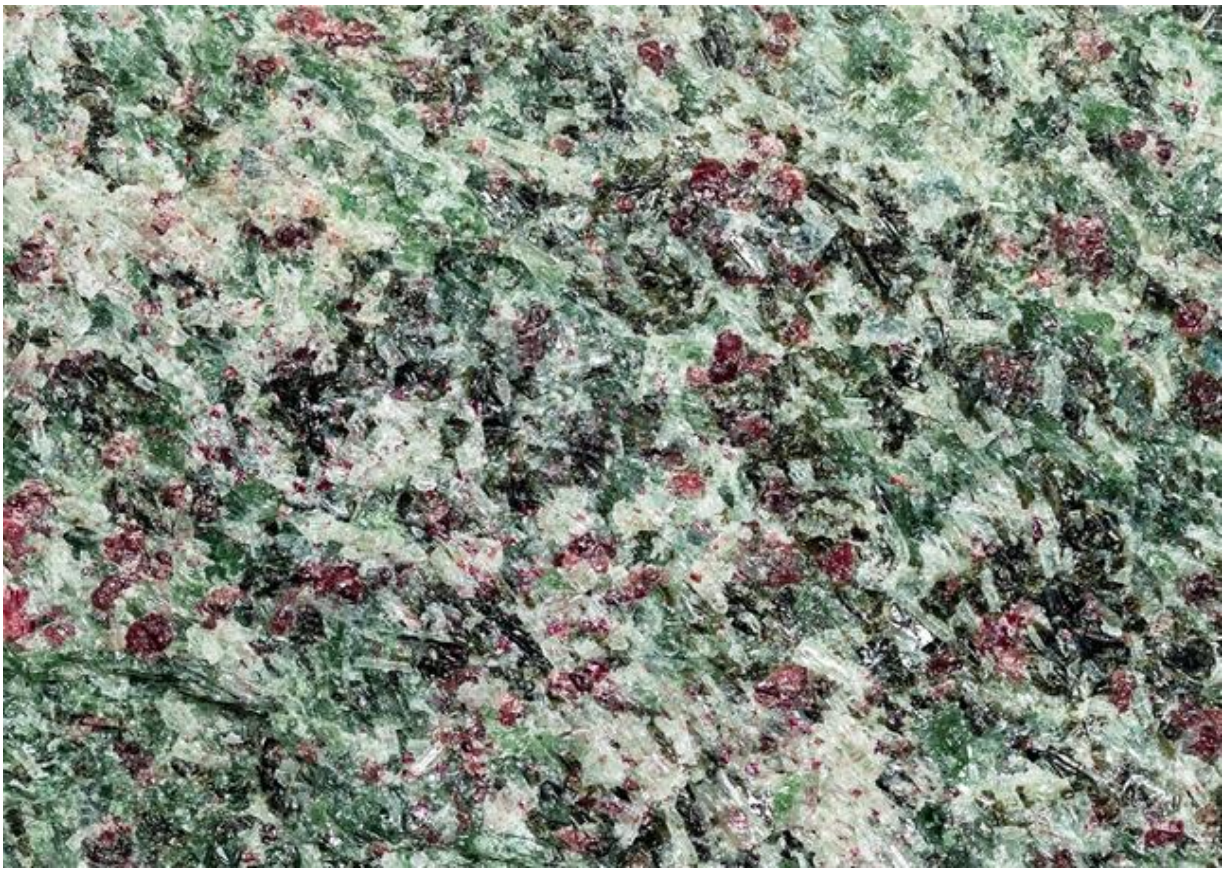

Figure 13. Appearance of eclogite from the type locality (Saualpe, Austria) [4 cm wide], (Tsujimori, 2021)

Since Finnish geologist Pentti Eskola established the idea of "metamorphic facies" in 1915, 1920, and 1939, eclogite has been used similarly with eclogite facies. The eclogite facies demonstrates a P-T field, in which the assemblage of eclogitic minerals is stable in both the crustal and mantle layers (Fig. 14). The eclogite facies is bounded on the low-T side by the blueschist facies, on the high-T side by the granulite facies, and on the lower-P side by the amphibolite and epidote-amphibolite facies (Fig. 14A). Eclogite forms gradually from other facies rocks in the P-T area, but this process can be slowed down by reaction kinetics that are strongly influenced by the fluid content of the rocks. Amphibole eclogite, epidote eclogite, lawsonite eclogite, and dry eclogite are the four subfacies that have been proposed (Fig. 14B). The eclogite facies include a broad range of P-T zones, from the deep crust to the mantle. Therefore, various eclogite occurrences represent various tectonic environments and host oceanic/continental crustal compositions (Tsujimori, 2021).

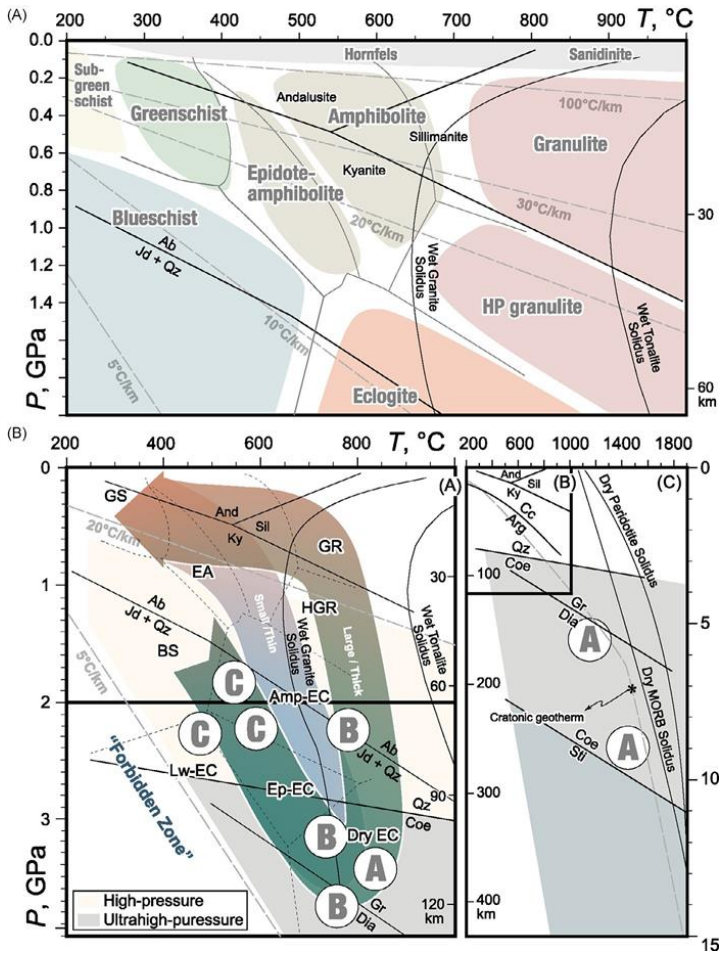

Figure 14. A) Pressure–temperature (P–T) diagram showing metamorphic facies. (B) P–T regime at different scales assigned to various metamorphic type: HP—high-pressure, UHP—ultrahigh-pressure, and "Forbidden Zone." Metamorphic facies abbreviations: BS—blueschist; AM—amphibolite; Lw-EC—lawsonite eclogite; Ep-EC—epidote eclogite; Amp-EC—amphibole eclogite; DryEC—dry eclogite; GS—greenschist; EA—epidote-amphibolite; GR—granulite; HGR—highpressure granulite. P–T paths of small/thin UHP terranes and large/thick terranes are also shown. The circled A, B, and C refer to the Coleman et al. (1965) classification (see text). (C) High-T limit of eclogite defined by dry MORB solidus. (B) Modified after Kylander-Clark ARC, Hacker BR, Mattinson CG (2012) Size and exhumation rate of ultrahigh-pressure terranes linked to orogenic stage. Earth and Planetary Science Letters 321–322: 115–120, (Tsujimori, 2021).

2.6.3.2. Occurrence of Eclogites

Subduction/Collision-Related Orogenic Eclogites

The Pacific-type and collision-type orogens are two paleo convergent plate-tectonic systems that have been discovered (Maruyama et al., 1996; Liou et al., 2004; Stern et al., 2013) (Fig. 15). Both types of orogenic belts contain orogenic eclogite (Smith, 1988; Carswell, 1990; Coleman and Wang, 1995) (Fig. 16).

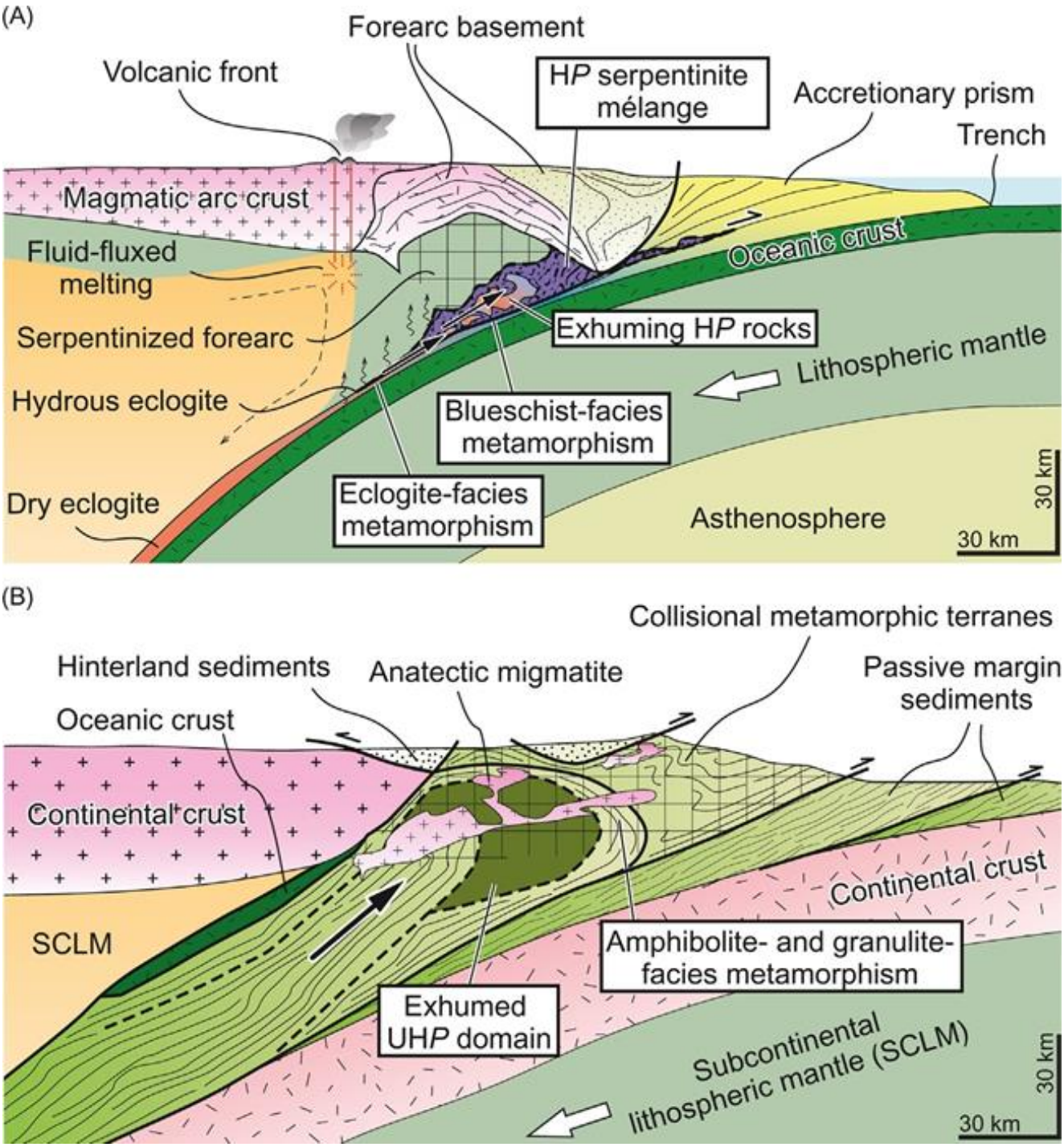

Figure 15. Cross sections showing two different convergent plate margins. (A) Pacific-type subduction zone. (B) Continental collision zone. Modified after Stern RJ, Tsujimori T, Harlow GE and Groat LA (2013) Plate tectonic gemstones. Geology 41: 723–726, (Tsujimori, 2021).

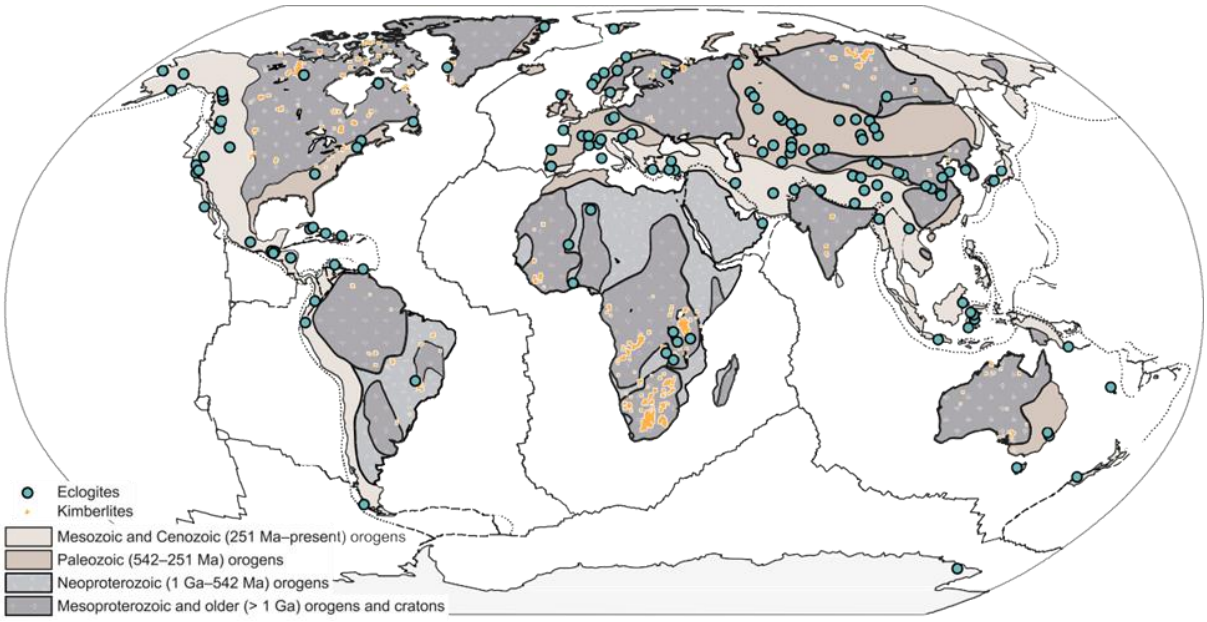

Figure 16. Global distribution of eclogites and kimberlites (modified after Tsujimori T, Ernst WG (2014) Lawsonite blueschists and lawsonite eclogites as proxies for palaeo-subduction zone processes: A review. Journal of Metamorphic Geology 32(5): 437–454). Kimberlite localities are based on a database of Giuliani A, Pearson DG (2019) Kimberlites: From deep earth to diamond mines. Elements 15(6): 377–380 (Tsujimori, 2021).

Pacific-type eclogites are typically found with serpentinite, blueschist, epidote-amphibolite, metachert and rare jadeitite (Fig. 17A–C). Most Pacific-type eclogites reveal an exhumation that occurred less than 10 to 15 Ma (Agard et al., 2009). According to recent zircon U-Pb investigations of Sambagawa eclogites, the process of eclogite-facies metamorphism seemed to last 30 Ma (Aoki et al., 2020) and may have involved recrystallization of subducted oceanic arc materials rather than a subducted accretionary complex. According to thermomechanical modeling, low-density, low-viscosity sedimentary rocks and serpentinites on the seafloor are essential for the exhumation of Pacific-type eclogites (Wang et al., 2019).

In comparison, collision-type eclogites are connected with continental rocks such as gneiss, aluminous metapelite, granulite, amphibolite, migmatite, impure marble, and rare garnet peridotite (Fig. 17E–H). Eclogites often have lenses and lenticular boudins contained within quartzo-feldspathic gneiss and migmatitic gneiss (Fig. 17F and H). Continental subduction and collision usually follow Pacific-type oceanic subduction. The key to the buoyancy-driven exhumation of collision-type eclogite is the underflow of continental crust (Ernst, 2001). Gerya et al. (2008) proposed a model based on numerical modeling of continental subduction/collision and exhumation of eclogites that states that the deeply subducted continental crust reaches temperatures of 700–900 C through intense viscous shear and radiogenic heating; as a result, the high-T results in buoyancy-driven upward extrusion of the UHP slab due to melting. Zircon U-Pb

geochronology of multiple eclogite-facies metamorphism in the Italian Western Alps suggests that the metamorphism of the eclogite-facies lasted for 25 million years (Rubatto et al., 2011).

Mantle Eclogites in Kimberlitic Pipes and Plume-Related Ocean Island Basalts

A variety of deep mantle fragments (xenoliths, xenocrysts), including mantle eclogites and bimineralic garnet clinopyroxenites, are found in kimberlites - potassic, volatile-rich ultramafic rocks (Fig. 17I and J). Since kimberlite eclogites contain diamonds, it is important to understand their origin and distribution (Tappert and Tappert, 2011). While orogenic eclogites older than 2.5 Ga have not been identified, eclogites containing diamonds are more typical in kimberlitic pipes with older ages (> 2.5 Ga) (Tsujimori, 2021). The discovery of nanodiamonds suggests that some eclogites were uplifted from depths greater than 180 km by mantle plumes (Wirth & Rocholl, 2003).

Figure 17. Representative appearances, textures, and occurrence of eclogites in different tectonic settings. (A) Lawsonite eclogite in the South Motagua Mélange, Guatemala, showing a foliation (Tsujimori et al., 2006). (B) Eclogite (EC) associated with blueschist (BS) in the Franciscan Complex (Jenner, California, United States). (C) Photomicrograph of the low-T Franciscan

eclogite from Healdsburg, California, United States (Sample 62-RGC-58: Coleman et al., 1965). Scale bar is 1 cm. (D) Eclogite 'knockers' of the Franciscan Complex (Tiburon Peninsula, California, United States). (E) Kyanite eclogites in the Western Gneiss Region, Nordfjord, Norway, showing a "Christmas rock" appearance. (F) Eclogite lenses (EC) enclosed in quartzo-feldspathic gneiss (qfg) in the Western Gneiss Region. (G) Photomicrograph of the Neoproterozoic medium-T eclogite of the Ufipa Terrane, Ubendian Belt. Scale bar is 1 cm. (H) Eclogite lenses (EC) enclosed in quartzofeldspathic gneiss (qfg) in North Qaidam, NW China. (I) Appearance of mantle eclogite xenoliths in kimberlitic pipes: RV—Roberts Victor, South Africa (Group I, and Group II, Photo credit: Akira Ishikawa); UD—Udachnaya, Siberia, Russia, GR—Garnet Ridge, Colorado, United States. Scale bars are 1 cm. (J) Photomicrograph of Udachnaya eclogite. Scale bar is 1 cm. (K) View of the Garnet Ridge diatremes of the Navajo Volcanic Field, Colorado, United States. Credits: (E) Kennet Flores, (I) Dmitry Zedgenizov, Akira Ishikawa, and Yoshihide Ogasawara, (J) Dmitry Zedgenizov, and (K) Yoshihide Ogasawara, (Tsujimori, 2021).

2.6.3.3. Tectonic Origin and Classification of Eclogites

Geologist Robert G. Coleman divided orogenic and mantle eclogites into three types based on mineral compositions and tectonic origin (Coleman et al., 1965). Group A high-T eclogites can be found as xenoliths in kimberlite (or lamprophyres) and layers in orogenic peridotite; Group B eclogites are linked to HP granulites in the crustal basement of collisional orogenic belts; while Group C eclogites are abundant in Pacific-type orogenic belts. According to the temperature of formation, Carswell (1990) suggested three categories: high-T at 900–1600 C, medium-T at 550–900 C, and low-T at 450–550 C. These correspond to Coleman's Group A, B, and C eclogites, respectively. Despite the fact that a number of eclogite classifications have been offered, Coleman's classification is still relevant today since various type eclogites have formed in different tectonic (P–T) settings (Tsujimori, 2021).

High-T (Group A) eclogites are primarily found as xenoliths in kimberlite and lamproite pipes in pre-Cambrian continental basement. These mantle eclogite xenoliths from kimberlitic pipes are fragments of subducted oceanic crust or HP cumulates from mantle melts. Medium-T (Group B) eclogites are widespread in continental collision zones. In terms of volume, HP–UHP eclogites are small components of gneissic metamorphic belts and the majority of eclogites have undergone significant retrogradation after exhumation. Rigid minerals including garnet, omphacite, phengite, epidote, and tourmaline all still contain minute amounts of coesite or micro-diamond inclusions. Minerals such as garnet, omphacite and even in phengite, epidote and tourmaline contain trace amounts of coesite or micro-diamond inclusions. Low-T (Group C) eclogites can be found as block or lenses (Fig. 17) in blueschist belts, and blueschist-bearing serpentinite mélanges of Pacific-type orogens (Tsujimori, 2021).

Figure 18 shows eclogites discovered during the field trip in October 2022 at locations such as Chaglinka, Kulet and Kumdy-Kol in North Kazakhstan.

Figure 18. Appearance and texture of eclogites of the Kokchetav massif, North Kazakhstan

2.5. Garnet

2.5.1 Introduction

Garnets are a large group of rock-forming silicate minerals (Fig. 19). The word garnet derives from the Middle English word ‘gernet’, meaning 'dark red'. Garnets are commonly found in metamorphic and in some in igneous rocks (Alderton, 2021). They form under the same extreme pressures and/or temperatures as those types of rocks. Geologists can use garnets to determine the temperature and pressure at which a particular rock containing garnet formed (Garnet, n.d.).

Figure 19. Garnet, (https://rocksminerals.flexiblelearning.auckland.ac.nz/minerals/garnet.html#:~:text=Garnet%20is%20commonly%20found%20in,particular%20garnet%2Dbearing%20rock%20formed .)

2.5.2 Classification and Chemistry

These minerals have similar physical properties and crystal structure, but differ in chemical composition. The garnet group has the general chemical formula of $X_3Y_2(SiO_4)_3$ (King, 2012). Divalent cations (Ca, Mg, Fe, Mn)$^{2+}$ typically occupy the X site and trivalent cations (Al, Fe, Mn,

V, Cr)$^{3+}$ in a dodecahedral and octahedral framework with [SiO4]$^{4-}$ occupying the tetrahedra. Most of the cation exchange in the garnets occurs in the divalent X sites and the trivalent Y sites. Garnets are classified into six main species, which indicate the end-members of solid solution series:

- Almandine - $Fe_3Al_2Si_3O_{12}$
- Pyrope - $Mg_3Al_2Si_3O_{12}$
- Spessartine - $Mn_3Al_2Si_3O_{12}$
- Andradite - $Ca_3Fe_2Si_3O_{12}$
- Grossular - $Ca_3Al_2Si_3O_{12}$
- Uvarovite - $Ca_3Cr_2Si_3O_{12}$

These garnets make up two solid solution series: pyralspite - almandine, pyrope, spessartine, with cation exchange in the X sites and ugrandite - andradite, grossular, uvarovite, with cation exchange in the Y sites (Alderton, 2021).

2.5.3 Optical Properties

Garnet comes in a variety of colors. While pyrope, almandine, and spessartine frequently have diverse shades of red, orange, brown, and black, grossular, andradite, and uvarovite typically have shades of green, yellow, brown, and black (Alderton, 2021). They crystallize in the cubic system and have a huge power of crystallization growing up to 1 m in size. Cubic and octahedral faces are poorly developed. Common shapes include rhombic dodecahedra (110) or icositetrahedra (=trapezohedra) (211) and these crystal structures are frequently visible in thin sections (Fig. 20).

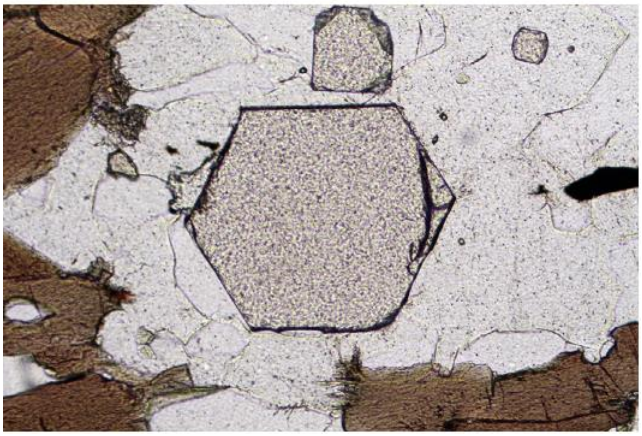

Figure 20. Well-formed crystal of garnet in a thin section of a granulite (plane polarized light). Field of view ¼ 1 mm, (Alderton, 2021).

2.5.4. Occurrences and geological Significance

Garnet is present in green-schist facies metamorphic rocks such as gneiss, hornblende schist, and mica schist because its crystal lattice structure is stable at high pressures and temperatures (Klein,

1985). Pyrope, which is typically found in peridotites and kimberlites as well as the serpentines that originate from them, is the component that is stable at the pressure and temperature conditions of the Earth's mantle. Garnets are special in that they can record the pressures and temperatures of peak metamorphism and are used as geothermometers and geobarometers in the study of geothermobarometry, which creates P-T paths.

Some garnets are carried up from the mantle during deep-source volcanic eruptions, despite the fact that the majority of the garnets found at the Earth's surface have developed within the crust. These eruptions transport xenoliths, or fragments of mantle rock, to the surface in the form of "pipes" (Fig. 21). The majority of diamonds found at or near the surface of the Earth come from these xenoliths. Despite xenoliths carry diamonds, they frequently also contain a huge number of garnets for every diamond, and those garnets tend to be larger. Compared to garnets found in the earth's crust at shallow depths, these garnets from deep sources are very different. So, searching for these distinctive garnets is an excellent strategy to prospect for diamonds. The garnets are used by geologists searching for diamond deposits as "indicator minerals"(King, 2012).

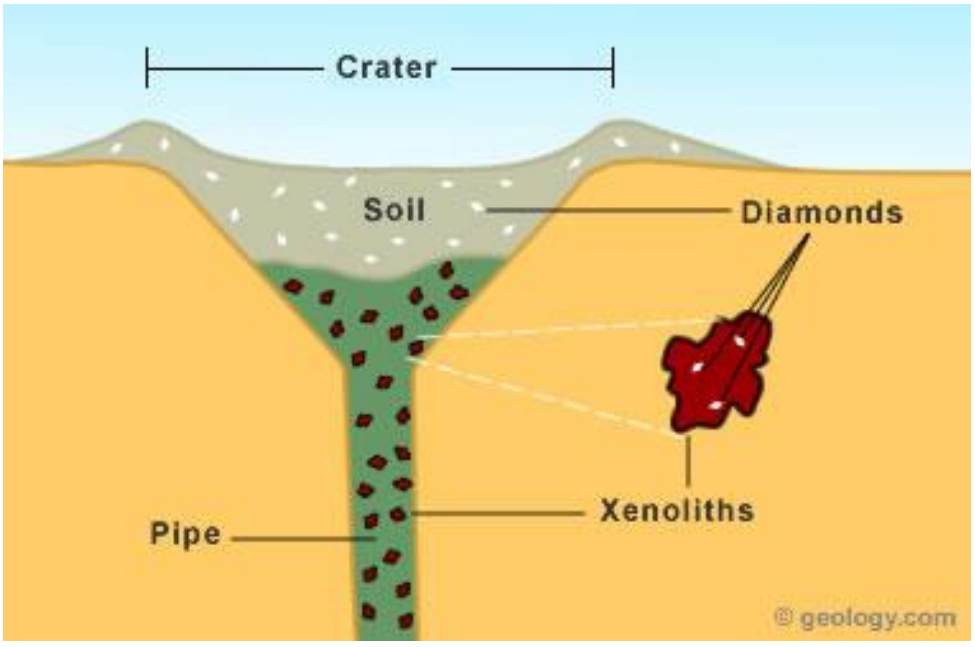

Figure 21. Diamond pipe: Simplified cross-section of a diamond pipe and residual soil deposit showing the relationships of xenoliths and diamonds with the pipe and residual soil, (King, 2012).

In summary, the Central Asian Orogenic Belt, which is one of the largest accretionary orogens in the world, includes island arcs, accretionary complexes and microcontinental fragments. The Kokchetav massif in northern Kazakhstan has undergone a strong metamorphism and is made up of ultrahigh pressure (UHP) and high pressure (HP) units. Microdiamonds are present as small inclusions in garnet and zircon. Kokchetav UHP-HP metamorphic belt consists of four units based on the lithofacies. Unit I is composed mainly of alternating siliceous schist (leptite) and

amphibolite; Unit II is composed mainly of pelitic–psammitic gneiss with locally abundant eclogite boudins and whiteschist; Unit III consists of alternating orthogneiss and amphibolite, with locally abundant large eclogite blocks; and Unit IV consists mainly of quartzite and siliceous schist. Whiteschist and pelitic-psammitic gneiss, which contain blocks of eclogite and make up Unit II, can be found in a number of places, including Barchi-Kol, Kumdy-Kol, Chaglinka, Sulu-Tube, Kulet, and Soldat-Kol in the west of the mapped area, and also extend to the north of Borovoye in the east. The overall thickness of units I–IV of the UHP-HP metamorphic belt is estimated to be around 2 km.

Eclogite is an extremely dense (3.3-3.5 g/cm3) metamorphic rock consisting mainly of bright green omphacite and red/pinkish garnet with small amounts of quartz (or coesite), kyanite, and rutile. Most Pacific-type eclogites reveal an exhumation that occurred less than 10 to 15 Ma. According to recent zircon U-Pb investigations of Sambagawa eclogites, the process of eclogite-facies metamorphism seemed to last 30 Ma. While orogenic eclogites older than 2.5 Ga have not been identified, eclogites containing diamonds are more typical in kimberlitic pipes with older ages (> 2.5 Ga).

Garnets are a large group of rock-forming silicate minerals and are commonly found in metamorphic and in some in igneous rocks. Garnets are special in that they can record the pressures and temperatures of peak metamorphism and are used as geothermometers and geobarometers in the study of geothermobarometry, which creates P-T paths. Some garnets are carried up from the mantle during deep-source volcanic eruptions, despite the fact that the majority of the garnets found at the Earth's surface have developed within the crust. These eruptions transport xenoliths, or fragments of mantle rock, to the surface in the form of "pipes".

2.7.2. Thesis timeline

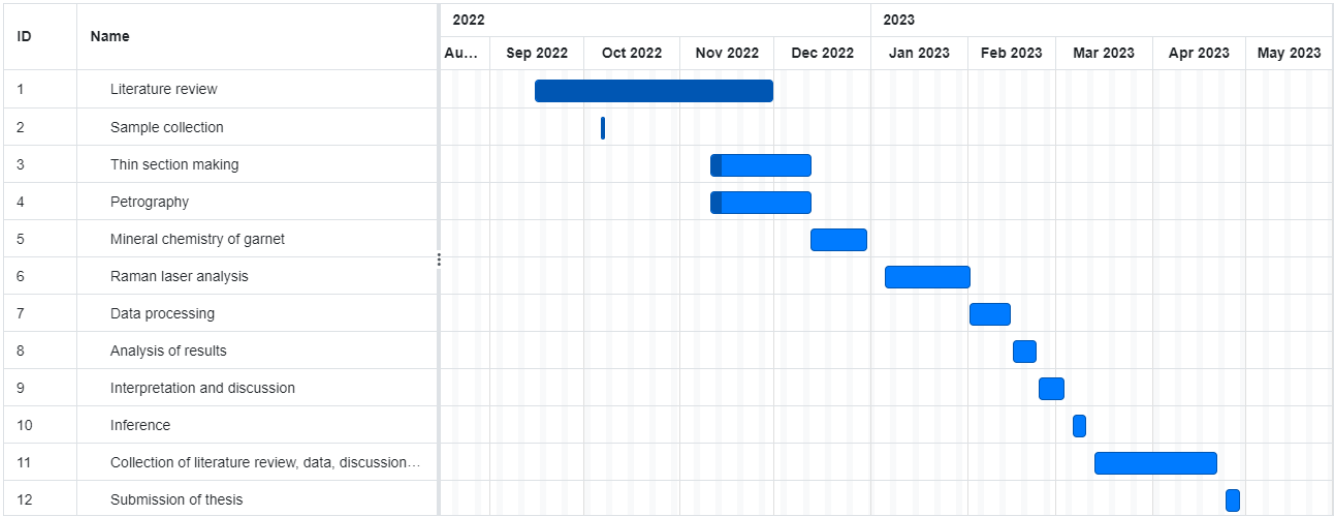

3. Methodology

First method was obtaining rocks during field trip to the Kokchetav massif. Then samples containing garnet were analyzed under microscope in thin section and the chemical composition of garnet was determined using the Scanning Electron Microscope (SEM).

The equipment for making thin sections of rock samples at the School of Mining and Geosciences NU Laboratory of Thin Sections include:

Rock cutting machine (Fig. 22); Set for impregnation and gluing samples (Fig. 23); Slicing machine (Fig. 24).

Figure 22. Rock cutting machine

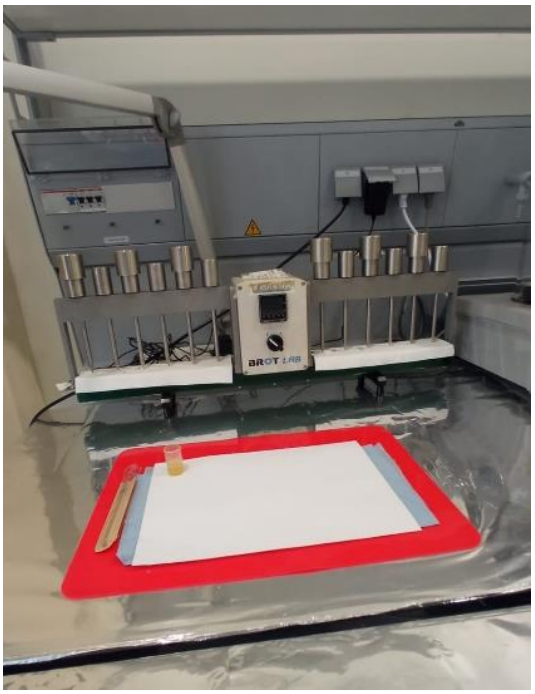

Figure 23. Set for impregnation and gluing samples

Figure 24. Slicing machine

A Scanning electron microscope (SEM) fitted with Energy Dispersion spectrometer (EDS) was used for imaging and to obtain chemical composition of various minerals in thin sections. The analytical conditions are shown with each of the back scattered images obtained and in the appendix, along with the data. (Fig. 25).

Figure 25. Scanning Electron Microscope with EDS at Core facilities of NU

4. Results

Figure 26 depicts geological map of the Kokchetav Massif with sample locations.

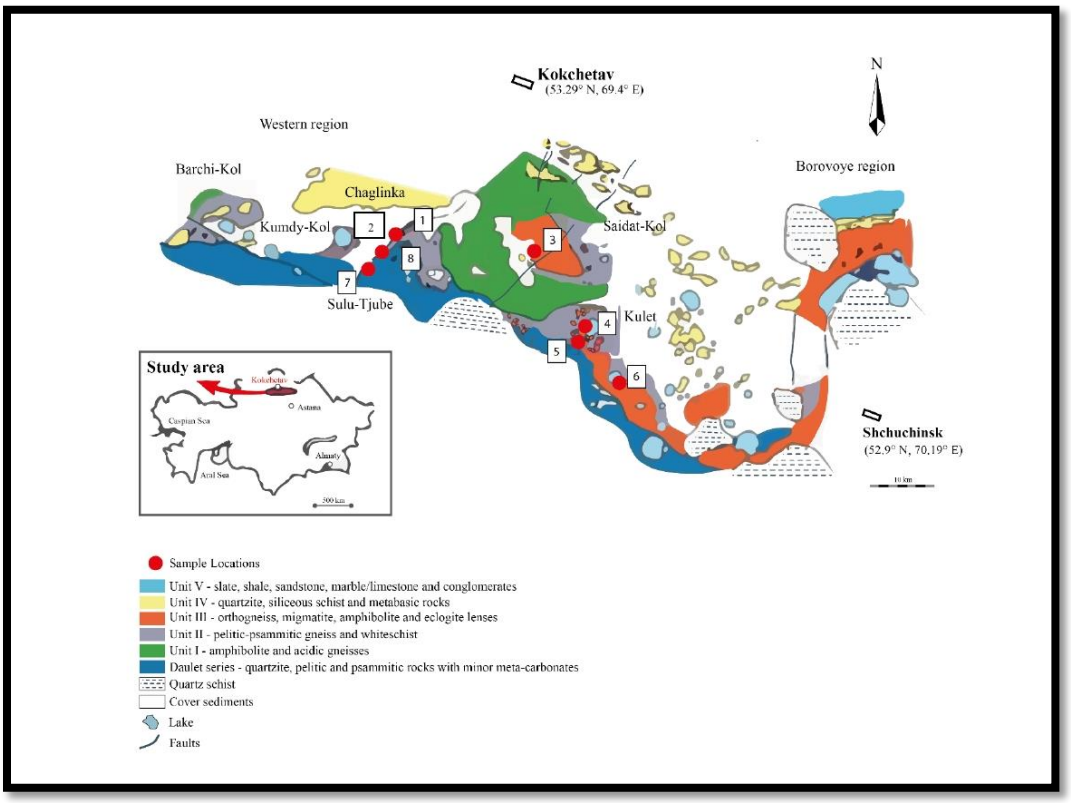

Figure 26. Simplified geological map of the Kokchetav Massif (after Kaneko et al., 2000) with the sample locations

GPS coordinates of locations of taken samples in the field are given in Table 1.

No.	Name of rock	Latitude, ° N	Longitude, ° E
1	Eclogite	53.1657	69.1242
2	Eclogite	53.1641	69.1209
3	Granite gneiss	53.1277	69.4376
4	Granite	53.0086	69.5471
5	Garnet amphibolite	52.9881	69.5402
6	Granite	52.9264	69.6206
7	Pelitic schist	53.1335	69.0641
8	Gabbro	53.1511	69.0906

Table 1. GPS coordinates of locations from the field

A complete list of rock samples is given in Table 2.

No.	Sample No.	Name of rock
1	1	Eclogite
2	2a	Eclogite
3	2b	Eclogite
4	3a	Granite gneiss
5	3b	Amphibolite
6	4	Granite
7	4a	Amphibolite
8	5	Garnet amphibolite
9	6	Granite
10	7a	Pelitic schist
11	7b	Eclogite
12	8a	Gabbro
13	8b	Pelitic schist

Table 2. A complete list of rock samples

4.1. Description of samples and outcrops during the field work

Location 1

There are eclogite rocks in this place. Location – Chaglinka. GPS locations are: 53.1657° N, 69.1242° E.

Location 2

This eclogite outcrop (Fig. 27 and 28) dips at an angle of about 40 degrees and is about 20 m long. Location – Chaglinka. GPS locations are: 53.1641° N, 69.1209° E.

Figure 27. Eclogite outcrop (Chaglinka, GK 2a)

Figure 28. Eclogite sample collected from the location

Location 3

This is a granite outcrop (Fig. 29). Rocks are highly fractured due to weathering. Granite is a coarse-grained intrusive igneous rock composed mostly of quartz, alkali feldspar, and plagioclase. It is light in color. Location – Zerendi District. GPS locations are: 53.1277° N, 69.4376° E

Figure 29. Granite outcrop (GK 3a)

Location 4

This is a granite outcrop (Fig. 30). Location – Kulet. GPS locations are: 53.0086° N, 69.5471° E

Figure 30. Granite outcrop

Location 5

Garnet amphibolite rocks contain coarse grains (Fig. 31). Location – Kulet. GPS locations are: 52.9881° N, 69.5402° E

Figure 31. Eclogite rocks

Location 6

This is a granite outcrop (Fig. 32). The rocks are light pink. Location – Karabulak. GPS locations are: 52.9264° N, 69.6206° E

Figure 32. Granite outcrop

Location 7a

The outcrop consists of pelitic schists (Fig. 33). Strike is N 40 W. Garnet crystals are big (porphyroblastic) (Fig. 34). There are eclogite rocks (Fig. 35). Pelitic schist is found next to eclogite. Rock is well foliated. Location – near Prirechnoye. GPS locations are: 53.1335° N, 69.0641° E

Figure 33. Pelitic schist outcrop (GK 7a)

Figure 34. Pelitic schist rock with garnet porphyroblasts (GK 7a)

Figure 35. Eclogite outcrop (GK 7b)

Location 8a

This is a gabbro outcrop (Fig. 36). Location - near Prirechnoye. GPS locations are: 53.1511° N, 69.0906° E

Figure 36. Gabbro outcrop (GK8a)

Location 8b

This is a pelitic schist outcrop (Fig. 37).

Figure 37. Pelitic schist outcrop (GK 8b)

4.2. Petrography of the selected garnet bearing samples

Of the 13 rock samples obtained during the field trip, we analyzed 8 thin sections under a microscope. The reason why they were chosen for analysis is that they all contain garnet. All samples were eclogites, except for GK 5 and 7a, which are garnet amphibolite and a pelitic schist, respectively.

GK 1

Figure 38 shows a microphotograph of GK 1. The mineral assemblage is Grt+Amph+Omph+Qtz. The sample mainly contains fine-grained minerals with a diameter of 0.2 to 1 mm. The rock has ameboid granoblastic texture which means that the crystals vary significantly in size are irregular. The mineral composition varies notably, the mode, percentage of each mineral present being roughly 40% garnet, 35% quartz, 15% omphacite, and 10% amphibole. Garnet has a subhedral shape, where grains are only partly bounded by crystal faces. Garnet grain size varies greatly, from very small to very large. The longest grain in the left is about 700 µm long and the widest grain in the top left corner is about 400 µm wide. The quartz grains also have a subhedral shape. The largest quartz grain is about 1 mm long and 600 µm wide. Omphacite also has a subhedral shape.

Part of it turned into amphibole. This means that rehydration has occurred, since amphibole belongs to the group of hydrous minerals. The length of the largest grain is about 500 µm. Garnet contains small inclusions of quartz and amphibole contains inclusions of garnet.

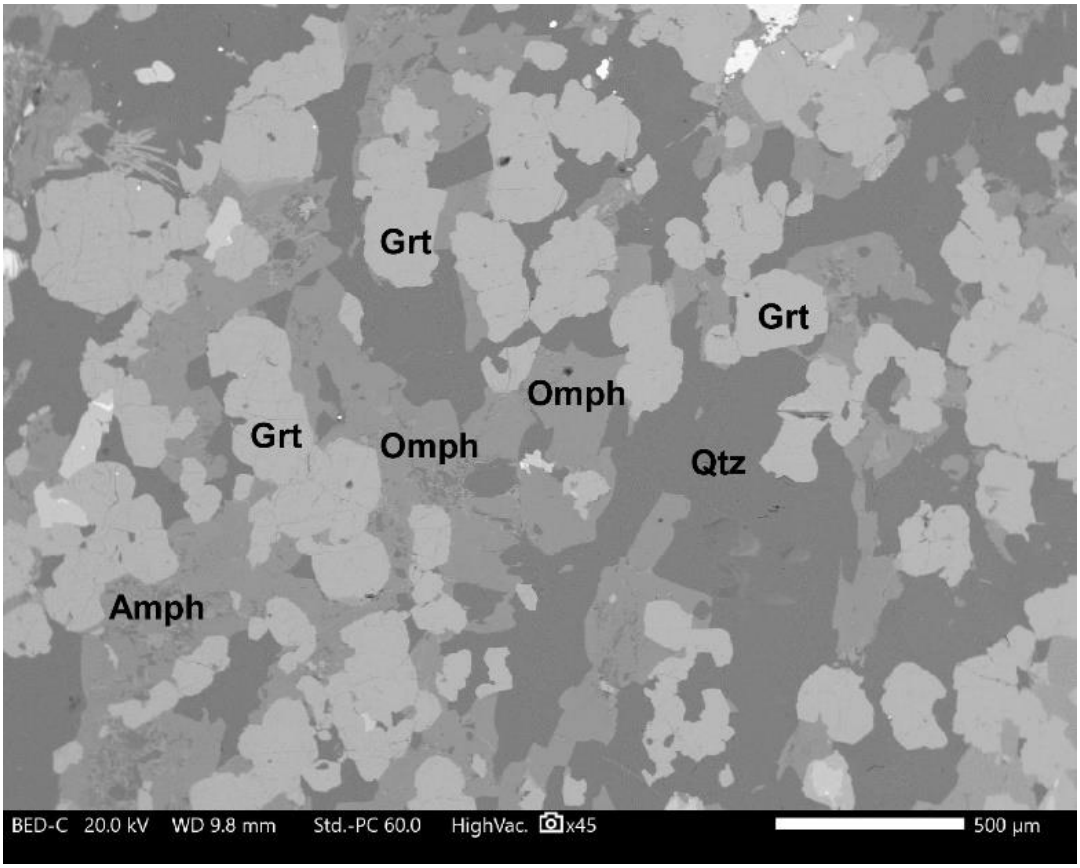

Figure 38. Back Scattered Electron image of sample GK 1

GK 2

Figure 39 shows a microphotograph of GK 2. The mineral assemblage is Grt+Amph+Omph+Qtz+Rt. The sample consists mainly of fine-grained grains with a diameter of 0.2 to 1 mm. The rock has ameboid granoblastic texture due to crystals that vary significantly in size and are irregular. The mineral composition of the sample is approximately the following: 40% omphacite, 30% quartz, 20% garnet, 5% amphibole and 5% rutile. Garnet has a subhedral shape. The grain size of the garnet varies. For example, there are tiny grains less than 0.1 mm long. The longest garnet grain, is over 0.4 mm. The grain at the bottom left is about 0.47 mm wide. Omphacite grains are surrounded by symplectite, a fine-grained intergrowth of several minerals that crystallized together and are usually the products of a metamorphic reaction during rapid exhumation. Most of the quartz occurs adjoining the omphacite grains. It has some small garnet inclusions. Rutile is present in small amounts and adjacent to garnet and omphacite grains. The longest rutile grain is about 0.32 mm long and 0.1 mm wide.

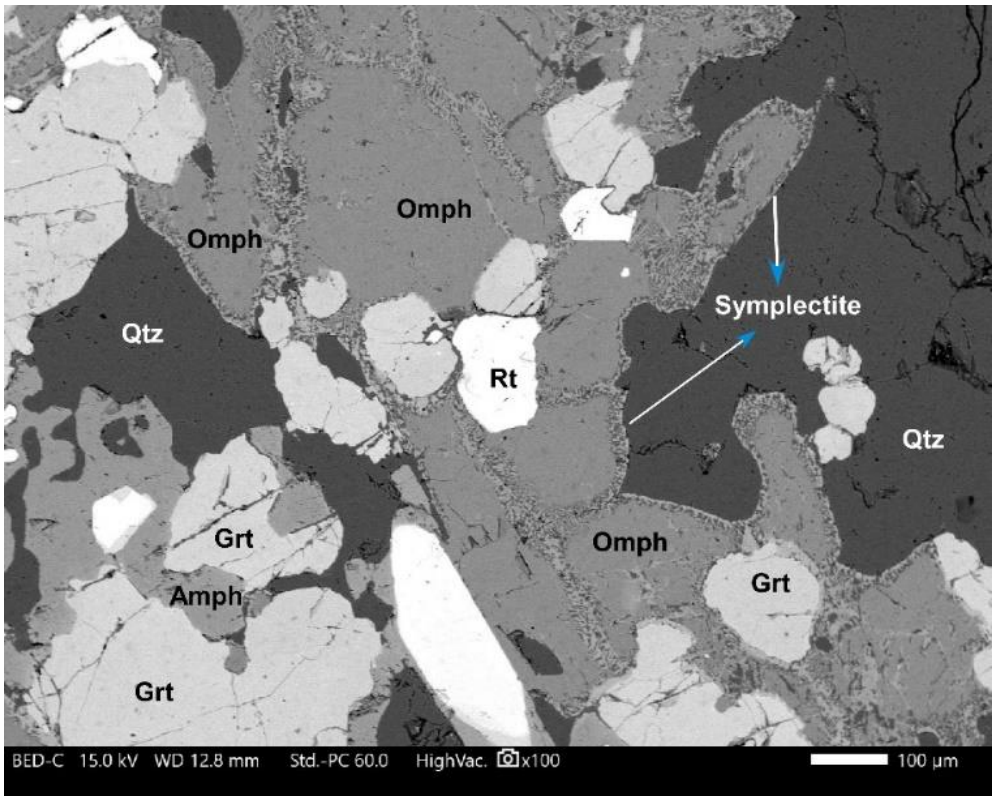

Figure 39. Back Scattered Electron image of sample GK 2

GK 2a

Figure 40 shows a microphotograph of GK 2a. The mineral assemblage is Grt+Qtz. The sample consists mainly of fine-grained grains with a diameter of 0.2 to 1 mm. Since the grains are basically all about the same size, it has a porphyroblastic texture. The sample is approximately 55% garnet, 40% symplectite, and 5% quartz. Garnet has a subhedral shape. The sizes of garnet grains in general do not vary much. The length of the longest grain is about 0.33 mm. The grain in the upper

part has a width of about 0.4 mm. Quartz is present in very small amounts and occur at the garnet grains boundary within the symplectite. Symplectite, occupies a vast area and surrounds garnet and quartz crystals.

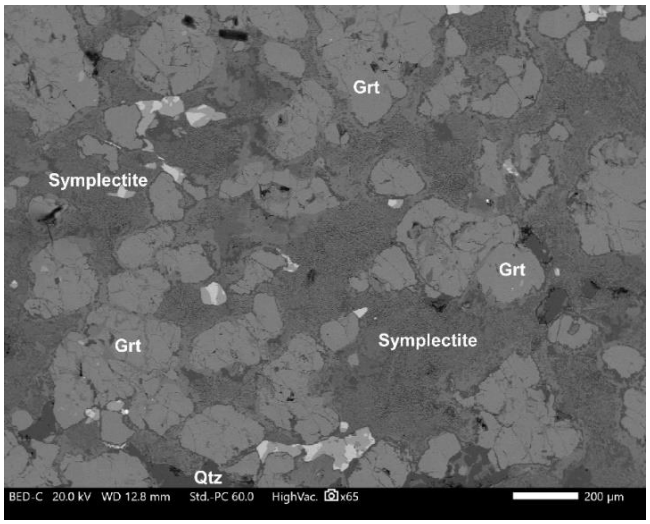

Figure 40. Back Scattered Electron image of sample GK 2a

GK 2b

Figure 41 shows a microphotograph of GK 2b. The mineral assemblage is Grt+Omph+Qtz+Rt. The sample consists mainly of garnet and omphacite grains with a diameter of 0.1 to 0.2 mm. Since the grains are basically all about the same size, it has a granoblastic texture. The sample is approximately 50% garnet, 45% omphacite, 3% rutile, and 2% quartz. Garnet has a subhedral shape. Rutile occurs at boundaries of garnet grains. Rutile minerals are euhedral because crystals are well developed with sharp, easily recognized faces. Small quartz inclusions are present inside omphacite grains.

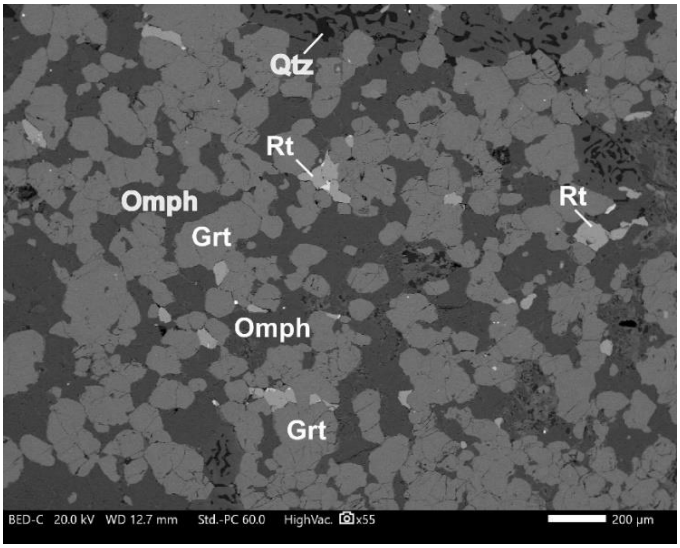

Figure 41. Back Scattered Electron image of sample GK 2b

GK 5

Figure 42 shows a microphotograph of GK 5. The mineral assemblage is Grt+Omph+Amph+Qtz. The sample consists mainly of fine-grained grains with a diameter of 0.2 to 1 mm. The rock is ameboid granoblastic texture due to crystals that vary significantly in size and are irregular. The approximate mineral composition of the sample is as follows: 45% amphibole, 40% garnet, 10% quartz and 5% omphacite. Garnet minerals have clearer and sharper geometric edges than in previous samples but still shows a subhedral shape. Omphacite grains are found as inclusions in amphibole. The length of the longest garnet grain is about 0.32 mm.

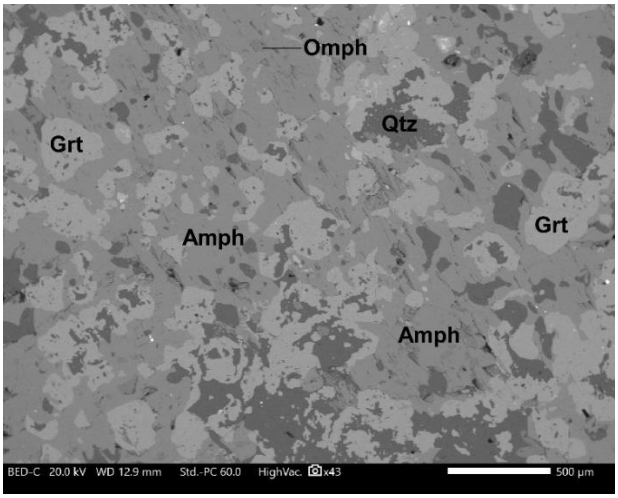

Figure 42. Back Scattered Electron image of sample GK 5

GK 7a

Figure 43 shows a microphotograph of GK 7a. The mineral assemblage is Grt+Phe+Qtz. The sample consists mainly of fine-grained grains with a diameter of 0.2 to 1 mm. The garnet grains appears as large porphyroblasts with a length 6 mm. The approximate mineral composition of the sample is as follows: 10% garnet, 60% quartz and 30% phengite mica. The phengite mica occur with the quartz as shown in the figure.

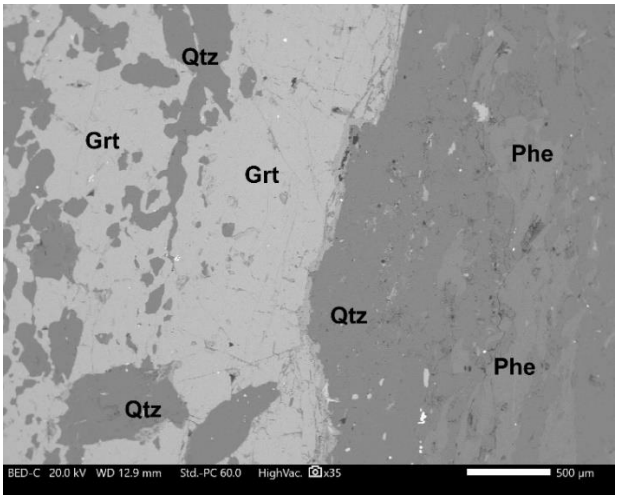

Figure 43. Back Scattered Electron image of sample GK 7a

GK 7b

Figure 44 shows a microphotograph of GK 7b. The mineral assemblage is Grt+Omph+Amph+Qtz. The sample consists mainly of fine-grained grains with a diameter of 0.2 to 1 mm. The rock ameboid granoblastic texture due to grains that vary significantly in size. The approximate mineral composition of the sample is as follows: 50% omphacite, 30% garnet, 15% amphibole and 5% quartz. Garnet has some flat crystal faces and therefore is considered to have a subhedral shape. The length of the longest grain, which is located in the center, is about 0.6 mm. Quartz grains are located inside the amphibole grains. Omphacite makes up most of the volume of the thin section.

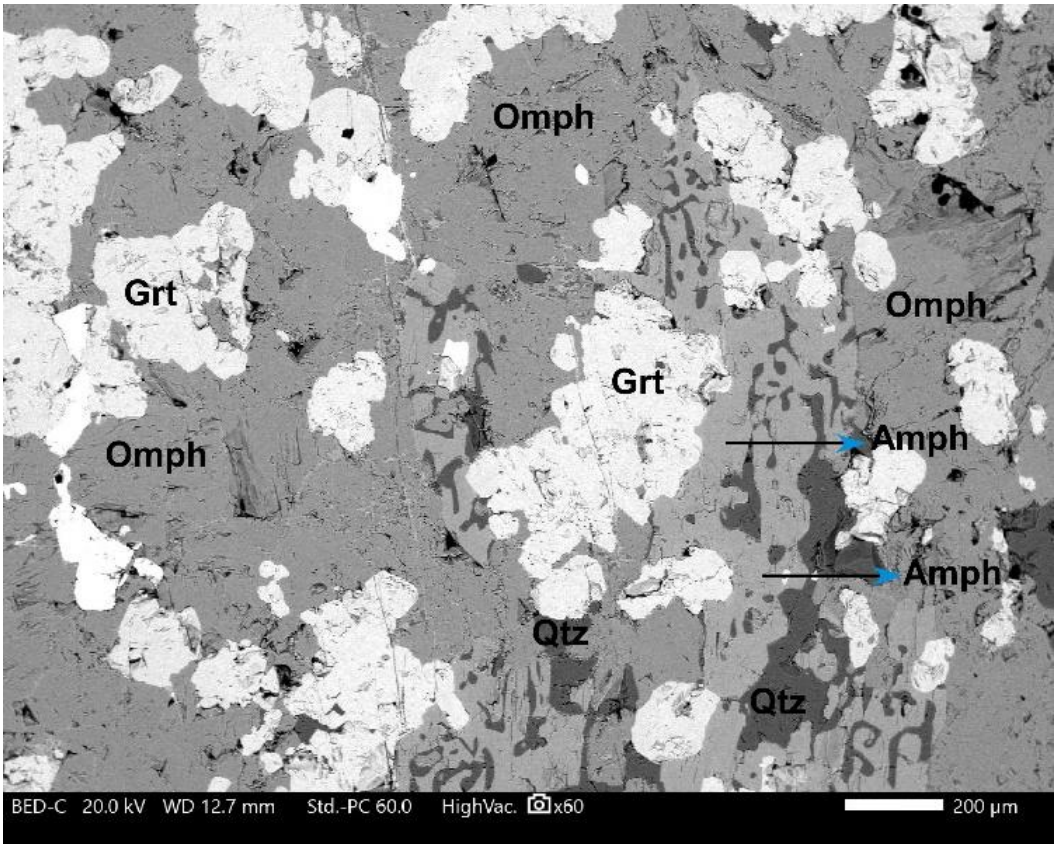

Figure 44. Back Scattered Electron image of sample GK 7b

GK 8a

Figure 45 shows a microphotograph of GK 8a. The mineral assemblage is Grt+Omph+Amph+Qtz+Rt. The sample consists mainly of fine-grained grains with a diameter of 0.2 to 1 mm. The rock has ameboid granoblastic texture due to grains that vary significantly in size. The approximate mineral composition of the sample is as follows: 50% omphacite, 25% quartz, 10% amphibole, 10% garnet and 5% rutile. Garnet has a subhedral shape. Garnet grains are mainly adjacent to omphacite. There are large quartz crystals. The length of the largest grain of omphacite is about 1.58 mm.

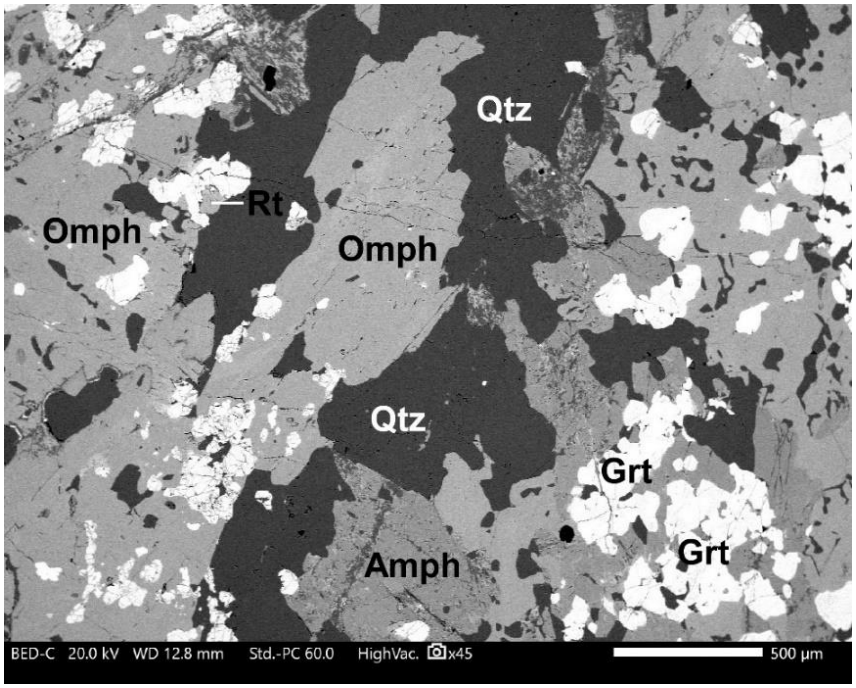

Figure 45. Back Scattered Electron image of sample GK 8a

4.3. Scanning Electron Microscope (SEM) analysis data

Please refer to the appendix to see the details of analyses and the data of each of the thin obtained through SEM-EDS technique. Only the major cation (Fe, Mg, Ca) obtained for the garnet analyses are shown in the tables below.

Tables 3-10 include data on the content of Mg, Fe and Ca cations and the *X* Fe values of each sample

GK 1

Cations	2	7	9	10	12
Mg	0.41	0.39	0.44	0.43	0.4
Fe	1.63	1.56	1.59	1.57	1.59
Ca	0.63	0.74	0.69	0.7	0.71
X Fe	0.799	0.8	0.783	0.785	0.799

Table 3. Mg, Fe and Ca cations and the *X* Fe= (Fe/Fe+Mg) values of garnets in sample GK 1

GK 2

Cations	2	5	8	10
Mg	0.54	0.71	0.55	0.52
Fe	1.3	1.34	1.24	1.34
Ca	0.8	0.56	0.83	0.85
X Fe	0.71	0.654	0.693	0.72

Table 4. Mg, Fe and Ca cations and the *X* Fe= (Fe/Fe+Mg) values of garnets in sample GK 2

GK 2a

Cations	1	5
Mg	0.67	0.54
Fe	1.48	1.35
Ca	0.61	0.89
X Fe	0.688	0.714

Table 5. Mg, Fe and Ca cations and the *X* Fe= (Fe/Fe+Mg) values of garnets in sample GK 2a

GK 2b

Cations	1	6
Mg	0.6	0.57
Fe	1.36	1.41
Ca	0.78	0.79
X Fe	0.694	0.712

Table 6. Mg, Fe and Ca cations and the *X* Fe= (Fe/Fe+Mg) values of garnets in sample GK 2b

GK 5

Cations	1	4	5	10
Mg	0.31	0.71	0.28	0.38
Fe	1.65	1.67	1.8	1.7
Ca	0.7	0.79	0.66	0.69
X Fe	0.842	0.843	0.865	0.817

Table 7. Mg, Fe and Ca cations and the *X* Fe= (Fe/Fe+Mg) values of garnets in sample GK 5

GK 7a

Cations	1	2	3
Mg	0.18	0.2	0.33
Fe	2.26	2.38	2.33
Ca	0.24	0.13	0.607
X Fe	0.926	0.922	0.876

Table 8. Mg, Fe and Ca cations and the *X* Fe= (Fe/Fe+Mg) values of garnets in sample GK 7a

GK 7b

Cations	1	4	3
Mg	0.62	0.58	0.58
Fe	1.32	1.36	1.34
Ca	0.82	0.84	0.88
X Fe	0.68	0.701	0.698

Table 9. Mg, Fe and Ca cations and the *X* Fe= (Fe/Fe+Mg) values of garnets in sample GK 7b

GK 8a

Cations	1	5
Mg	0.66	0.65
Fe	1.26	1.29
Ca	0.81	0.81
X Fe	0.656	0.665

Table 10. Mg, Fe and Ca cations and the *X* Fe= (Fe/Fe+Mg) values of garnets in sample GK 8a

5. Discussion

It is evident from the *X* Fe values presented in the tables (Tables 3-10) that the Fe content is varying with samples, although some of them are similar. Sample GK 1 *X* Fe values are very similar with values such as 0.799, 0.8, 0.783, 0.785 and 0.799 (Table 3). The *X* Fe values of sample GK 2 are less than in GK 1 i.e., of 0.71, 0.654, 0.693 and 0.72 (Table 4). The *X* Fe values of GK 2a and 2b are similar to GK 2 and equal to 0.688 and 0.714; 0.694 and 0.712, respectively. This may be due to the fact that rocks 2, 2a, and 2b were located close to each other in the field, as mentioned above on section 4. The *X* Fe values of GK 5 are greater than in the previous samples and equal to 0.842, 0.843, 0.865 and 0.817. However, the *X* Fe values of GK 7a are the highest among all samples and are equal to 0.926, 0.922 and 0.876. The *X* Fe values GK 7b are very similar to those in GK 2, 2a and 2b with values of 0.68, 0.701 and 0.698. Lastly, the *X* Fe values of GK 8a are the lowest among all the above samples and are equal to 0.656 and 0.665.

Figure 46 shows the variations in the garnet composition of all the analyzed samples.

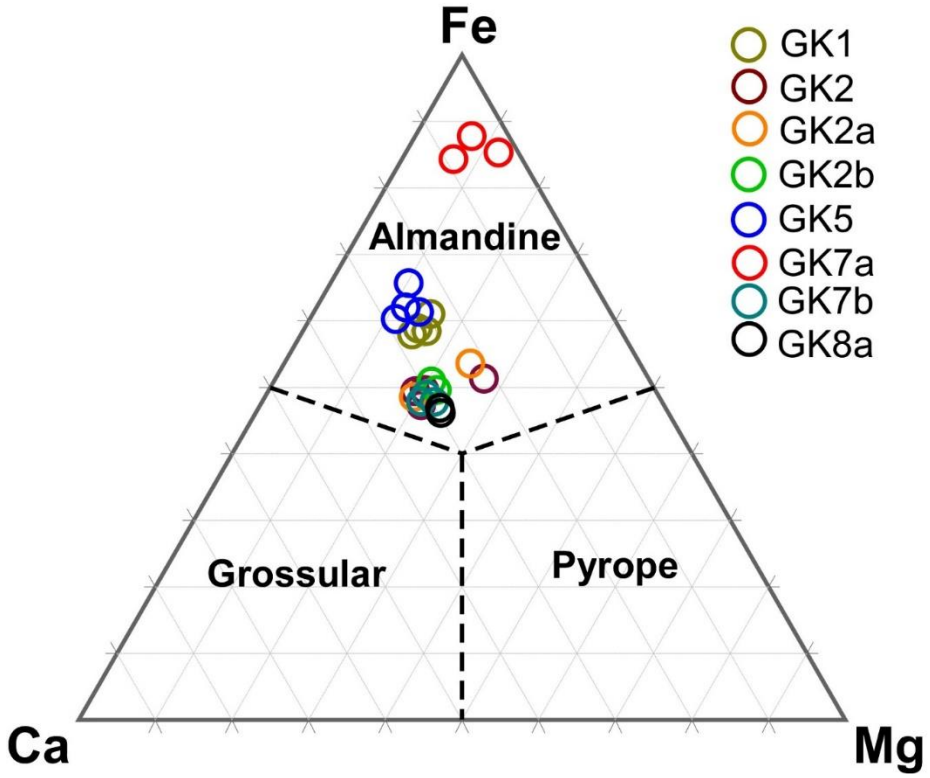

Figure 46. Triplot diagram for magnesium (Mg), calcium (Ca) and iron (Fe) in garnet of samples

The diagram shows that all garnet minerals of all samples belong to almandine, an iron rich variant of the garnet group, as discussed in section 2.5.2. In general, the garnet composition of all GK sample are similar in content (see the appendix). Almost all the samples have similar silica (39-41 Wt %) and Al content of ~ 22 Wt %. In case of Mg, Fe and Ca they are key cations the variations of which that decides the end members Pyrope, Almandine and Grossular, respectively. GK 1 and 5 have a similar composition in the almandine region. Most of the samples, namely GK 2, 2a, 2b, 7b, and 8a are located close to each other in the lower part of the almandine region in the diagram and therefore also have a similar mineral composition. As can be seen from the diagram, they contain a small amount of iron cations with values from 1.24 to 1.41. On the other hand, the magnesium and calcium content of these samples mentioned above are high. The calcium cationic values range from 0.56 to 0.89, the most common value being around 0.8. From each GK 2 and 2a, there is only one sample point with a relatively low calcium content (see table no). However, the most noteworthy fact is the elemental composition of the garnet in GK 7a sample is very different from other samples. Magnesium and calcium cations in GK 7a garnets are 0.33 and 0.24, respectively, which is very low compared to garnets of other samples. The sample points fall near to A-axis where Fe is 100%, which means that the iron content of the garnets is very high, and calcium and magnesium are very low compared to garnets in other GK samples. The average value of the Fe among the three sample points is 2.32, while the iron cations in other samples do not exceed 1.8. At the same time, the maximum content of magnesium and calcium cations in GK 7a garnets is 0.33 and 0.24, respectively, which is very low compared to garnets of other samples.

From the above discussion, it is evident that the composition of the garnet samples vary with samples esp. with Fe content, although there are samples with similar Fe content. As mentioned in the introduction the factors that determines the mineral composition are the physico-chemical conditions that prevails during the formation. All of the rock types included in this study have had experienced high-pressure metamorphism, and therefore it can be postulated that these rocks were affected by similar physical conditions i.e., pressure, temperature, as also mentioned in section 2. However, the depth of metamorphism could be different. Both eclogites/gabbro samples (GK 1, 2, 2a, 2b, 7b, 8a) and garnet amphibolite (GK 5) have been more deeper levels than the pelitic schist (phengite schist) GK 7a. The changes in the depth of metamorphism can be a fact that affect the garnet composition, as there is change in *P-T* conditions with increasing geothermal gradient. However, more than the physical conditions, the sharp variations in the Fe indicate towards differences in the source or in other words the protolith. The protolith bulk chemistry have a major role in the composition of the rocks or minerals. In this case, the eclogite, gabbro, or garnet amphibolite have a basaltic parentage and are hence formed out of magma. Basaltic magma are generally Mg rich when it is formed at the source and tend to get Fe rich as it get fractionated and rise towards the crust (see Keleman et al., 2016). Therefore, the source rock of eclogites or gabbro or the garnet amphibolite has a mixed source crustal and mantle source. However, the pelitic schist on the other hand is not only rich in Fe, also has considerable high amount of Al and K (in phengite mica) with less Ca and Mg. Such composition points towards a crustal source, rightly so as the pelites are originally clay. Therefore, the major element chemistry of garnet in the garnet bearing rocks indicates that rocks were formed in a setting with a mixed crustal and mantle source. In other words, the garnet composition of various rock types of the Kokchetav massif shows a crust-mantle interaction during their formation. What else can be a good indicator of subduction processes

where a dense, cold crustal plate (oceanic?) sinks into the mantle causing dehydration of the crustal plate and mantle melting? Our results hence endorses the previous studies that proposed subduction related magmatism and subsequent h-pressure metamorphism (see section 2.3.4). Our study therefore proves that major element composition of garnet reflects well its source like their trace element chemistry does, esp. in metamorphic rocks. If put together, both major element and trace element chemistry of garnet from various rocks could be a good indicator of source and the paleo crustal processes.

6. Conclusions and future directions

The objectives of this project included petrographic analysis of garnet bearing rocks using thin section and after compare the chemical composition of garnets in rock samples obtained during field work on the Kokchetav massif. While observing the thin sections under microscope, it was revealed that minerals such as garnet, omphacite, amphibole, quartz, phengite mica and rutile are present in various rock samples. The analyses using the SEM-EDS technique show that all garnets of all rock samples are more or less rich in iron and are therefore a member of a group of garnets called almandine. The most ferruginous among all the others are garnets in pelitic schist, represented by sample GK 7a. This means that the pelitic schist originated from a source with more crustal input than the other garnet bearing rocks that has basaltic parentage although rich in Fe indicated by almandine variety of garnet. Such mixed source points towards crust-mantle interaction which is best possible during subduction, as also proposed by previous studies from the region. This study also underscores the fact that major element chemistry of garnet can be a good indicator of the source of rocks esp. metamorphic rocks and could bring more insights to the crustal processes.

This study has several limitations such as lesser number sample were collected or studied from a large area like Kokchetav massif. Large number of sample from various locations will give a broad picture of garnet chemistry of the region. Another major limitation of this study is lack of a detailed analyses such as elemental mapping of the garnets, to understand zoning. Elemental map and profile on garnet chemistry is required for establishing *P-T-x* scenario of the garnet. The mineral chemistry required for this study was obtained using SEM-EDS technique. Although the technique yielded desired results, it is considered as an inferior technique when compared to Wave Dispersion Spectrometry (WDS), which has a high resolution compared to EDS as it is done without proper standardization. However, in the absence of WDS facility in NU, EDS was the only best and quicker method. In future, these thin sections will be analyzed using WDS given the opportunity comes within Kazakhstan or elsewhere. It is also proposed to study the mineral composition using LA-ICP-MS technique in thin sections which is best technique available to determine the trace element composition of garnet. Moreover, the whole rock composition of these rocks is also necessary to unravel the source and originals setting of these rocks, which could be done in the near future, with the availability of facility and after development of protocol including standardization.

7. References

- Geological Society - Metamorphism. (n.d.). Www.geolsoc.org.uk. https://www.geolsoc.org.uk/ks3/gsl/education/resources/rockcycle/page3576.html

- Clarke, G. L., Daczko, N. R., & Miescher, D. (2013). Identifying Relic Igneous Garnet and Clinopyroxene in Eclogite and Granulite, Breaksea Orthogneiss, New Zealand. *Journal of Petrology, 54*(9), 1921–1938. https://doi.org/10.1093/petrology/egt036

- Schertl, H.-P. ., & Sobolev, N. V. (2013). The Kokchetav Massif, Kazakhstan: "Type locality" of diamond-bearing UHP metamorphic rocks. *Journal of Asian Earth Sciences, 63*, 5–38. https://doi.org/10.1016/j.jseaes.2012.10.032

- Dobretsov, N. L., Buslov, M. M., & Vernikovsky, V. A. (2003). Neoproterozoic to Early Ordovician Evolution of the Paleo-Asian Ocean: Implications to the Break-up of Rodinia. *Gondwana Research, 6*(2), 143–159. https://doi.org/10.1016/s1342-937x(05)70966-7
- Windley, B. F., Alexeiev, D., Xiao, W., KrönerA., & Badarch, G. (2007). Tectonic models for accretion of the Central Asian Orogenic Belt. *Journal of the Geological Society, 164*(1), 31–47. https://doi.org/10.1144/0016-76492006-022
- Buslov, M. M., Fujiwara, Y., Iwata, K., & Semakov, N. N. (2004). Late Paleozoic-Early Mesozoic Geodynamics of Central Asia. *Gondwana Research, 7*(3), 791–808. https://doi.org/10.1016/s1342-937x(05)71064-9
- Buslov, M. M. (2011). Tectonics and geodynamics of the Central Asian Foldbelt: the role of Late Paleozoic large-amplitude strike-slip faults. *Russian Geology and Geophysics, 52*(1), 52–71. https://doi.org/10.1016/j.rgg.2010.12.005
- Glorie, S., De Grave, J., Buslov, M. M., Zhimulev, F. I., Izmer, A., Vandoorne, W., Ryabinin, A., Van den haute, P., Vanhaecke, F., & Elburg, M. A. (2011a). Formation and Palaeozoic evolution of the Gorny-Altai–Altai-Mongolia suture zone (South Siberia): Zircon U/Pb constraints on the igneous record. *Gondwana Research, 20*(2-3), 465–484. https://doi.org/10.1016/j.gr.2011.03.003
- Dobretsov, N. L., Sobolev, N. V., Shatsky, V. S., Coleman, R. G., & Ernst, W. G. (1995). Geotectonic evolution of diamondiferous paragneisses, Kokchetav Complex, northern Kazakhstan: The geologic enigma of ultrahigh-pressure crustal rocks within a Paleozoic foldbelt. *The Island Arc, 4*(4), 267–279. https://doi.org/10.1111/j.1440-1738.1995.tb00149.x
- Ernst, W. G., Liou, J. G., & Coleman, R. G. (1995). Comparative Petrotectonic Study of Five Eurasian Ultrahigh-Pressure Metamorphic Complexes. *International Geology Review, 37*(3), 191–211. https://doi.org/10.1080/00206819509465400
- Kaneko, Y., Maruyama, S., Terabayashi, M., Yamamoto, H., Ishikawa, M., Anma, R., Parkinson, C. D., Ota, T., Nakajima, Y., Katayama, I., Yamamoto, J., & Yamauchi, K. (2000). Geology of the Kokchetav UHP-HP metamorphic belt, Northern Kazakhstan. *The Island Arc, 9*(3), 264–283. https://doi.org/10.1046/j.1440-1738.2000.00278.x

- Sobolev, N. V., & Shatsky, V. S. (1990). Diamond inclusions in garnets from metamorphic rocks: a new environment for diamond formation. *Nature*, *343*(6260), 742–746. https://doi.org/10.1038/343742a0
- Zhang, R. Y., Liou, J. G., Ernst, W. G., Coleman, R. G., Sobolev, N. V., & Shatsky, V. S. (1997). Metamorphic evolution of diamond-bearing and associated rocks from the Kokchetav Massif, northern Kazakhstan. Journal of Metamorphic Geology, 15(4), 479–496. https://doi.org/10.1111/j.1525-1314.1997.00035.x
- Letnikov, F. A. (1983). Diamond origin in deep-seated tectonic zones. Doklady Akademii Nauk SSSR, 271, 433-435.
- Lavrova, L. D. (1991). New type of diamond deposits. Priroda, 12, 62-68.
- Ekimova, T. E. (1992). Diamond inclusions in rock-forming minerals of metamorphic rocks. In Doklady Akademiya Nauk (Vol. 322, pp. 366-368).
- Lavrova, L. D., Petchnikov, V. A., Petrova, M. A., Ekimova, T. E., & Nadezhdina, E. D. (1995, September). New genetic type of diamond deposits-geological peculiarities and origin. In International Kimberlite Conference: Extended Abstracts (Vol. 6, pp. 311-313).
- Maruyama, S., Isozaki, Y., Kimura, G., & Terabayashi, M. (1997). Paleogeographic maps of the Japanese Islands: Plate tectonic synthesis from 750 Ma to the present. *The Island Arc*, *6*(1), 121–142. https://doi.org/10.1111/j.1440-1738.1997.tb00043.x
- Ishikawa, M. (1998). Structures of ultra-high pressure terrain: Sulu-Tube, Kokchetav, Kazakhstan. EOS Transactions of the American Geophysical Union, 79, F983.
- Kaneko, Y. (1998). Geology of the eastern Kokchetav metamorphic belt, northern Kazakhstan. EOS Transactions of the American Geophysical Union, 79, F983.
- Jagoutz, E. (1990). Sr-Nd-Pb isotopic study of ultrahigh PT rocks from Kokchetav massif. EOS Transactions of the American Geophysical Union, 71, 1707.
- Claoué-Long, J. C., Sobolev, N. V., Shatsky, V. S., & Sobolev, A. V. (1991). Zircon response to diamond-pressure metamorphism in the Kokchetav massif, USSR. Geology, 19(7), 710-713. https://doi.org/2.3.co;2%22%3E10.1130/0091-7613(1991)019%3C0710:zrtdpm%3E2.3.co;2
- Shatsky, V. S. (1993). The age and origin of eclogites from Kokchetav massif, North Kazakhstan. Geologiya i Geofizika, 34, 47-58.
- Okamoto, K., & Maruyama, S. (1998). Multi-anvil re-equilibration experiments of a Dabie Shan ultrahigh-pressure eclogite within the diamond-stability fields. *The Island Arc*, *7*(1-2), 52–69. https://doi.org/10.1046/j.1440-1738.1998.00179.x
- Desmons, J. and Smulikowski, W. (2007). A systematic nomenclature for metamorphic rocks: 4. High P/T metamorphic rocks. In: Douglas F and Desmons J (eds.) Metamorphic Rocks: A Classification and Glossary of Terms: Recommendations of the International Union of Geological Sciences Subcommission on the Systematics of Metamorphic Rocks, pp. 32–35. New York: Cambridge University Press.
- Tsujimori, T., & Mattinson, C. (2021). Eclogites in Different Tectonic Settings. *Encyclopedia of Geology*, 561–568. https://doi.org/10.1016/b978-0-08-102908-4.00104-1

- Coleman, R. G., Lee, D. E., Beatty, L. B., & Brannock, W. W. (1965). Eclogites and Eclogites: Their Differences and Similarities. *Geological Society of America Bulletin, 76*(5), 483. https://doi.org/10.1130/0016-7606(1965)76[483:eaetda]2.0.co;2
- D. C. Smith, "Eclogites and Eclogite Facies Rocks," Elsevier Science, New York, 1988, p. 524. Scientific Research Publishing. (n.d.). Scirp.org. https://scirp.org/reference/referencespapers.aspx?referenceid=1102735
- Carswell DA. (1990). Eclogites and eclogite facies: Definitions and classifications. In: Carswell DA (ed.) Eclogite Facies Rocks, pp. 1–13. New York: Blackie and Son Ltd.
- Coleman RG and Wang X (eds.). (1995). Ultrahigh Pressure Metamorphism. Cambridge: Cambridge University Press, 540.
- Agard, P., Yamato, P., Jolivet, L., & Burov, E. (2009). Exhumation of oceanic blueschists and eclogites in subduction zones: Timing and mechanisms. *Earth-Science Reviews, 92*(1-2), 53–79. https://doi.org/10.1016/j.earscirev.2008.11.002
- Wang, Y., Zhang, L., Li, Z., Li, Q., & Bader, T. (2019). The Exhumation of Subducted Oceanic-Derived Eclogites: Insights From Phase Equilibrium and Thermomechanical Modeling. *Tectonics, 38*(5), 1764–1797. https://doi.org/10.1029/2018tc005349
- Ernst, W. G. (2001). Subduction, ultrahigh-pressure metamorphism, and regurgitation of buoyant crustal slices — implications for arcs and continental growth. *Physics of the Earth and Planetary Interiors, 127*(1-4), 253–275. https://doi.org/10.1016/s0031-9201(01)00231-x
- Gerya, T. V., Perchuk, L. L., & Burg, J.-P. . (2008). Transient hot channels: Perpetrating and regurgitating ultrahigh-pressure, high-temperature crust–mantle associations in collision belts. *Lithos, 103*(1-2), 236–256. https://doi.org/10.1016/j.lithos.2007.09.017
- Rubatto, D., Regis, D., Hermann, J., Boston, K., Engi, M., Beltrando, M., & McAlpine, S. R. B. (2011). Yo-yo subduction recorded by accessory minerals in the Italian Western Alps. *Nature Geoscience, 4*(5), 338–342. https://doi.org/10.1038/ngeo1124
- Tappert R and Tappert MC. (2011). Diamonds in Nature: A Guide to Rough Diamonds. Springer Science & Business Media.
- Wirth, R., & Rocholl, A. (2003). Nanocrystalline diamond from the Earth's mantle underneath Hawaii. Earth and Planetary Science Letters, 211(3-4), 357–369. https://doi.org/10.1016/s0012-821x(03)00204-8
- Carswell DA. (1990). Eclogites and eclogite facies: Definitions and classifications. In: Carswell DA (ed.) Eclogite Facies Rocks, pp. 1–13. New York: Blackie and Son Ltd.
- Alderton, D. (2021). Garnets. *Encyclopedia of Geology*, 350-357. https://doi.org/10.1016/B978-0-08-102908-4.00172-7
- Garnet. (n.d.). Geology - rocks and minerals. https://rocksminerals.flexiblelearning.auckland.ac.nz/minerals/garnet.html#:~:text=Garnet%20is%20commonly%20found%20in,particular%20garnet%2Dbearing%20rock%20formed.

- King, H. M. (2012). *Garnet: a mineral, a gem, an abrasive, a filter and more!* Geology.com https://geology.com/minerals/garnet.shtml
- Klein, C; Hurlbut, C.D. (1985). Manual of Mineralogy. New York: John Wiley and Sons. pp. 375–378.

Appendix

GK 1
Garnet

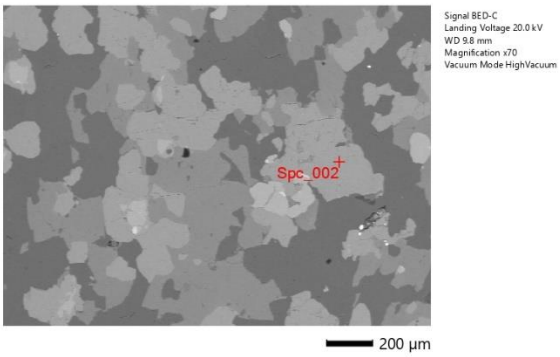

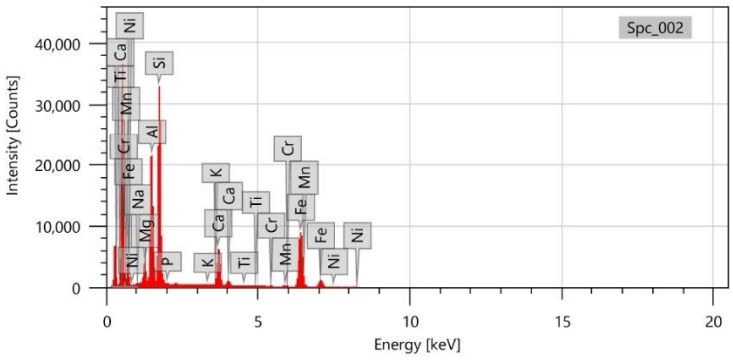

Items	Value
measurement conditions	
Acceleration voltage	20.00 kV
Probe current	-
Magnification	x 70
Process time	T3
Measurement detector	First
Live time	30.00 seconds
Real time	38.95 seconds
Dead time	23.00 %
Count rate	49425.00 CPS

Display name	Standard data	Quantification method	Result Type
Spc_002	Standardless	ZAF	Oxide (Number of oxygen 12)

Chemical formula	Line	Mass%	Mol%	Cations
O	K			
Na2O	K	0.24±0.02	0.27±0.02	0.04
MgO	K	3.57±0.03	6.00±0.06	0.41
Al2O3	K	22.29±0.08	14.81±0.05	2.03
SiO2	K	40.08±0.11	45.19±0.13	3.09
P2O5	K	0.24±0.02	0.12±0.01	0.02
K2O	K	nd	nd	-
CaO	K	7.61±0.04	9.20±0.05	0.63
TiO2	K	0.07±0.01	0.06±0.01	0.00
Cr2O3	K	0.10±0.01	0.04±0.01	0.01
MnO	K	0.54±0.02	0.52±0.02	0.04
FeO	K	25.25±0.09	23.80±0.09	1.63
NiO	K	nd	nd	-
Total		100.00	100.00	
Spc_002				Fitting ratio 0.3281

Figure 47. SEM-EDS analysis data of garnet

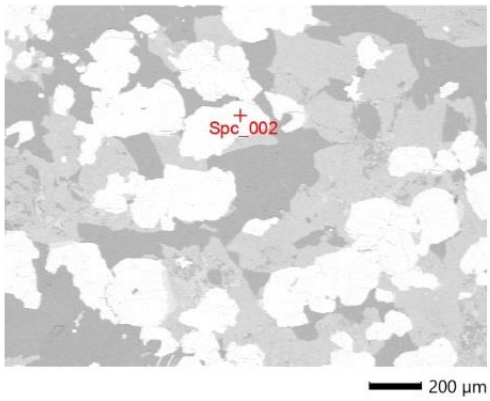

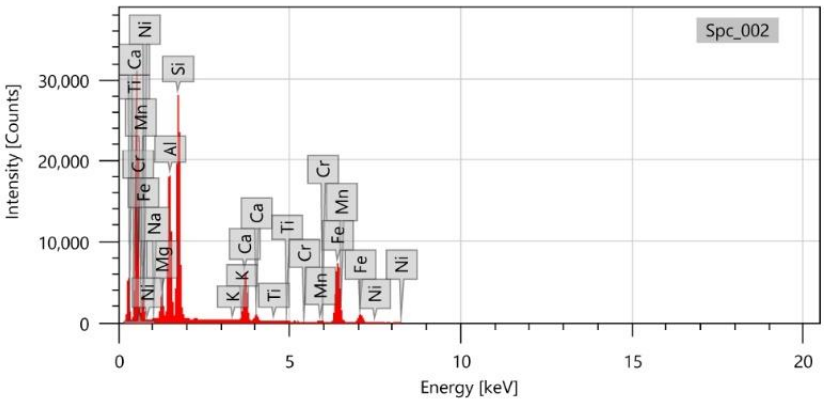

Items	Value
measurement conditions	
Acceleration voltage	20.00 kV
Probe current	-
Magnification	x 70
Process time	T3
Measurement detector	First
Live time	30.00 seconds
Real time	37.49 seconds
Dead time	20.00 %
Count rate	41584.00 CPS

Display name	Standard data	Quantification method	Result Type
Spc_002	Standardless	ZAF	Oxide (Number of oxygen 12)

Chemical formula	Line	Mass%	Mol%	Cations
O	K			
Na2O	K	0.18±0.02	0.20±0.02	0.03
MgO	K	3.41±0.04	5.70±0.06	0.39
Al2O3	K	22.06±0.08	14.59±0.06	2.00
SiO2	K	40.42±0.12	45.35±0.14	3.11
K2O	K	nd	nd	-
CaO	K	8.95±0.05	10.76±0.06	0.74
TiO2	K	0.17±0.01	0.14±0.01	0.01
Cr2O3	K	0.05±0.01	0.02±0.01	0.00
MnO	K	0.49±0.02	0.46±0.02	0.03
FeO	K	24.21±0.10	22.72±0.09	1.56
NiO	K	0.06±0.02	0.06±0.01	0.00
Total		100.00	100.00	
Spc_002				Fitting ratio 0.3258

Figure 48. SEM-EDS analysis data of garnet

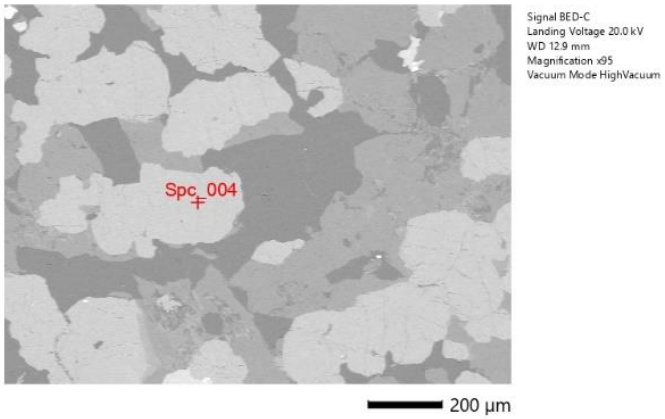

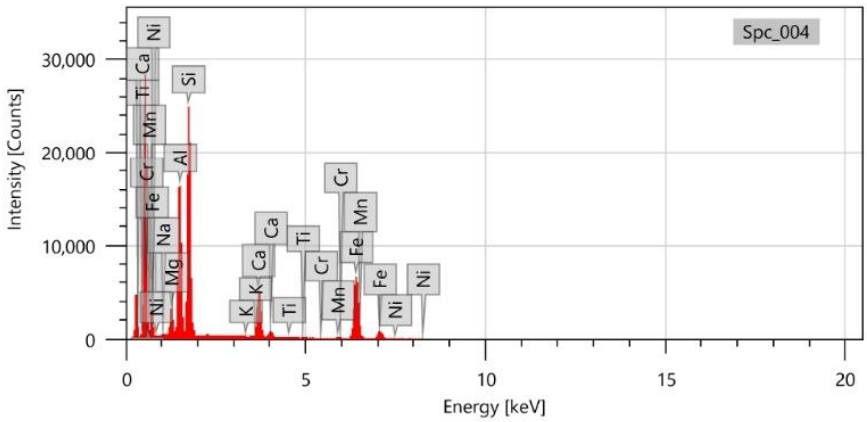

Items	Value
measurement conditions	
Acceleration voltage	20.00 kV
Probe current	-
Magnification	x 95
Process time	T3
Measurement detector	First
Live time	30.00 seconds
Real time	36.66 seconds
Dead time	18.00 %
Count rate	37287.00 CPS

Display name	Standard data	Quantification method	Result Type
Spc_004	Standardless	ZAF	Oxide (Number of oxygen 12)

Chemical formula	Line	Mass%	Mol%	Cations
O	K			
Na2O	K	0.26±0.02	0.28±0.02	0.04
MgO	K	3.79±0.04	6.34±0.07	0.44
Al2O3	K	22.28±0.09	14.73±0.06	2.02
SiO2	K	40.02±0.13	44.90±0.14	3.09
K2O	K	nd	nd	-
CaO	K	8.30±0.05	9.98±0.06	0.69
TiO2	K	0.25±0.02	0.21±0.01	0.01
Cr2O3	K	0.02±0.01	0.01±0.01	0.00
MnO	K	0.49±0.02	0.47±0.02	0.03
FeO	K	24.59±0.10	23.07±0.10	1.59
NiO	K	nd	nd	-
Total		100.00	100.00	
Spc_004				Fitting ratio 0.3262

Figure 49. SEM-EDS analysis data of garnet

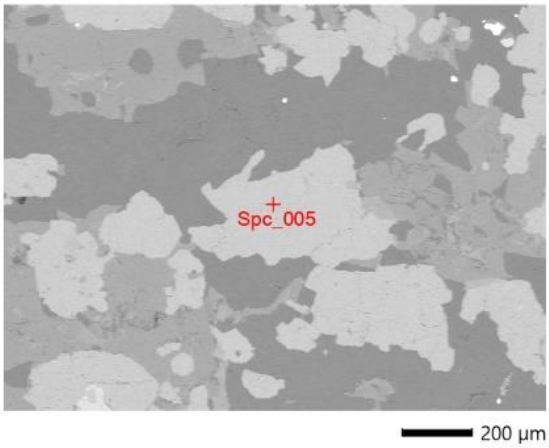

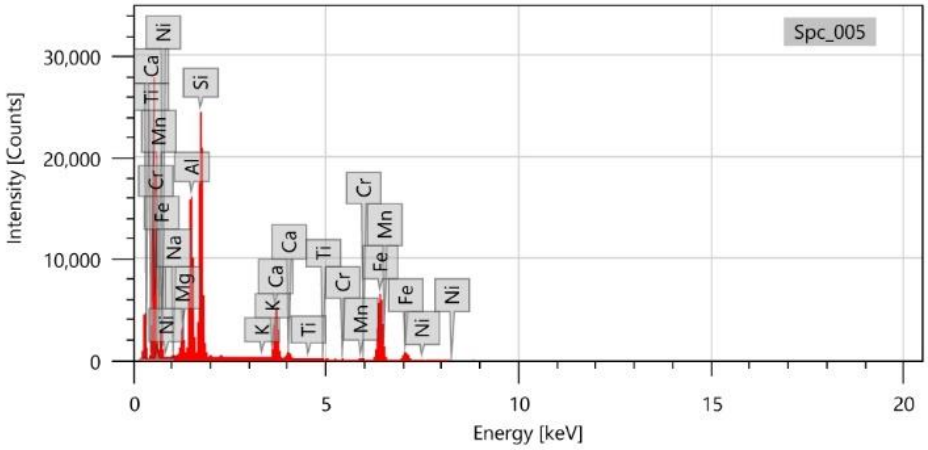

Items	Value
measurement conditions	
Acceleration voltage	20.00 kV
Probe current	-
Magnification	x 85
Process time	T3
Measurement detector	First
Live time	30.00 seconds
Real time	36.61 seconds
Dead time	18.00 %
Count rate	36780.00 CPS

Display name	Standard data	Quantification method	Result Type
Spc_005	Standardless	ZAF	Oxide (Number of oxygen 12)

Chemical formula	Line	Mass%	Mol%	Cations
O	K			
Na2O	K	0.21±0.02	0.23±0.02	0.03
MgO	K	3.75±0.04	6.27±0.07	0.43
Al2O3	K	22.21±0.09	14.68±0.06	2.02
SiO2	K	40.18±0.13	45.07±0.15	3.10
K2O	K	nd	nd	-
CaO	K	8.48±0.05	10.19±0.06	0.70
TiO2	K	0.08±0.01	0.07±0.01	0.00
Cr2O3	K	0.09±0.01	0.04±0.01	0.01
MnO	K	0.52±0.02	0.49±0.02	0.03
FeO	K	24.40±0.10	22.89±0.10	1.57
NiO	K	0.08±0.02	0.08±0.02	0.01
Total		100.00	100.00	
Spc_005				Fitting ratio 0.3232

Figure 50. SEM-EDS analysis data of garnet

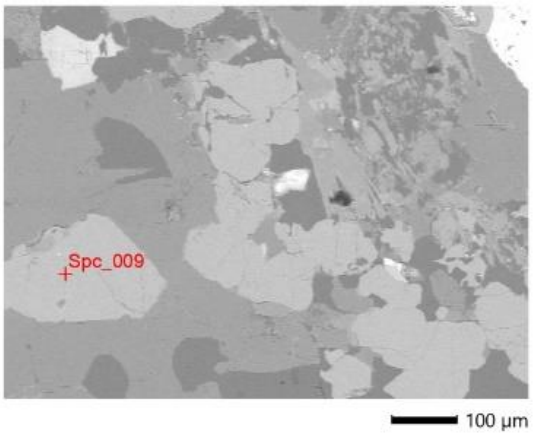

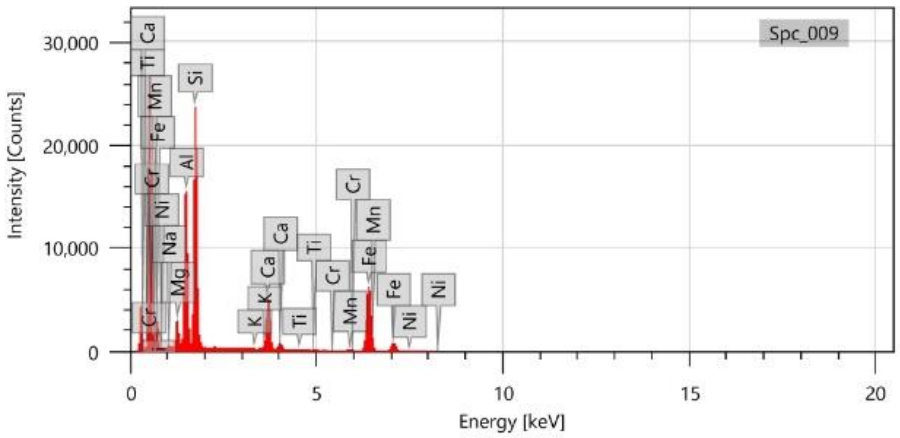

Items	Value
measurement conditions	
Acceleration voltage	20.00 kV
Probe current	-
Magnification	x 160
Process time	T3
Measurement detector	First
Live time	30.00 seconds
Real time	36.28 seconds
Dead time	17.00 %
Count rate	35109.00 CPS

Display name	Standard data	Quantification method	Result Type
Spc_009	Standardless	ZAF	Oxide (Number of oxygen 12)

Chemical formula	Line	Mass%	Mol%	Cations
O	K			
Na2O	K	0.25±0.02	0.27±0.02	0.04
MgO	K	3.63±0.04	6.07±0.07	0.42
Al2O3	K	22.13±0.09	14.64±0.06	2.01
SiO2	K	40.03±0.13	44.93±0.15	3.09
K2O	K	nd	nd	-
CaO	K	8.55±0.05	10.28±0.06	0.71
TiO2	K	0.13±0.01	0.11±0.01	0.01
Cr2O3	K	0.11±0.02	0.05±0.01	0.01
MnO	K	0.52±0.02	0.49±0.02	0.03
FeO	K	24.64±0.11	23.13±0.10	1.59
NiO	K	0.02±0.02	0.02±0.02	0.00
Total		100.00	100.00	
Spc_009				Fitting ratio 0.3228

Figure 51. SEM-EDS analysis data of garnet

Omphacite

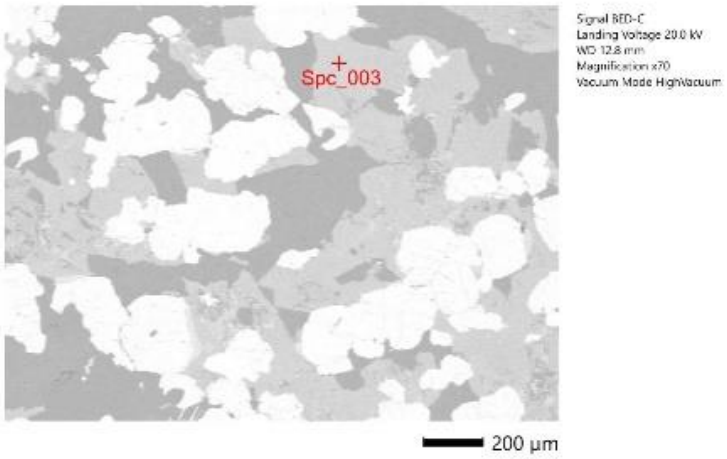

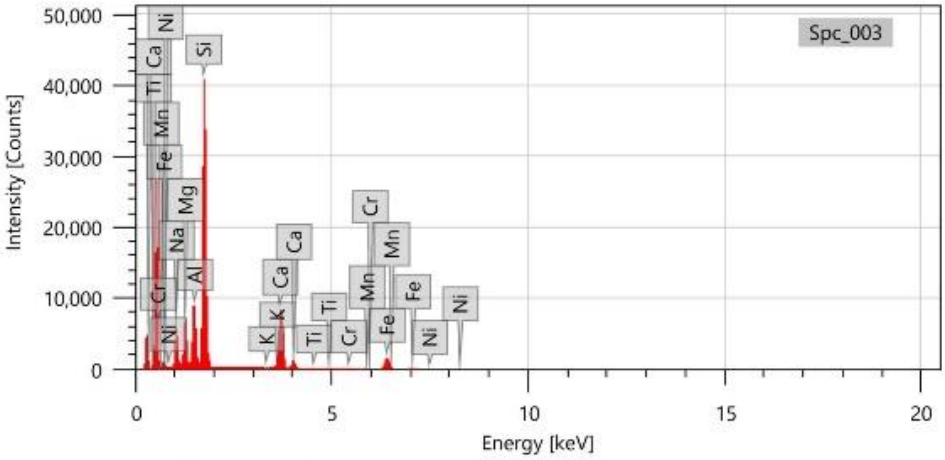

Items	Value
measurement conditions	
Acceleration voltage	20.00 kV
Probe current	-
Magnification	x 70
Process time	T3
Measurement detector	First
Live time	30.00 seconds
Real time	36.90 seconds
Dead time	19.00 %
Count rate	39373.00 CPS

Display name	Standard data	Quantification method	Result Type
Spc_003	Standardless	ZAF	Oxide (Number of oxygen 6)

Chemical formula	Line	Mass%	Mol%	Cations
O	K			
Na2O	K	6.89±0.05	6.74±0.05	0.48
MgO	K	7.76±0.05	11.66±0.07	0.41
Al2O3	K	10.52±0.06	6.25±0.04	0.44
SiO2	K	55.80±0.14	56.26±0.14	2.00
K2O	K	nd	nd	-
CaO	K	13.17±0.06	14.22±0.06	0.50
TiO2	K	0.16±0.01	0.12±0.01	0.00
Cr2O3	K	0.12±0.01	0.05±0.01	0.00
MnO	K	0.02±0.01	0.01±0.01	0.00
FeO	K	5.53±0.05	4.66±0.04	0.17
NiO	K	0.03±0.01	0.03±0.01	0.00
Total		100.00	100.00	
Spc_003				Fitting ratio 0.3293

Figure 52. SEM-EDS analysis data of omphacite

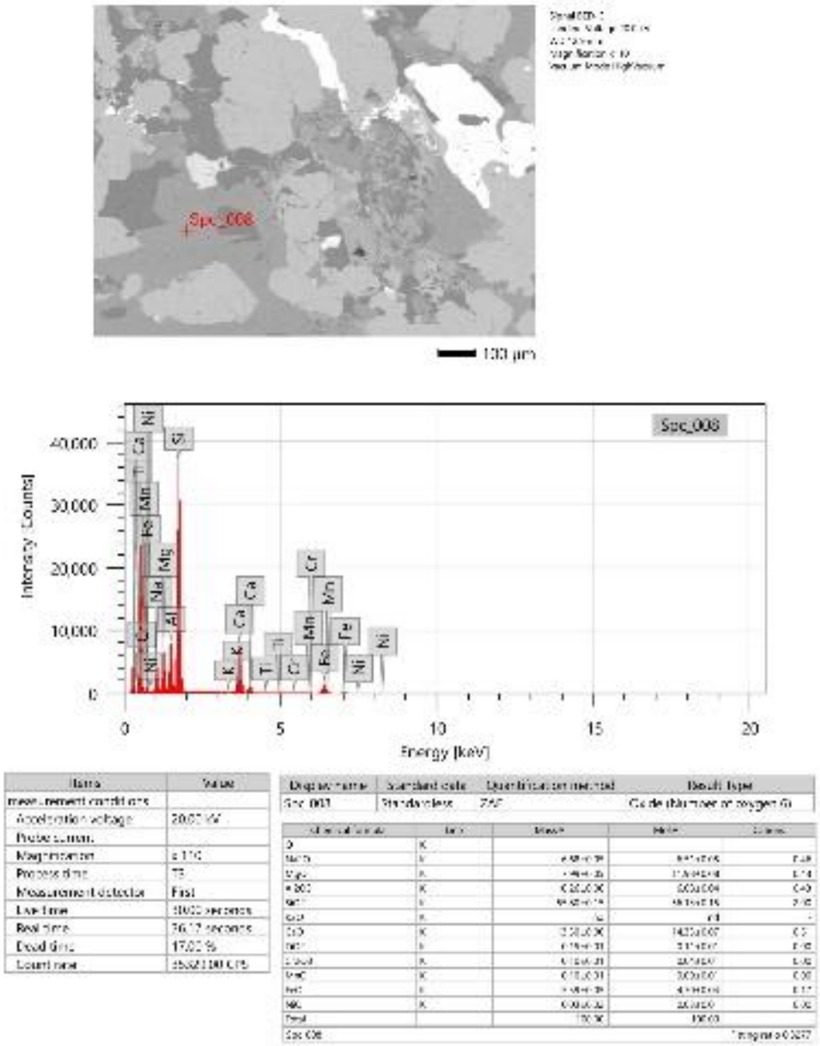

Figure 53. SEM-EDS analysis data of omphacite

Amphibole

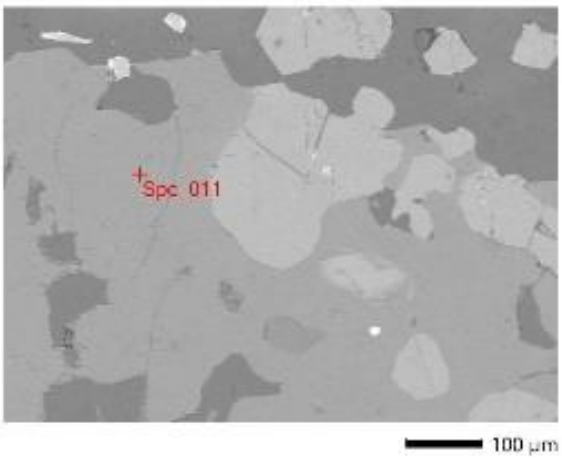

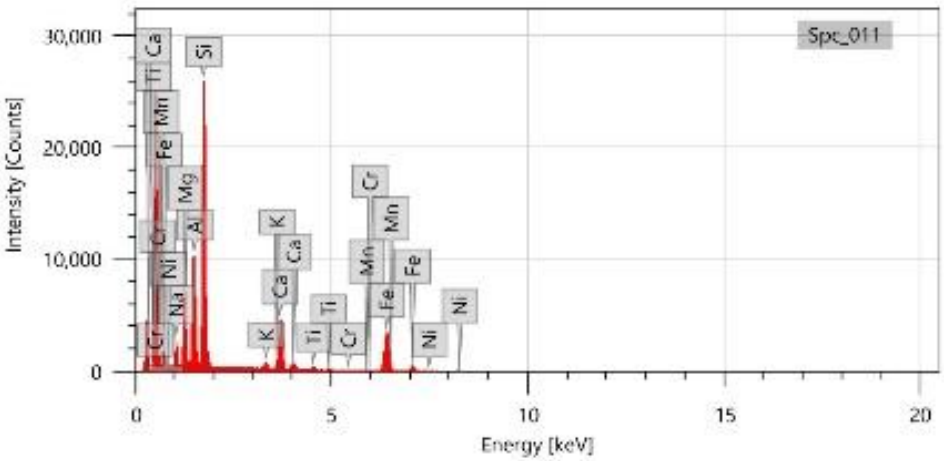

Items	Value
measurement conditions	
Acceleration voltage	20.00 kV
Probe current	
Magnification	x 180
Process time	T3
Measurement detector	First
Live time	30.00 seconds
Real time	35.76 seconds
Dead time	16.00 %
Count rate	32795.000 CPS

Display name	Standard data	Quantification method	Result Type
Spc_011	Standardless	ZAF	Oxide (Number of oxygen 22)

Chemical formula	Line	Mass%	Mol%	Cations
O	K			
Na2O	K	3.96±0.04	4.00±0.04	1.05
MgO	K	9.02±0.06	15.24±0.10	2.00
Al2O3	K	15.09±0.06	9.03±0.05	1.33
SiO2	K	45.82±0.14	47.71±0.15	6.26
K2O	K	0.73±0.02	0.49±0.01	0.13
CaO	K	9.61±0.06	9.01±0.06	1.26
TiO2	K	0.77±0.03	0.60±0.02	0.08
Cr2O3	K	n.d.	n.d.	-
MnO	K	0.08±0.02	0.07±0.01	0.01
FeO	K	14.50±0.09	12.63±0.07	1.66
NiO	K	0.01±0.02	0.01±0.01	0.00
Total		100.00	100.00	

Spc_011 Fitting ratio 0.7496

Figure 54. SEM-EDS analysis data of amphibole

GK 2
Garnet

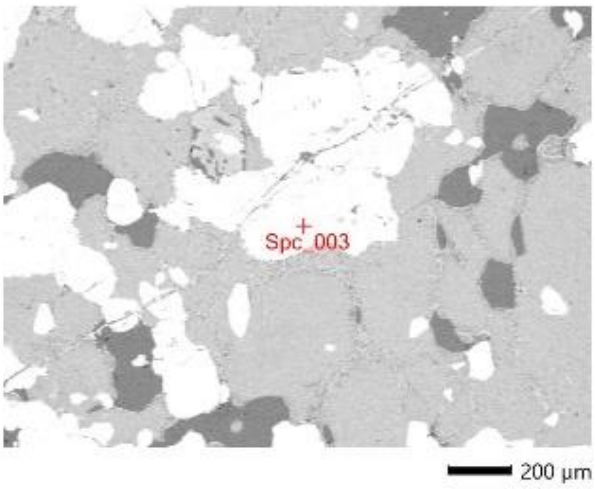

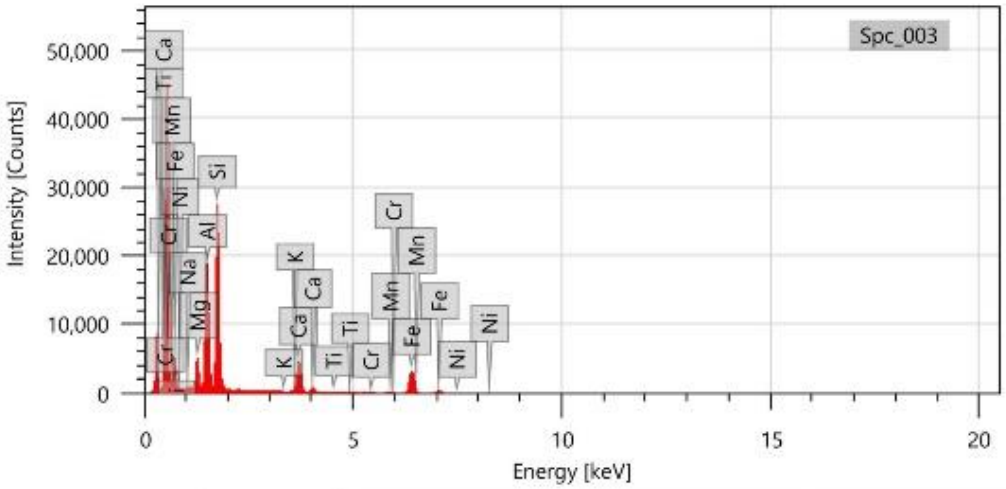

Items	Value
measurement conditions	
Acceleration voltage	15.00 kV
Probe current	-
Magnification	x 70
Process time	T3
Measurement detector	First
Live time	30.00 seconds
Real time	37.40 seconds
Dead time	20.00 %
Count rate	42800.00 CPS

Display name	Standard data	Quantification method	Result Type
Spc_003	Standardless	ZAF	Oxide (Number of oxygen 12)

Chemical formula	Line	Mass%	Mol%	Cations
O	K			
Na2O	K	0.28±0.02	0.30±0.02	0.04
MgO	K	4.81±0.04	7.95±0.07	0.54
Al2O3	K	22.78±0.06	14.89±0.06	2.04
SiO2	K	40.96±0.12	45.43±0.14	3.11
K2O	K	nd	nd	-
CaO	K	9.78±0.06	11.63±0.07	0.80
TiO2	K	0.16±0.02	0.13±0.02	0.01
Cr2O3	K	0.06±0.02	0.03±0.01	0.00
MnO	K	0.42±0.03	0.39±0.03	0.03
FeO	K	20.77±0.13	19.26±0.12	1.52
NiO	K	nd	nd	-
Total		100.00	100.00	
Spc_003				Fitting ratio 0.4553

Figure 55. SEM-EDS analysis data of garnet

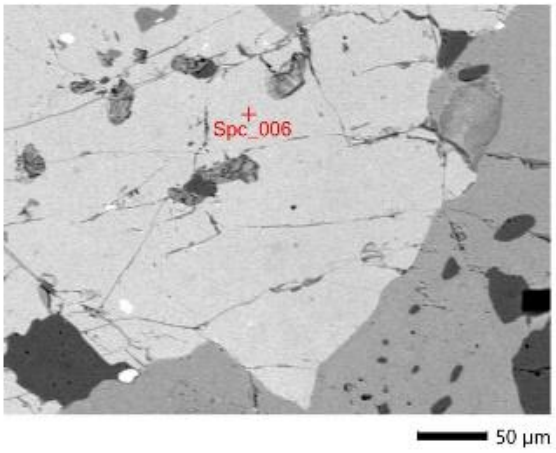

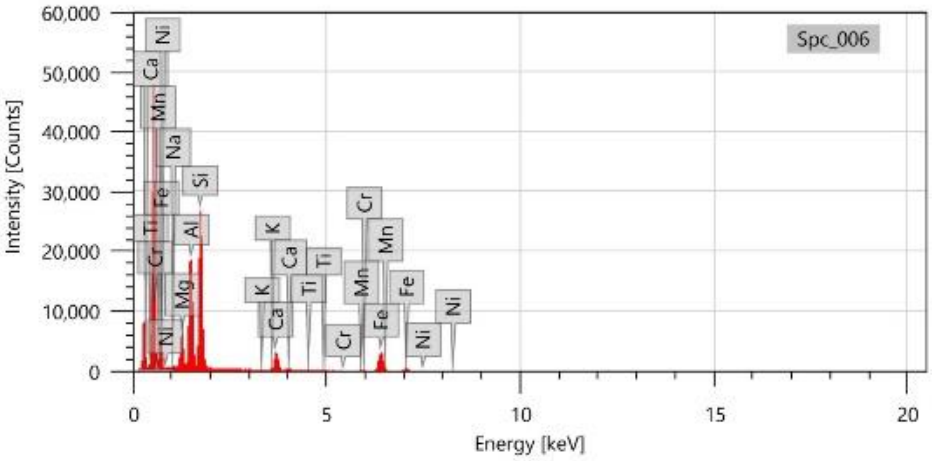

Items	Value
measurement conditions	
Acceleration voltage	15.00 kV
Probe current	-
Magnification	x 330
Process time	T3
Measurement detector	First
Live time	30.00 seconds
Real time	37.29 seconds
Dead time	19.00 %
Count rate	42440.00 CPS

Display name	Standard data	Quantification method	Result Type
Spc_006	Standardless	ZAF	Oxide (Number of oxygen 12)

Chemical formula	Line	Mass%	Mol%	Cations
O	K			
Na2O	K	0.25±0.02	0.27±0.02	0.04
MgO	K	6.29±0.04	10.38±0.07	0.71
Al2O3	K	23.26±0.09	15.17±0.06	2.07
SiO2	K	41.21±0.13	45.60±0.14	3.11
K2O	K	nd	nd	-
CaO	K	6.91±0.05	8.19±0.06	0.56
TiO2	K	0.14±0.02	0.12±0.02	0.01
Cr2O3	K	0.04±0.02	0.02±0.01	0.00
MnO	K	0.51±0.03	0.48±0.03	0.03
FeO	K	21.32±0.13	19.73±0.12	1.34
NiO	K	0.05±0.03	0.06±0.03	0.00
Total		100.00	100.00	
Spc_006				Fitting ratio 0.4737

Figure 56 SEM-EDS analysis data of garnet

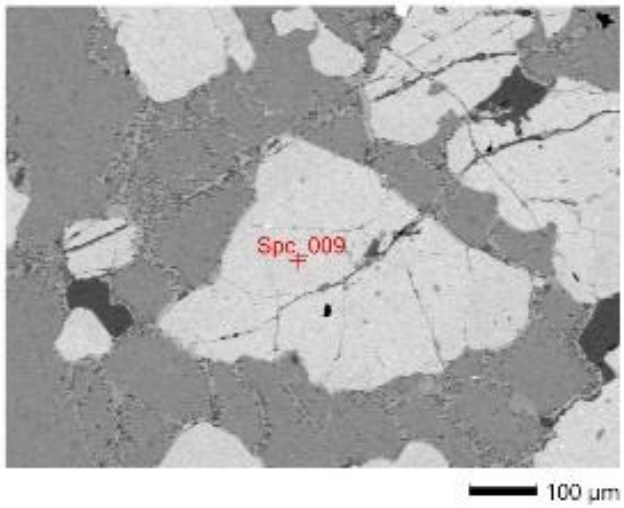

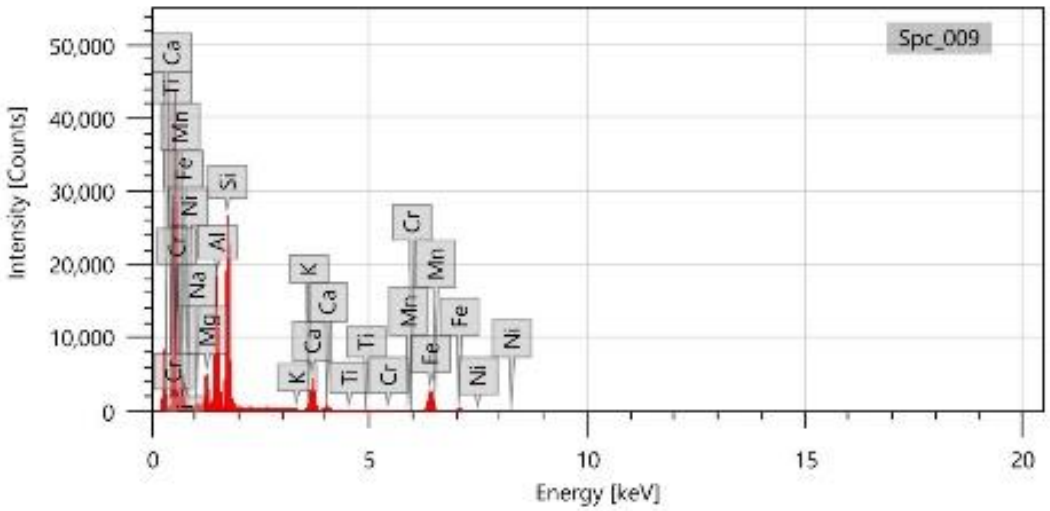

Items	Value
measurement conditions	
Acceleration voltage	15.00 kV
Probe current	-
Magnification	x 140
Process time	T3
Measurement detector	First
Live time	30.00 seconds
Real time	37.17 seconds
Dead time	19.00 %
Count rate	41604.00 CPS

Display name	Standard data	Quantification method	Result Type
Spc_009	Standardless	ZAF	Oxide (Number of oxygen 12)

Chemical formula	Line	Mass%	Mol%	Cations
O	K			
Na2O	K	0.41±0.07	0.44±0.07	0.03
MgO	K	4.89±0.04	8.07±0.07	0.45
Al2O3	K	22.01±0.09	14.25±0.05	2.04
SiO2	K	40.99±0.13	45.40±0.14	3.10
K2O	K	nd	nd	-
CaO	K	10.30±0.08	12.32±0.08	0.83
TiO2	K	0.35±0.07	0.29±0.07	0.02
Cr2O3	K	0.08±0.02	0.04±0.01	0.01
MnO	K	0.47±0.03	0.44±0.03	0.03
FeO	K	19.60±0.13	18.15±0.12	1.24
NiO	K	nd	nd	-
Total		100.00	100.00	
Spc_009				Fitting ratio 0.4683

Figure 57. SEM-EDS analysis data of garnet

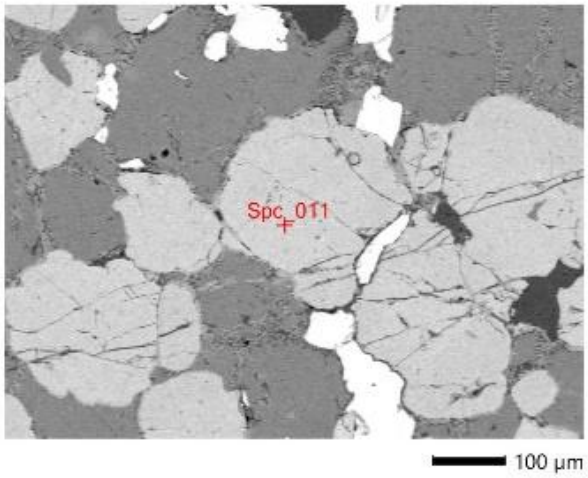

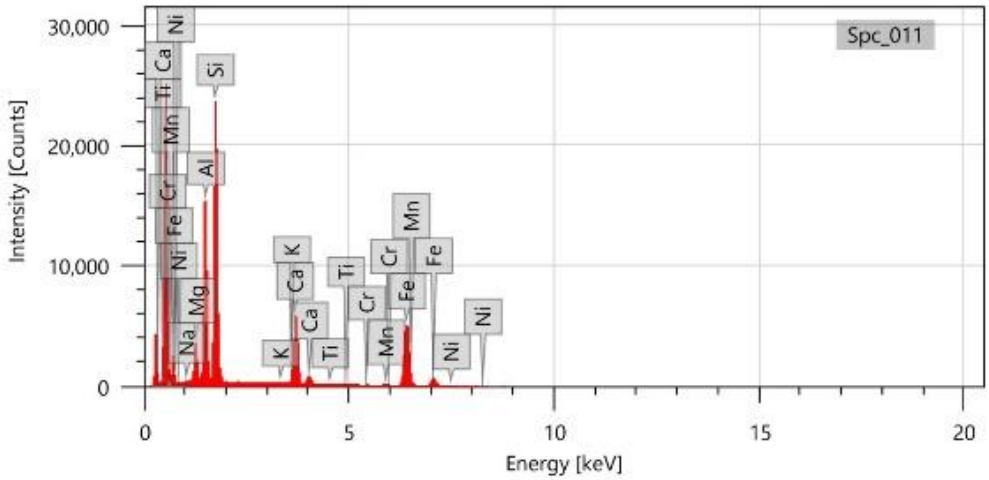

Items	Value
measurement conditions	
Acceleration voltage	20.00 kV
Probe current	-
Magnification	x 160
Process time	T3
Measurement detector	First
Live time	30.00 seconds
Real time	36.12 seconds
Dead time	17.00 %
Count rate	34336.00 CPS

Display name	Standard data	Quantification method	Result Type
Spc_011	Standardless	ZAF	Oxide (Number of oxygen 12)

Chemical formula	Line	Mass%	Mol%	Cations
O	K			
Na2O	K	0.15±0.02	0.17±0.02	0.02
MgO	K	4.56±0.04	7.54±0.07	0.52
Al2O3	K	22.48±0.09	14.70±0.06	2.02
SiO2	K	40.63±0.13	45.09±0.15	3.10
K2O	K	nd	nd	-
CaO	K	10.38±0.06	12.34±0.07	0.85
TiO2	K	0.10±0.01	0.08±0.01	0.01
Cr2O3	K	0.11±0.02	0.05±0.01	0.01
MnO	K	0.51±0.02	0.48±0.02	0.03
FeO	K	21.09±0.10	19.57±0.09	1.34
NiO	K	nd	nd	-
Total		100.00	100.00	
Spc_011				Fitting ratio 0.3249

Figure 58. SEM-EDS analysis data of garnet

Omphacite

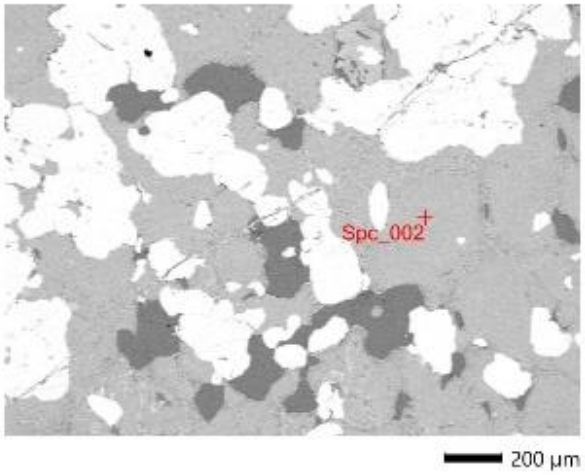

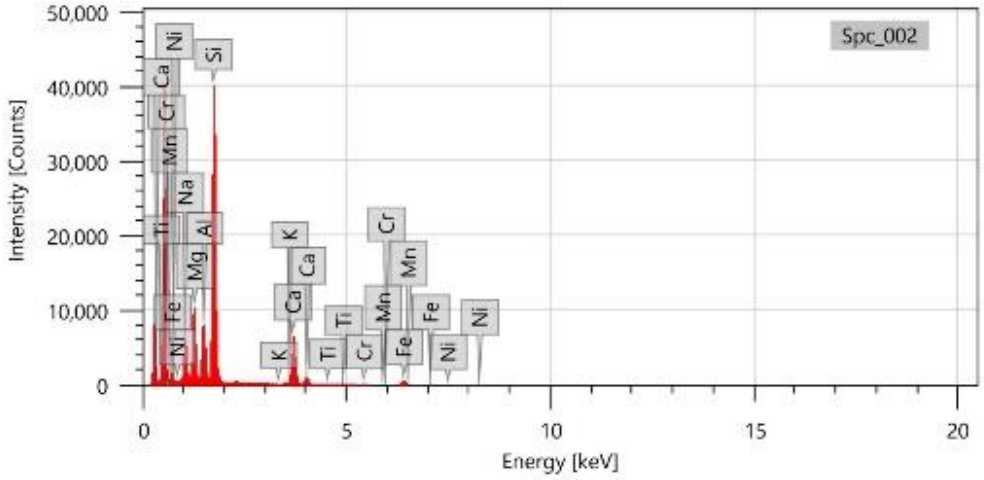

Items	Value
measurement conditions	
Acceleration voltage	15.00 kV
Probe current	-
Magnification	x 65
Process time	T3
Measurement detector	First
Live time	30.00 seconds
Real time	37.16 seconds
Dead time	19.00 %
Count rate	41860.00 CPS

Display name	Standard data	Quantification method	Result Type
Spc_002	Standardless	ZAF	Oxide (Number of oxygen 6)

Chemical formula	Line	Mass%	Mol%	Cations
O	K			
Na2O	K	5.57±0.04	5.33±0.04	0.39
MgO	K	10.26±0.05	15.08±0.08	0.55
Al2O3	K	8.89±0.06	5.17±0.03	0.37
SiO2	K	55.80±0.14	55.04±0.14	1.98
K2O	K	nd	nd	-
CaO	K	14.57±0.07	15.39±0.08	0.56
TiO2	K	0.14±0.02	0.10±0.01	0.00
Cr2O3	K	0.11±0.02	0.04±0.01	0.00
MnO	K	0.10±0.02	0.08±0.02	0.00
FeO	K	4.56±0.06	3.76±0.05	0.14
NiO	K	nd	nd	-
Total		100.00	100.00	
Spc_002				Fitting ratio 0.4401

Figure 59. SEM-EDS analysis data of omphacite

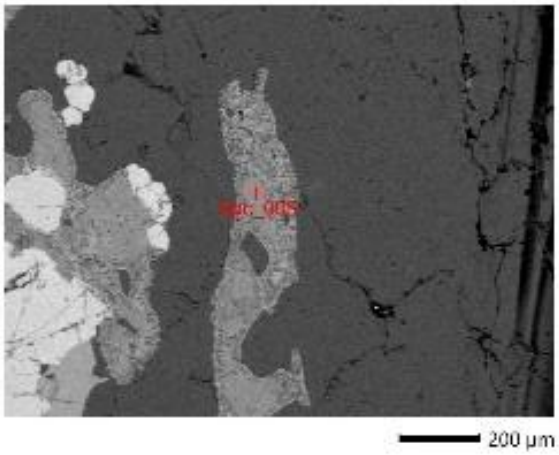

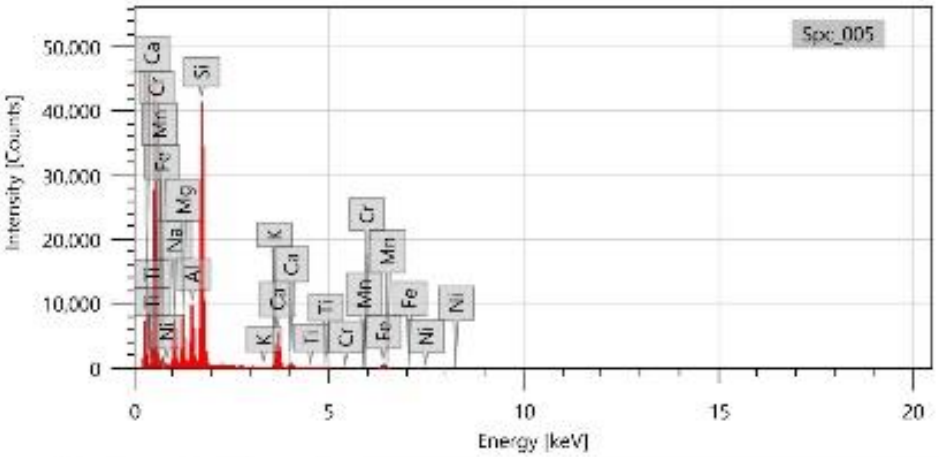

Items	Value
measurement conditions	
Acceleration voltage	15.00 kV
Probe current	-
Magnification	x 95
Process time	T3
Measurement detector	First
Live time	30.00 seconds
Real time	37.36 seconds
Dead time	20.00 %
Count rate	4901.7 00 CPS

Display name	Standard data	Quantification method	Result Type
Spc_005	Standardless	ZAF	Oxide (Number of oxygen 6)

Chemical formula	Line	Wt%	Wt%A	Category
O	K			
Na2O	K	6.82±0.04	6.82±0.07	0.47
MgO	K	8.24±0.05	12.28±0.07	0.42
Al2O3	K	11.12±0.06	6.55±0.04	0.48
SiO2	K	57.13±0.14	57.13±0.16	2.00
K2O	K	0.00	0.00	
CaO	K	13.48±0.07	13.43±0.07	0.47
TiO2	K	0.15±0.00	0.11±0.01	0.00
Cr2O3	K	0.23±0.00	0.04±0.01	0.00
MnO	K	0.28±0.00	0.07±0.00	0.00
FeO	K	4.27±0.03	3.42±0.03	0.12
NiO	K	0.12±0.01	0.03±0.02	0.00
Total		100.00	100.00	

Spc_005 Fitting ratio 0.4015

Figure 60. SEM-EDS analysis data of omphacite

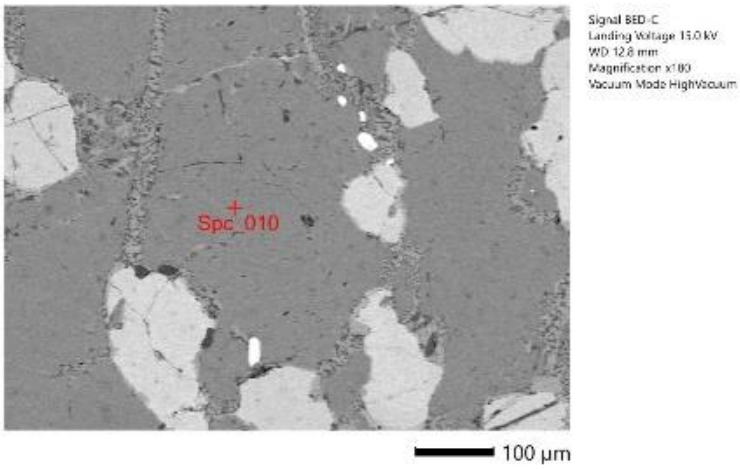

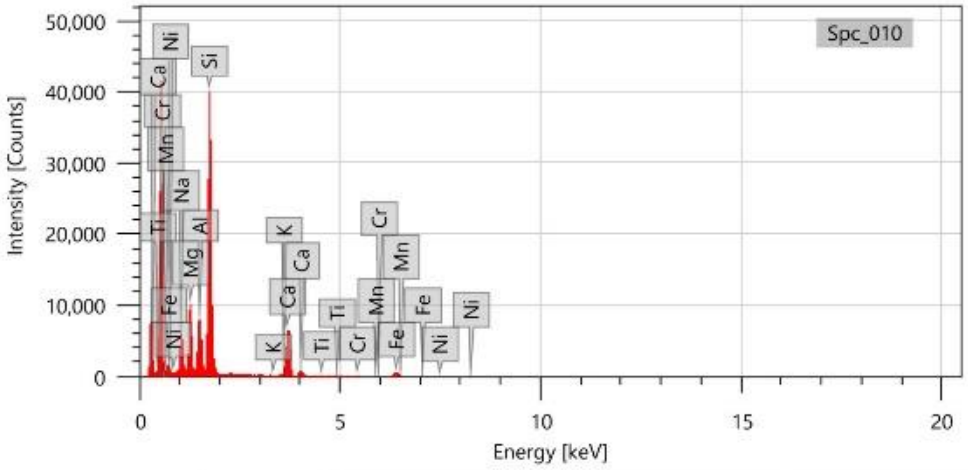

Items	Value
measurement conditions	
Acceleration voltage	15.00 kV
Probe current	-
Magnification	x 180
Process time	T3
Measurement detector	First
Live time	30.00 seconds
Real time	37.17 seconds
Dead time	19.00 %
Count rate	42133.00 CPS

Display name	Standard data	Quantification method	Result Type
Spc_010	Standardless	ZAF	Oxide (Number of oxygen 6)

Chemical formula	Line	Mass%	Mol%	Cations
O	K			
Na2O	K	5.59±0.04	5.35±0.04	0.39
MgO	K	10.21±0.06	15.02±0.08	0.54
Al2O3	K	8.91±0.06	5.18±0.03	0.38
SiO2	K	55.61±0.14	54.88±0.14	1.99
K2O	K	nd	nd	-
CaO	K	14.68±0.07	15.53±0.08	0.56
TiO2	K	0.11±0.02	0.08±0.01	0.00
Cr2O3	K	0.18±0.02	0.07±0.01	0.01
MnO	K	nd	nd	-
FeO	K	4.71±0.06	3.88±0.05	0.14
NiO	K	nd	nd	-
Total		100.00	100.00	
Spc_010				Fitting ratio 0.4395

Figure 61. *SEM-EDS* analysis data of omphacite

Amphibole

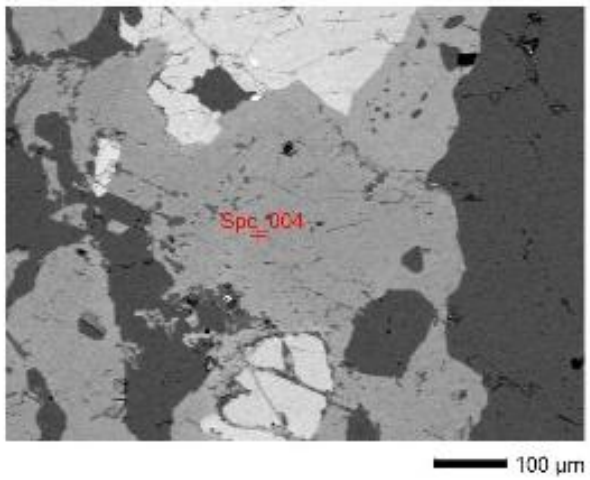

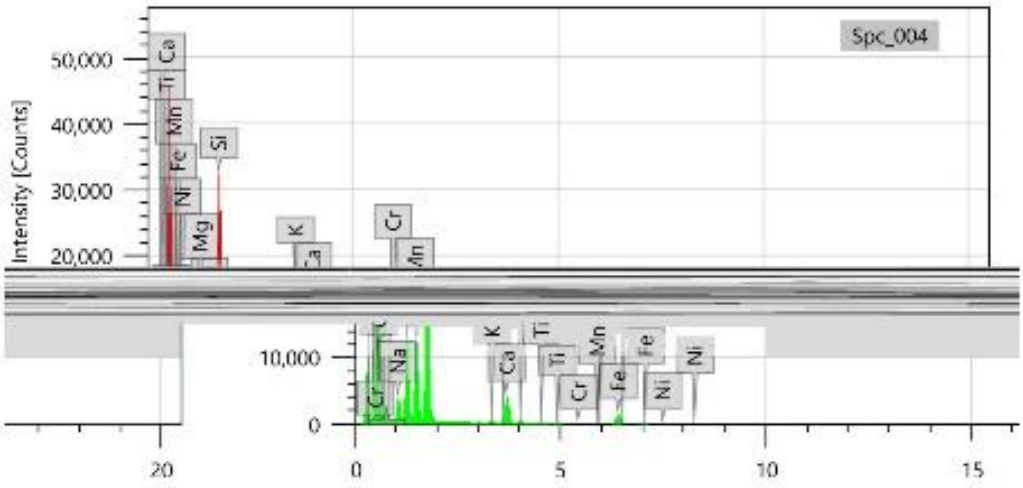

Items	Value
measurement conditions	
Acceleration voltage	15.00 kV
Probe current	-
Magnification	x 160
Process time	T3
Measurement detector	First
Live time	30.00 seconds
Real time	37.24 seconds
Dead time	19.00 %
Count rate	42418.00 CPS

Display name	Standard data	Quantification method	Result Type
Spc_004	Standardless	ZAF	Oxide (Number of oxygen 22)

Chemical formula	Line	Mass%	Mol%	Cations
O	K			
Na2O	K	3.40±0.05	3.56±0.03	0.03
MgO	K	12.25±0.06	15.80±0.07	2.57
Al2O3	K	15.37±0.07	9.12±0.04	2.40
SiO2	K	48.21±0.14	48.71±0.14	6.42
CaO	K	0.55±0.02	0.56±0.02	0.05
Cr2O3	K	0.04±0.06	0.03±0.04	0.00
TiO2	K	0.07±0.05	0.05±0.03	0.01
Cr2O3	K	0.11±0.05	0.08±0.03	0.01
MnO	K	0.27±0.07	0.20±0.05	0.03
FeO	K	9.02±0.09	5.95±0.06	0.79
NiO	K	0.07±0.05	0.05±0.03	0.01
Total		100.00	100.00	
Spc_004				Timing ratio (Live/Real)

Figure 62. SEM-EDS analysis data of amphibole

Rutile

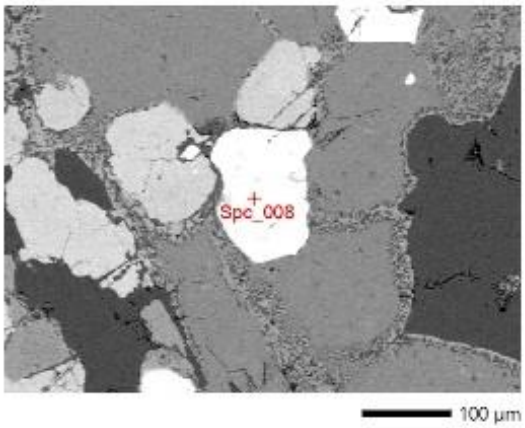

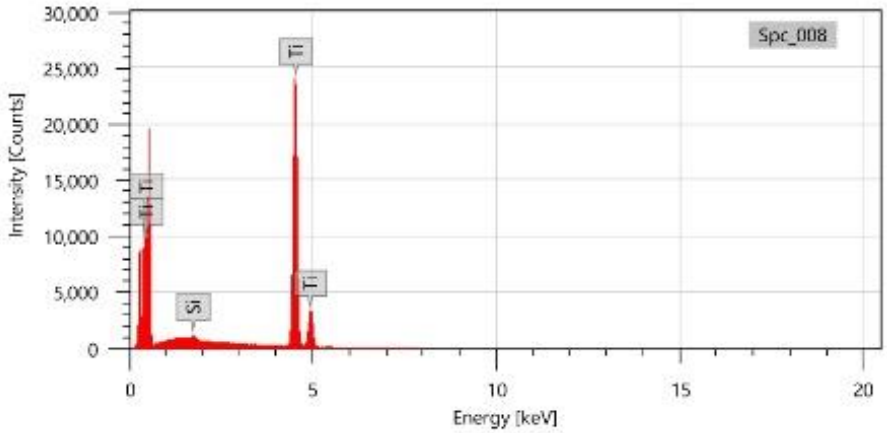

Items	Value
measurement conditions	
Acceleration voltage	15.00 kV
Probe current	-
Magnification	x 220
Process time	T3
Measurement detector	First
Live time	30.00 seconds
Real time	35.98 seconds
Dead time	17.00 %
Count rate	33529.00 CPS

Display name	Standard data	Quantification method	Result Type
Spc_008	Standardless	ZAF	Oxide (Number of oxygen 2)

Chemical formula	Line	Mass%	Mol%	Cations
O	K			
SiO2	K	0.44±0.02	0.59±0.03	0.01
TiO2	K	99.56±0.24	99.41±0.24	0.99
Total		100.00	100.00	
Spc_008				Fitting ratio 0.2455

Figure 63. SEM-EDS analysis data of rutile

GK 2a
Garnet

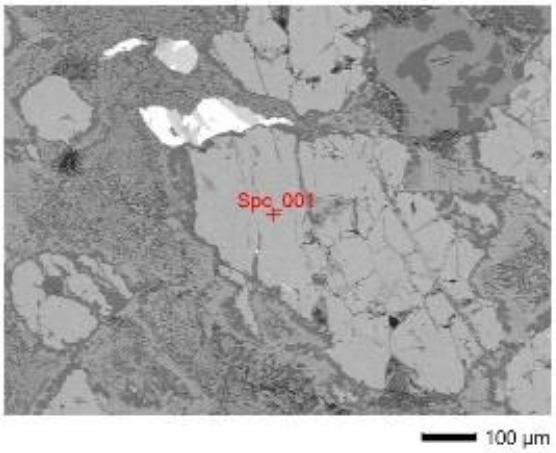

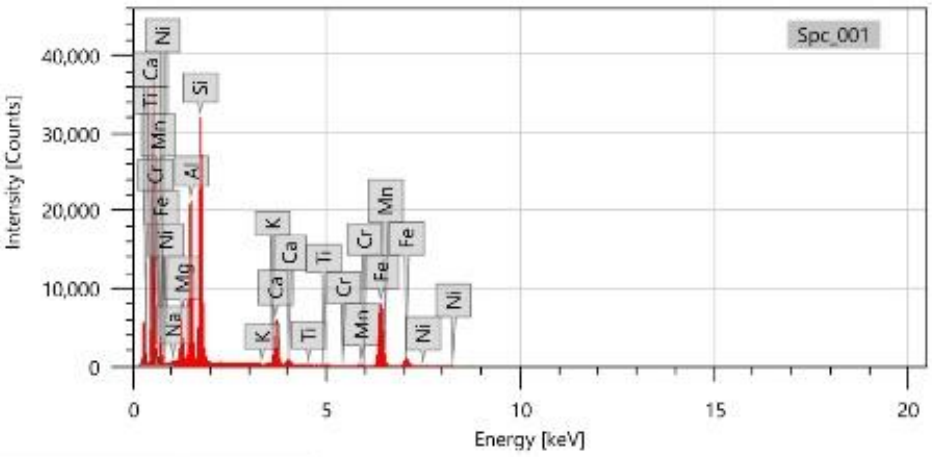

Items	Value
measurement conditions	
Acceleration voltage	20.00 kV
Probe current	
Magnification	x 130
Process time	T3
Measurement detector	First
Live time	30.00 seconds
Real time	38.65 seconds
Dead time	22.00 %
Count rate	47728.00 CPS

Display name	Standard data	Quantification method	Result Type
Spc_001	Standerdless	ZAF	Oxide (Number of oxygen 12)

Chemical formula	Line	Mass%	Mol%	Cation
O	K			
Na2O	K	0.20±0.02	0.22±0.02	0.03
MgO	K	5.84±0.04	9.71±0.07	0.97
Al2O3	K	22.41±0.08	14.62±0.05	2.02
SiO2	K	40.34±0.11	44.68±0.13	5.08
CrO	K	nd	nd	
CaO	K	7.41±0.04	8.79±0.05	0.81
TiO2	K	0.04±0.01	0.03±0.01	0.00
Cr2O3	K	0.07±0.01	0.03±0.01	0.00
MnO	K	0.50±0.02	0.47±0.02	0.05
FeO	K	28.14±0.09	21.48±0.08	1.48
NiO	K	0.01±0.01	0.01±0.01	0.00
Total		100.00	100.00	
Spc_001				Fitting ratio 0.8278

Figure 64. SEM-EDS analysis data of garnet

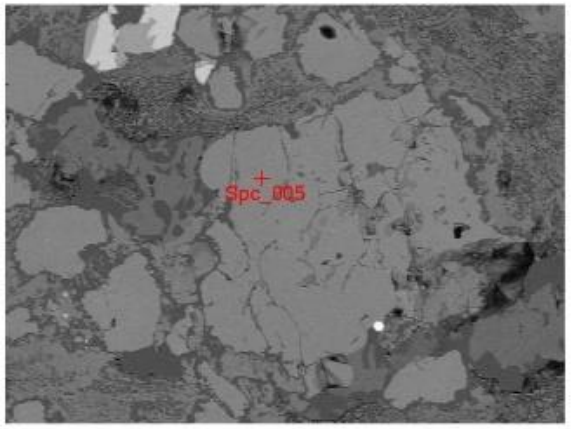

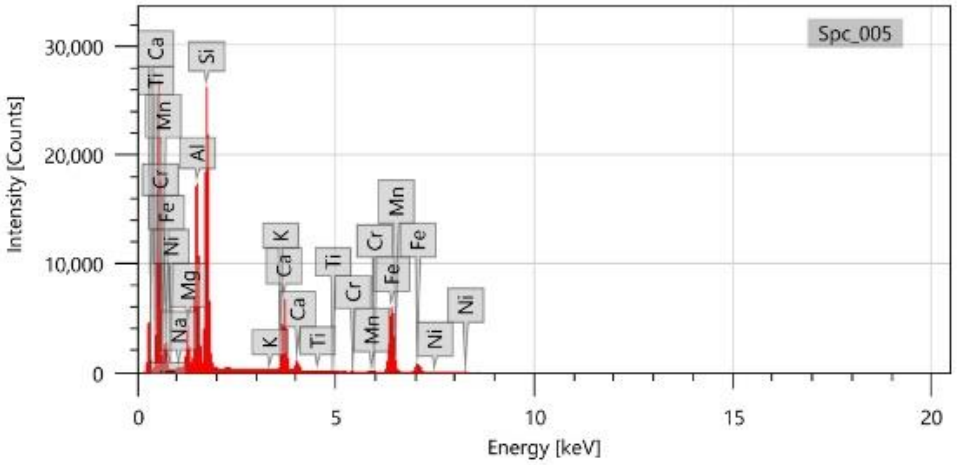

Items	Value
measurement conditions	
Acceleration voltage	20.00 kV
Probe current	-
Magnification	x 140
Process time	T3
Measurement detector	First
Live time	30.00 seconds
Real time	36.81 seconds
Dead time	18.00 %
Count rate	37867.00 CPS

Display name	Standard data	Quantification method	Result Type
Spc_005	Standardless	ZAF	Oxide (Number of oxygen 12)

Chemical formula	Line	Mass%	Mol%	Cations
O	K			
Na2O	K	0.17±0.02	0.19±0.02	0.03
MgO	K	4.71±0.04	7.77±0.07	0.54
Al2O3	K	22.19±0.09	14.47±0.06	2.00
SiO2	K	40.32±0.13	44.62±0.14	3.08
K2O	K	nd	nd	-
CaO	K	10.84±0.05	12.85±0.06	0.89
TiO2	K	0.05±0.01	0.04±0.01	0.00
Cr2O3	K	0.08±0.01	0.04±0.01	0.01
MnO	K	0.45±0.02	0.42±0.02	0.03
FeO	K	21.13±0.10	19.55±0.09	1.35
NiO	K	0.05±0.02	0.05±0.01	0.00
Total		100.00	100.00	
Spc_005				Fitting ratio 0.3115

Figure 65. SEM-EDS analysis data of garnet

GK 2b
Garnet

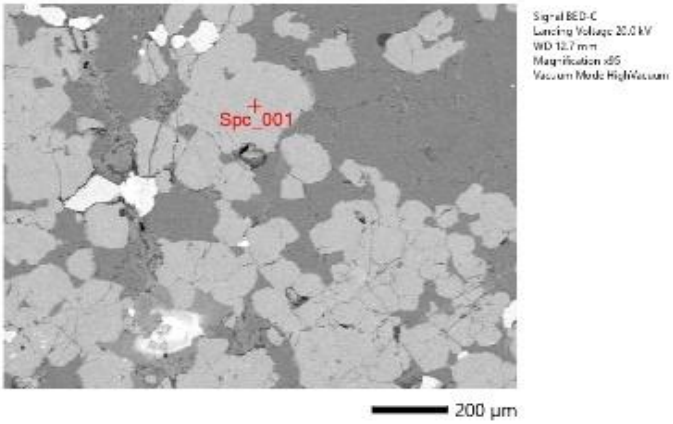

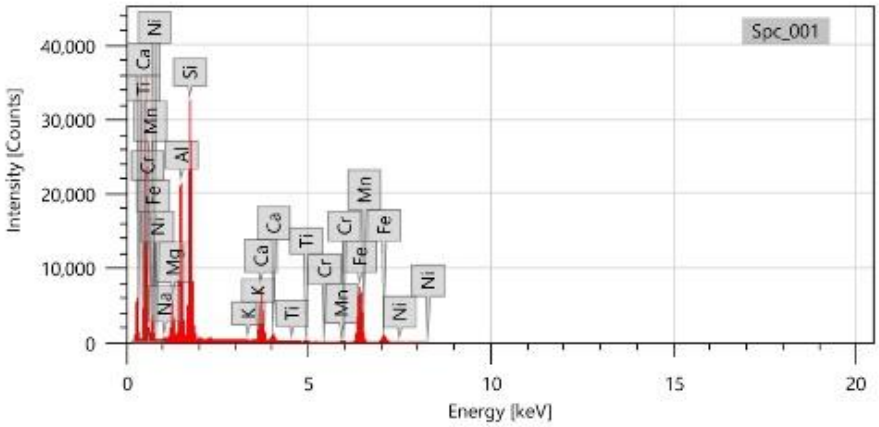

Items	Value
measurement conditions	
Acceleration voltage	20.00 kV
Probe current	-
Magnification	x 95
Process time	T3
Measurement detector	First
Live time	30.00 seconds
Real time	38.67 seconds
Dead time	22.00 %
Count rate	47846.00 CPS

Display name	Standard data	Quantification method	Result Type
Spc_001	Standardless	ZAF	Oxide (Number of oxygen 12)

Chemical formula	Line	Mass%	Mol%	Cation
O	K			
Na2O	K	0.21±0.02	0.23±0.02	0.03
MgO	K	5.26±0.04	8.67±0.06	0.80
Al2O3	K	22.34±0.08	14.55±0.05	2.01
SiO2	K	48.63±0.11	44.90±0.13	3.09
K2O	K	nd	nd	-
CaO	K	9.51±0.03	11.27±0.05	0.78
TiO2	K	0.22±0.01	0.19±0.01	0.01
Cr2O3	K	0.00±0.01	0.00±0.01	0.00
MnO	K	0.44±0.02	0.41±0.02	0.03
FeO	K	21.37±0.09	19.78±0.08	1.36
NiO	K	0.03±0.01	0.03±0.01	0.00
Total		100.00	100.00	
Spc_001				Filling ratio 0.3085

Figure 66. SEM-EDS analysis data of garnet

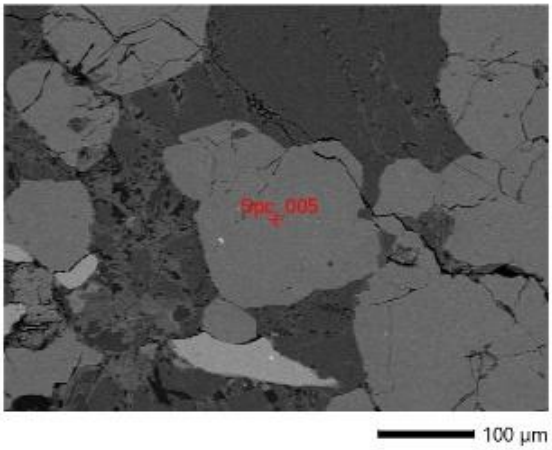

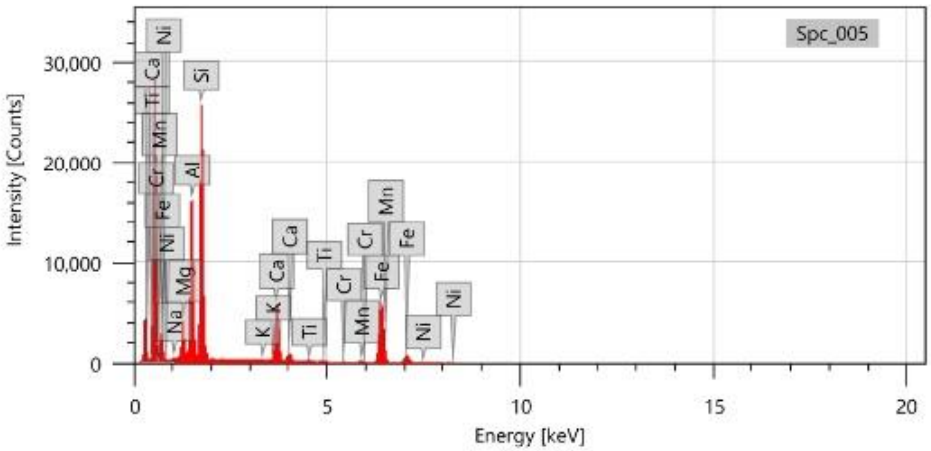

Items	Value
measurement conditions	
Acceleration voltage	20.00 kV
Probe current	-
Magnification	x 230
Process time	T3
Measurement detector	First
Live time	30.00 seconds
Real time	36.71 seconds
Dead time	18.00 %
Count rate	37475.00 CPS

Display name	Standard data	Quantification method	Result Type
Spc_005	Standardless	ZAF	Oxide (Number of oxygen 12)

Chemical formula	Line	Mass%	Mol%	Cations
O	K			
Na2O	K	0.27±0.02	0.23±0.02	0.03
MgO	K	4.98±0.04	8.22±0.07	0.57
Al2O3	K	21.69±0.09	14.14±0.06	1.96
SiO2	K	40.49±0.13	44.79±0.14	3.10
K2O	K	nd	nd	
CaO	K	9.64±0.05	11.43±0.06	0.79
TiO2	K	0.35±0.02	0.29±0.01	0.02
Cr2O3	K	0.10±0.01	0.05±0.01	0.01
MnO	K	0.46±0.02	0.43±0.02	0.03
FeO	K	20.07±0.10	20.43±0.09	1.41
NiO	K	0.01±0.02	0.01±0.01	0.00
Total		100.00	100.00	
Spc_005				Fitting ratio 0.3229

Figure 67. SEM-EDS analysis data of garnet

Omphacite

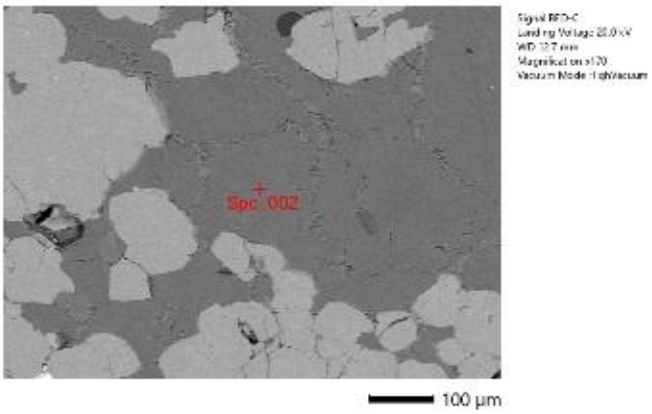

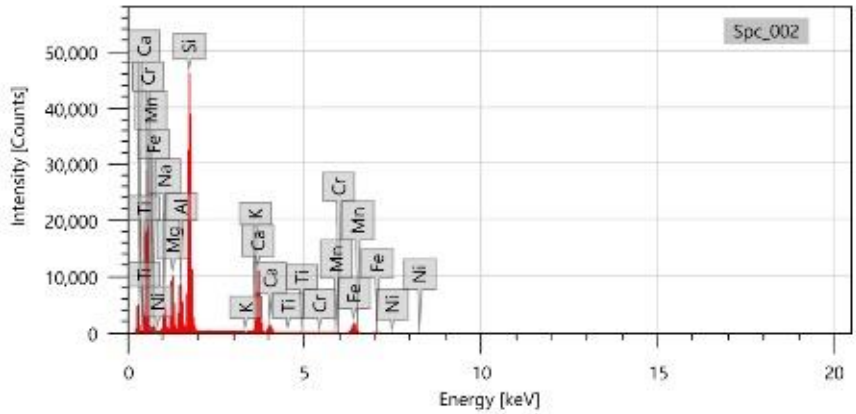

Items	Value
measurement conditions	
Acceleration voltage	20.00 kV
Probe current	-
Magnification	x 170
Process time	T3
Measurement detector	First
Live time	30.00 seconds
Real time	37.92 seconds
Dead time	21.00 %
Count rate	44552.00 CPS

Display name	Standard data	Quantification method	Result Type
Spc 002	Standardless	ZAF	Oxide (Number of oxygen 6)

Chemical formula	Line	Mass%	Mol%	Cations
O	K			
Na2O	K	5.81±0.04	5.69±0.04	0.37
MgO	K	9.72±0.05	14.33±0.07	0.52
Al2O3	K	8.72±0.05	5.09±0.03	0.37
SiO2	K	55.34±0.13	54.74±0.13	1.99
K2O	K	nd	nd	-
CaO	K	15.20±0.06	16.11±0.06	0.58
TiO2	K	0.21±0.01	0.16±0.01	0.01
Cr2O3	K	0.15±0.01	0.06±0.01	0.00
MnO	K	0.03±0.01	0.02±0.01	0.00
FeO	K	5.81±0.05	4.89±0.04	0.16
NiO	K	0.02±0.01	0.02±0.01	0.00
Total		100.00	100.00	
Spc_002				Fitting ratio 0.3170

Figure 68. SEM-EDS analysis data of omphacite

Rutile

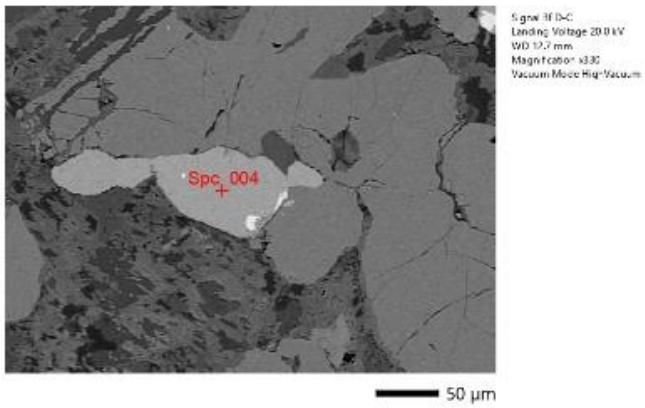

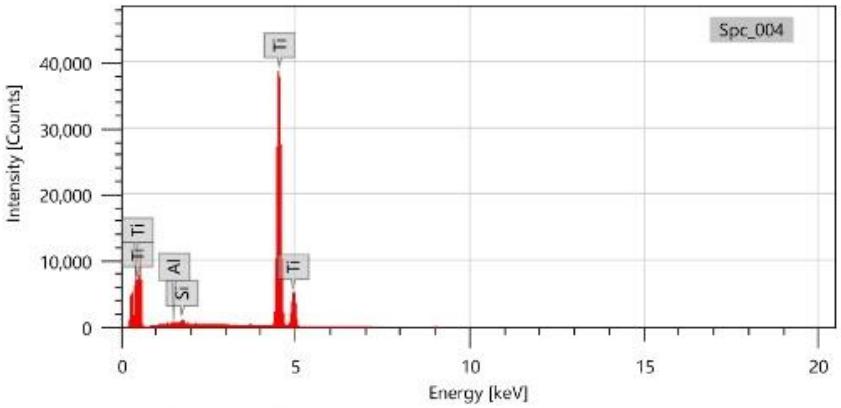

Items	Value
measurement conditions	
Acceleration voltage	20.00 kV
Probe current	-
Magnification	x 330
Process time	T3
Measurement detector	First
Live time	30.00 seconds
Real time	37.08 seconds
Dead time	19.00 %
Count rate	37322.00 CPS

Display name	Standard data	Quantification method	Result Type
Spc_004	Standardless	ZAF	Oxide (Number of oxygen ?)

Chemical formula	Line	Mass%	Mol%	Cations
O	K			
Al2O3	K	0.21±0.02	0.17±0.02	0.00
SiO2	K	0.58±0.02	0.77±0.03	0.01
TiO2	K	99.20±0.19	99.06±0.19	0.99
Total		100.00	100.00	
Spc_004				Fitting ratio 0.1007

Figure 69. SEM-EDS analysis data of rutile

GK 5
Garnet

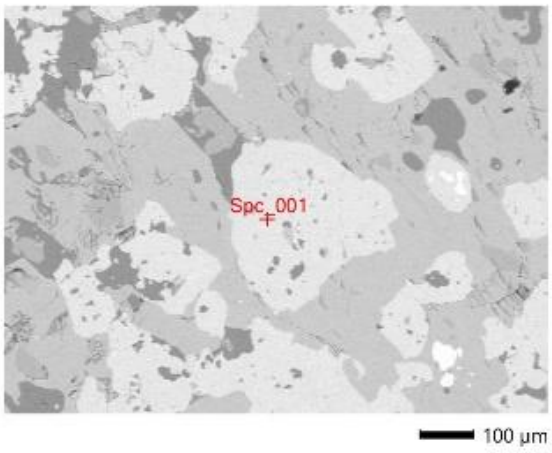

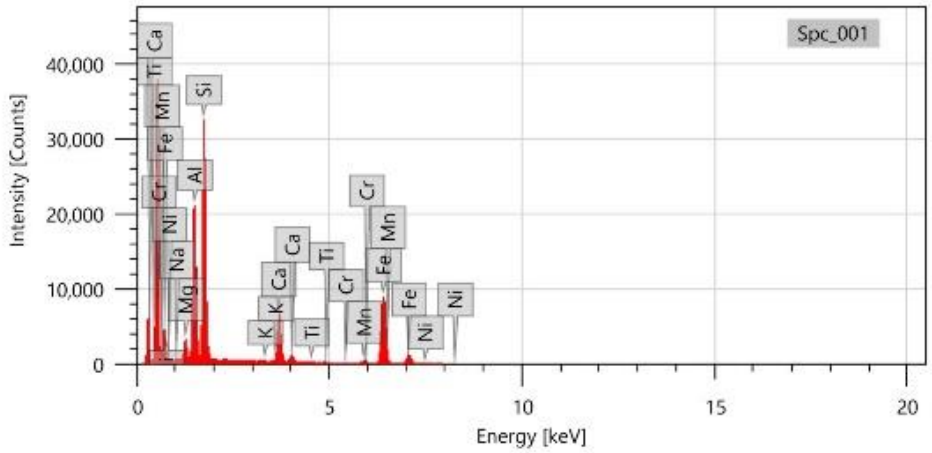

Items	Value
measurement conditions	
Acceleration voltage	20.00 kV
Probe current	-
Magnification	x 130
Process time	T3
Measurement detector	First
Live time	30.00 seconds
Real time	38.90 seconds
Dead time	23.00 %
Count rate	48808.00 CPS

Display name	Standard data	Quantification method	Result Type
Spc_001	Standardless	ZAF	Oxide (Number of oxygen 12)

Chemical formula	Line	Mass%	Mol%	Cations
O	K			
Na2O	K	0.20±0.02	0.22±0.02	0.03
MgO	K	2.64±0.03	4.45±0.05	0.31
Al2O3	K	21.07±0.05	14.56±0.05	2.00
SiO2	K	40.41±0.11	43.65±0.13	3.13
K2O	K	nd	nd	
CaO	K	8.39±0.04	10.15±0.05	0.70
TiO2	K	0.14±0.01	0.12±0.01	0.01
Cr2O3	K	0.09±0.01	0.04±0.01	0.01
MnO	K	0.76±0.02	0.72±0.02	0.05
FeO	K	25.49±0.09	24.08±0.09	1.63
NiO	K	0.00±0.01	0.00±0.01	0.00
Total		100.00	100.00	
Spc_001				Fitting ratio 0.3286

Figure 70. SEM-EDS analysis data of garnet

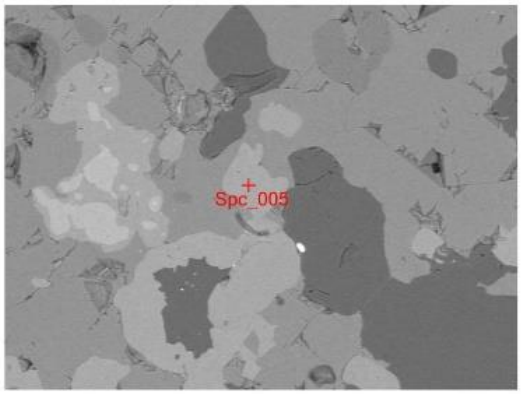

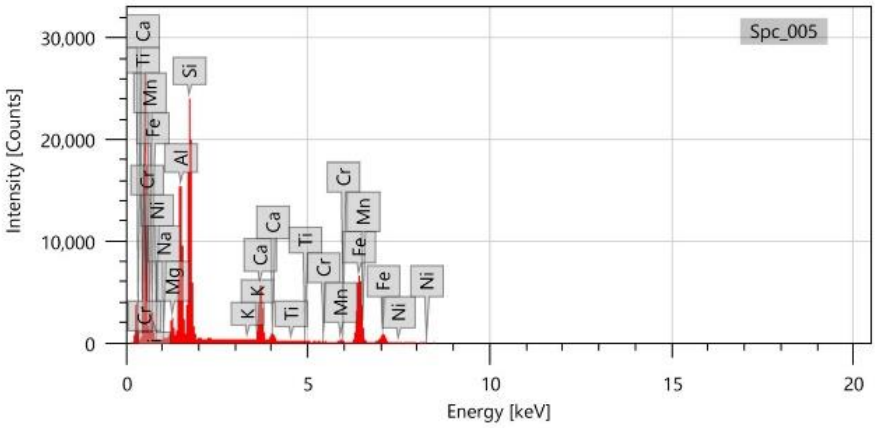

Items	Value
measurement conditions	
Acceleration voltage	20.00 kV
Probe current	-
Magnification	x 200
Process time	T3
Measurement detector	First
Live time	30.00 seconds
Real time	36.41 seconds
Dead time	17.00 %
Count rate	35623.00 CPS

Display name	Standard data	Quantification method	Result Type
Spc_005	Standardless	ZAF	Oxide (Number of oxygen 12)

Chemical formula	Line	Mass%	Mol%	Cations
O	K			
Na2O	K	0.16±0.02	0.16±0.02	0.02
MgO	K	2.70±0.03	4.53±0.06	0.31
Al2O3	K	21.72±0.09	14.42±0.06	2.00
SiO2	K	39.48±0.13	44.49±0.15	3.08
K2O	K	nd	nd	-
CaO	K	9.50±0.05	11.47±0.06	0.79
TiO2	K	0.16±0.02	0.14±0.01	0.01
Cr2O3	K	0.00±0.01	0.00±0.01	0.00
MnO	K	0.69±0.02	0.66±0.02	0.05
FeO	K	25.57±0.11	24.09±0.10	1.67
NiO	K	0.02±0.02	0.01±0.02	0.00
Total		100.00	100.00	
Spc_005				Fitting ratio 0.3108

Figure 71. SEM-EDS analysis data of garnet

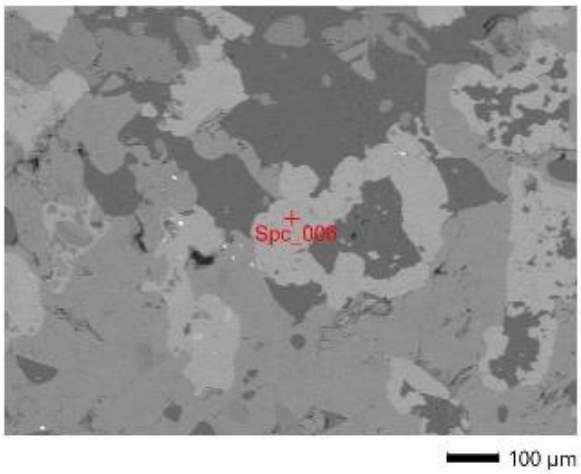

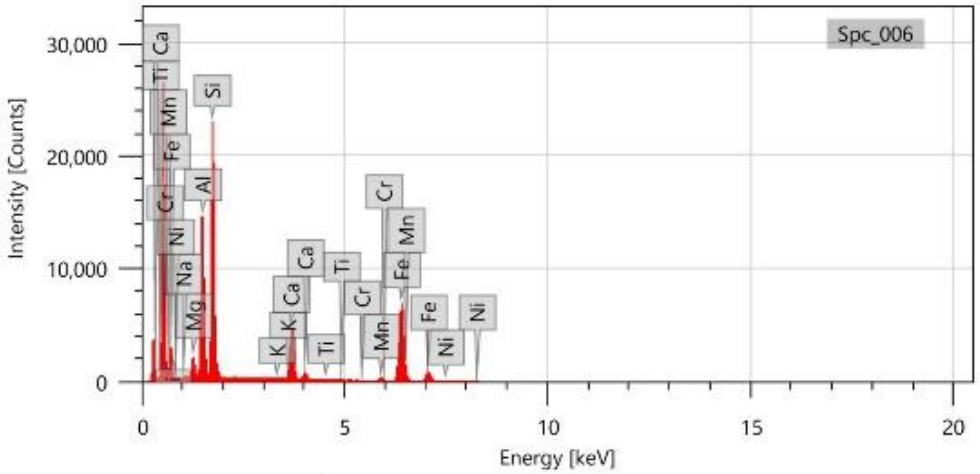

Items	Value
measurement conditions	
Acceleration voltage	20.00 kV
Probe current	-
Magnification	x 120
Process time	T3
Measurement detector	First
Live time	30.00 seconds
Real time	36.29 seconds
Dead time	17.00 %
Count rate	34855.00 CPS

Display name	Standard data	Quantification method	Result Type
Spc_006	Standardless	ZAF	Oxide (Number of oxygen 12)

Chemical formula	Line	Mass%	Mol%	Cations
O	K			
Na2O	K	0.21±0.02	0.23±0.02	0.03
MgO	K	2.41±0.03	4.07±0.06	0.28
Al2O3	K	21.40±0.09	14.29±0.06	1.98
SiO2	K	39.36±0.13	44.61±0.15	3.09
K2O	K	nd	nd	-
CaO	K	7.91±0.05	9.60±0.06	0.66
TiO2	K	0.21±0.02	0.18±0.01	0.01
Cr2O3	K	nd	nd	-
MnO	K	1.00±0.03	0.96±0.03	0.07
FeO	K	27.46±0.11	25.02±0.11	1.80
NiO	K	0.04±0.02	0.04±0.02	0.00
Total		100.00	100.00	
Spc_006				Fitting ratio 0.3116

Figure 72. SEM-EDS analysis data of garnet

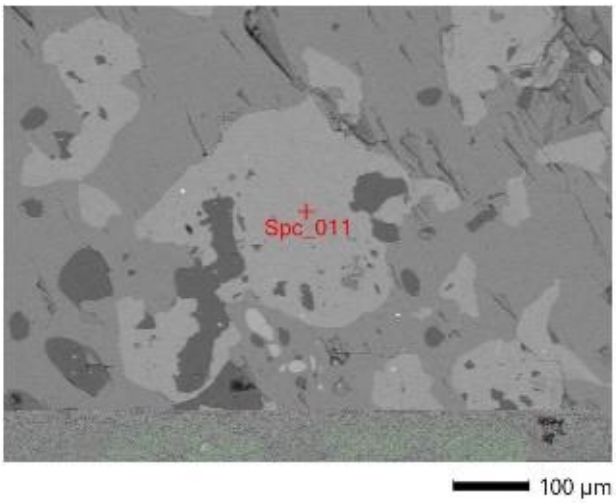

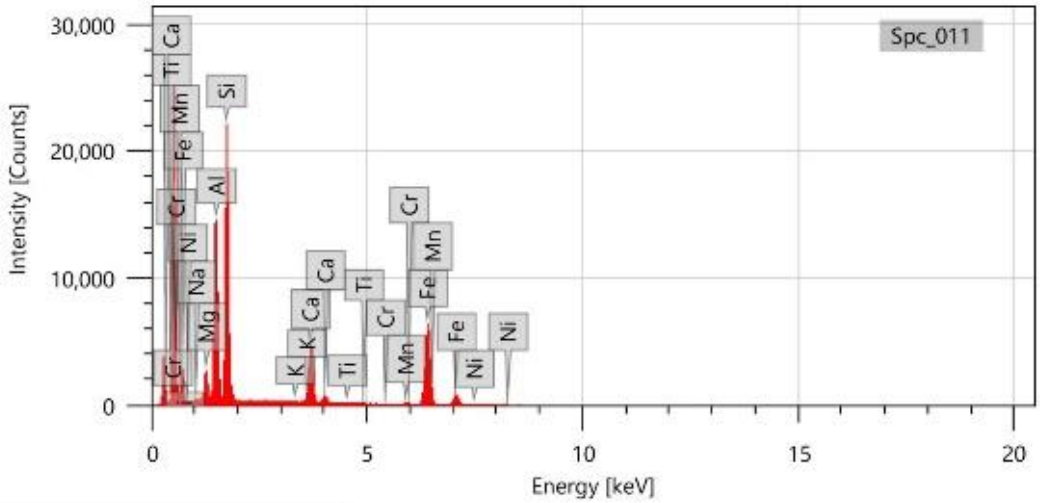

Items	Value
measurement conditions	
Acceleration voltage	20.00 kV
Probe current	-
Magnification	x 160
Process time	T3
Measurement detector	First
Live time	30.00 seconds
Real time	35.92 seconds
Dead time	16.00 %
Count rate	33145.00 CPS

Display name	Standard data	Quantification method	Result Type
Spc_011	Standardless	ZAF	Oxide (Number of oxygen 12)

Chemical formula	Line	Mass%	Mol%	Cations
O	K			
Na2O	K	0.26±0.02	0.29±0.02	0.04
MgO	K	3.26±0.04	5.48±0.07	0.38
Al2O3	K	21.94±0.09	14.56±0.06	2.01
SiO2	K	39.58±0.14	44.58±0.15	3.08
K2O	K	0.01±0.01	0.01±0.01	0.00
CaO	K	8.23±0.05	9.95±0.06	0.69
TiO2	K	0.06±0.01	0.05±0.01	0.00
Cr2O3	K	0.01±0.01	0.01±0.01	0.00
MnO	K	0.46±0.02	0.44±0.02	0.03
FeO	K	26.17±0.11	24.64±0.11	1.70
NiO	K	nd	nd	-
Total		100.00	100.00	
Spc_011				Fitting ratio 0.3161

Figure 73. SEM-EDS analysis data of garnet

Omphacite

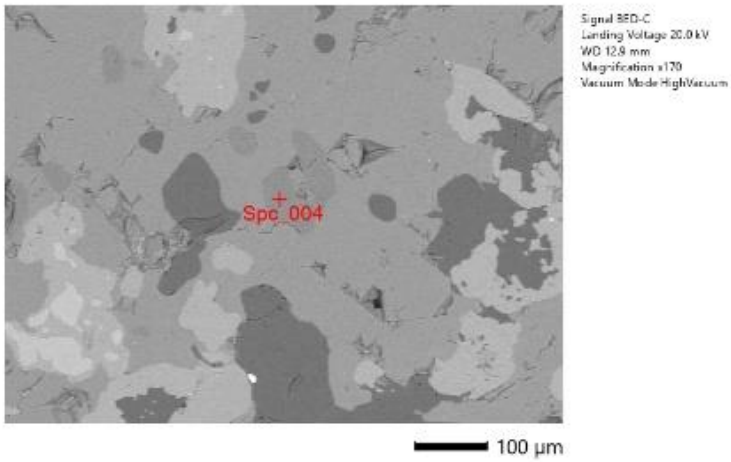

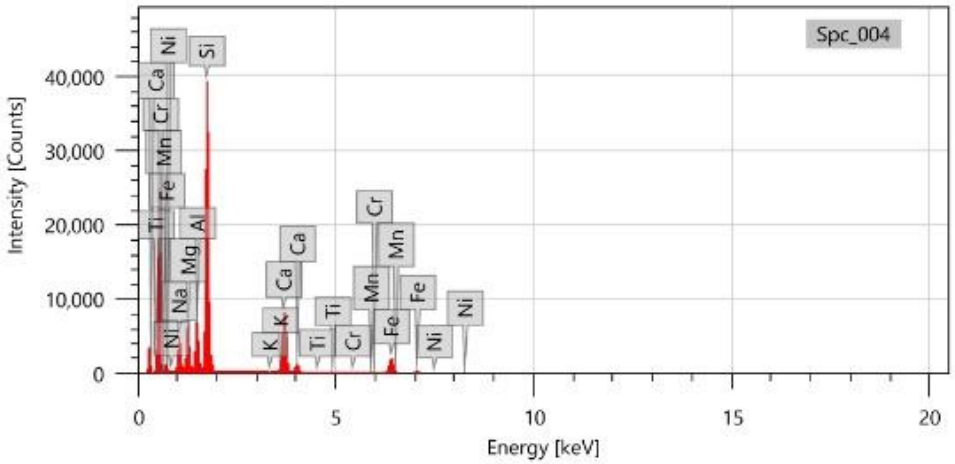

Items	Value
measurement conditions	
Acceleration voltage	20.00 kV
Probe current	-
Magnification	x 170
Process time	T3
Measurement detector	First
Live time	30.00 seconds
Real time	36.57 seconds
Dead time	18.00 %
Count rate	37139.00 CPS

Display name	Standard data	Quantification method	Result Type
Spc_004	Standardless	ZAF	Oxide (Number of oxygen 6)

Chemical formula	Line	Mass%	Mol%	Cations
O	K			
Na2O	K	6.52±0.05	6.33±0.05	0.46
MgO	K	7.91±0.05	11.01±0.08	0.43
Al2O3	K	8.54±0.06	5.04±0.03	0.36
SiO2	K	55.62±0.14	55.74±0.14	2.01
K2O	K	nd	nd	
CaO	K	13.56±0.06	14.56±0.07	0.53
TiO2	K	0.15±0.01	0.11±0.01	0.00
Cr2O3	K	0.12±0.01	0.05±0.01	0.00
MnO	K	0.01±0.01	0.01±0.01	0.00
FeO	K	7.49±0.06	6.20±0.05	0.23
NiO	K	0.08±0.02	0.06±0.01	0.00
Total		100.00	100.00	
Spc_004				Fitting ratio 0.3145

Figure 74. SEM-EDS analysis data of omphacite

Amphibole

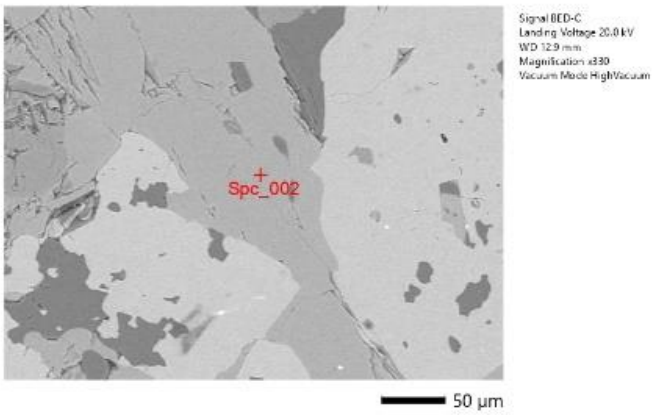

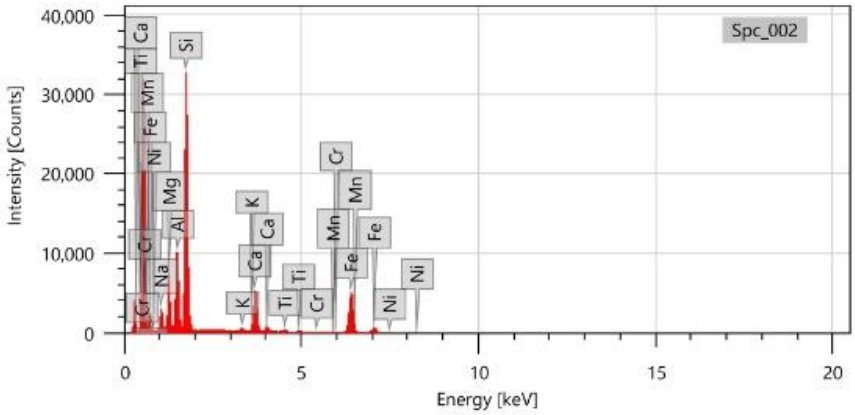

Items	Value
measurement conditions	
Acceleration voltage	20.00 kV
Probe current	-
Magnification	x 330
Process time	T3
Measurement detector	First
Live time	30.00 seconds
Real time	37.07 seconds
Dead time	19.00 %
Count rate	39861.00 CPS

Display name	Standard data	Quantification method	Result Type
Spc_002	Standardless	ZAF	Oxide (Number of oxygen 22)

Chemical formula	Line	Mass%	Mol%	Cations
O	K			
Na2O	K	3.90±0.04	3.94±0.04	1.04
MgO	K	8.41±0.05	13.06±0.08	1.73
Al2O3	K	13.08±0.07	8.03±0.04	2.13
SiO2	K	47.55±0.13	49.55±0.14	6.56
K2O	K	0.37±0.01	0.25±0.01	0.07
CaO	K	8.07±0.05	9.01±0.05	1.19
TiO2	K	0.70±0.02	0.54±0.02	0.07
Cr2O3	K	0.02±0.01	0.01±0.01	0.00
MnO	K	0.05±0.01	0.04±0.01	0.01
FeO	K	17.85±0.09	15.56±0.08	2.06
NiO	K	0.01±0.02	0.01±0.01	0.00
Total		100.00	100.00	
Spc_002				Fitting ratio 0.3471

Figure 75. SEM-EDS analysis data of amphibole

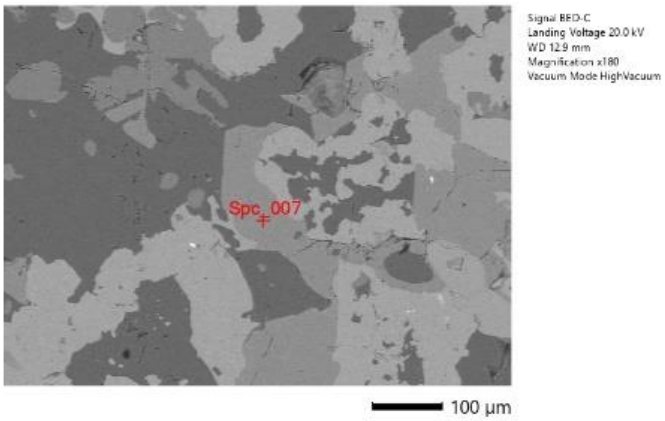

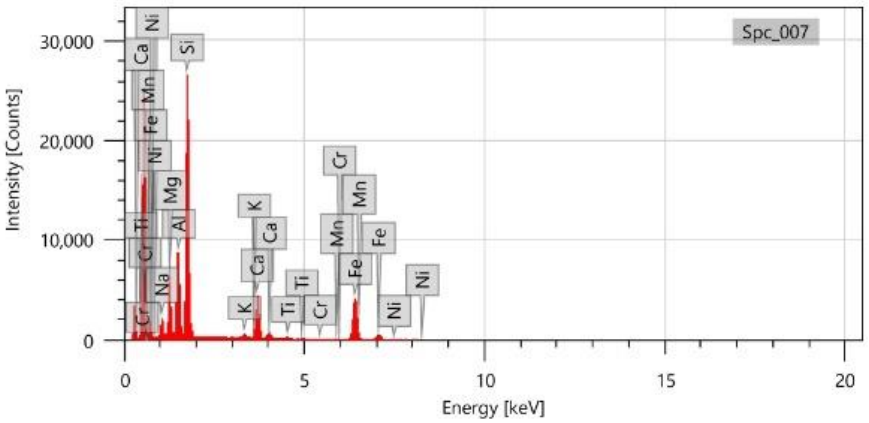

Items	Value
measurement conditions	
Acceleration voltage	20.00 kV
Probe current	-
Magnification	x 180
Process time	T3
Measurement detector	First
Live time	30.00 seconds
Real time	35.72 seconds
Dead time	16.00 %
Count rate	32421.00 CPS

Display name	Standard data	Quantification method	Result Type
Spc_007	Standardless	ZAF	Oxide (Number of oxygen 22)

Chemical formula	Line	Mass%	Mol%	Cations
O	K			
Na2O	K	3.30±0.04	3.33±0.04	0.88
MgO	K	8.87±0.06	13.78±0.09	1.82
Al2O3	K	13.62±0.08	8.36±0.05	2.21
SiO2	K	47.14±0.15	49.11±0.15	6.50
K2O	K	0.58±0.02	0.38±0.01	0.10
CaO	K	8.26±0.05	9.22±0.06	1.22
TiO2	K	0.54±0.02	0.43±0.02	0.06
Cr2O3	K	0.05±0.02	0.02±0.01	0.01
MnO	K	0.08±0.02	0.07±0.01	0.01
FeO	K	17.56±0.09	15.30±0.08	2.02
NiO	K	nd	nd	-
Total		100.00	100.00	
Spc_007				Fitting ratio 0.3396

Figure 76. SEM-EDS analysis data of amphibole

GK 7a
Garnet

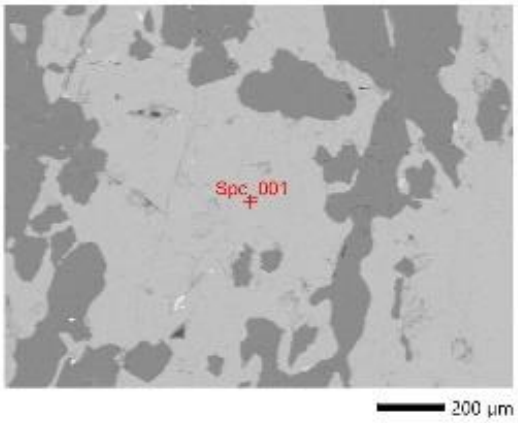

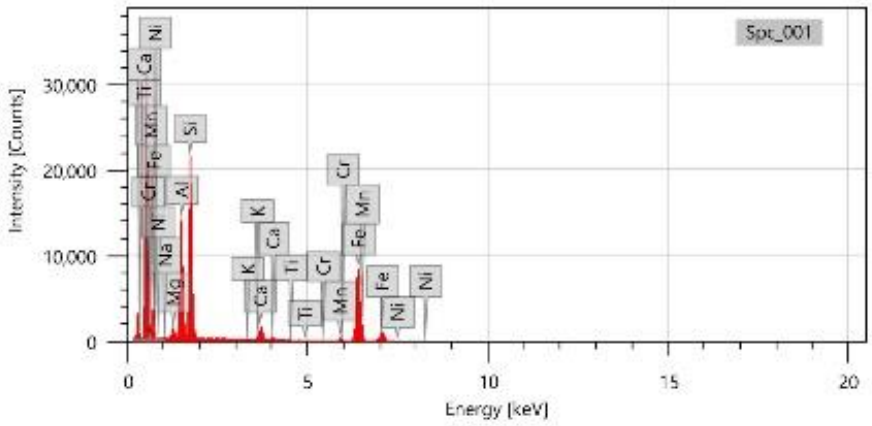

Items	Value
measurement conditions	
Acceleration voltage	20.00 kV
Probe current	
Magnification	x 85
Process time	T3
Measurement detector	First
Live time	30.00 seconds
Real time	36.29 seconds
Dead time	17.30 %
Count rate	35059.00 CPS

Display name	Standard data	Quantification method	Result Type
Spc_001	Standardless	ZAF	Oxide (Number of oxygen 12)

Chemical formula	Line	Mass%	Mol%	Cations
O	K			
Na2O	K	0.11±0.02	0.12±0.03	0.02
MgO	K	1.56±0.03	2.58±0.05	0.18
Al2O3	K	21.62±0.23	14.76±0.06	2.03
SiO2	K	38.09±0.19	45.06±0.15	3.10
K2O	K	n.d.	n.d.	-
CaO	K	2.62±0.13	3.39±0.16	0.25
TiO2	K	0.00±0.11	0.00±0.09	0.00
Cr2O3	K	0.00±0.17	0.00±0.09	0.00
MnO	K	0.55±0.12	0.50±0.10	0.06
FeO	K	34.80±0.18	32.95±0.12	2.68
NiO	K	0.00±0.22	0.01±0.00	0.00
Total		100.00	100.00	

Spc_001 Fitting ref. 0.3355

Figure 77. SEM-EDS analysis data of garnet

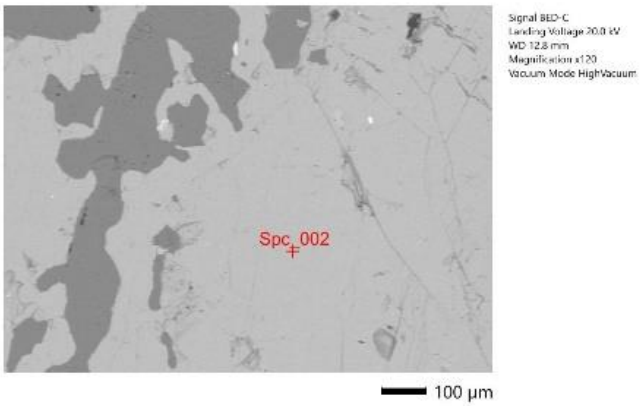

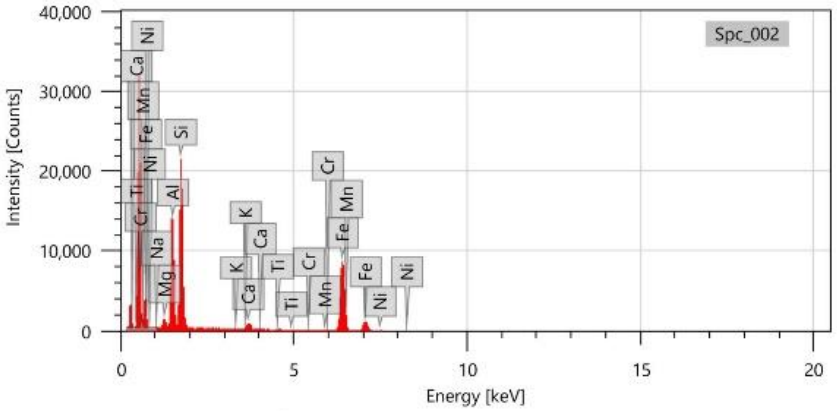

Items	Value
measurement conditions	
Acceleration voltage	20.00 kV
Probe current	-
Magnification	x 120
Process time	T3
Measurement detector	First
Live time	30.00 seconds
Real time	36.27 seconds
Dead time	17.00 %
Count rate	34990.00 CPS

Display name	Standard data	Quantification method	Result Type
Spc_002	Standardless	ZAF	Oxide (Number of oxygen 12)

Chemical formula	Line	Mass%	Mol%	Cations
O	K			
Na2O	K	0.18±0.02	0.20±0.02	0.03
MgO	K	1.70±0.03	2.94±0.05	0.20
Al2O3	K	21.77±0.09	14.90±0.06	2.05
SiO2	K	38.73±0.13	45.00±0.16	3.09
K2O	K	0.01±0.01	0.00±0.01	0.00
CaO	K	1.51±0.02	1.88±0.03	0.13
TiO2	K	0.02±0.01	0.02±0.01	0.00
Cr2O3	K	0.02±0.01	0.01±0.01	0.00
MnO	K	0.35±0.02	0.34±0.02	0.02
FeO	K	35.70±0.13	34.69±0.13	2.38
NiO	K	0.02±0.02	0.02±0.02	0.00
Total		100.00	100.00	
Spc_002				Fitting ratio 0.8391

Figure 78. SEM-EDS analysis data of garnet

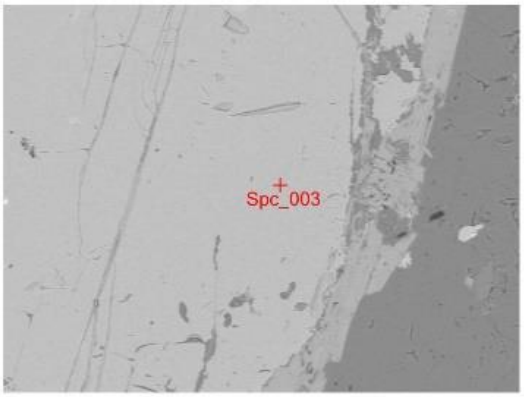

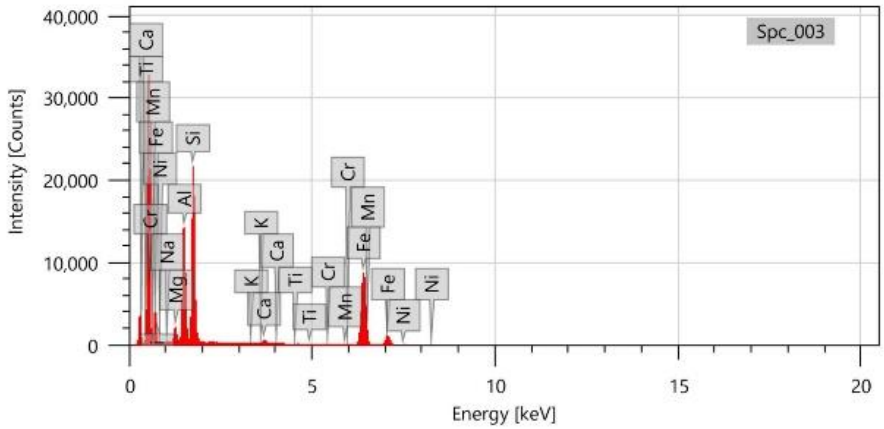

Items	Value
measurement conditions	
Acceleration voltage	20.00 kV
Probe current	-
Magnification	x 270
Process time	T3
Measurement detector	First
Live time	30.00 seconds
Real time	36.25 seconds
Dead time	17.00 %
Count rate	34912.00 CPS

Display name	Standard data	Quantification method	Result Type
Spc_003	Standardless	ZAF	Oxide (Number of oxygen 12)

Chemical formula	Line	Mass%	Mol%	Cations
O	K			
Na2O	K	0.22±0.02	0.25±0.02	0.03
MgO	K	2.77±0.04	4.76±0.06	0.33
Al2O3	K	21.98±0.09	14.96±0.06	2.05
SiO2	K	38.89±0.13	44.92±0.16	3.08
K2O	K	nd	nd	-
CaO	K	0.77±0.02	0.96±0.02	0.07
TiO2	K	nd	nd	-
Cr2O3	K	0.01±0.01	0.00±0.01	0.00
MnO	K	0.16±0.02	0.15±0.02	0.01
FeO	K	35.14±0.13	33.94±0.12	2.33
NiO	K	0.06±0.02	0.06±0.02	0.00
Total		100.00	100.00	
Spc_003				Fitting ratio 0.3451

Figure 79. SEM-EDS analysis data of garnet

Phengite mica

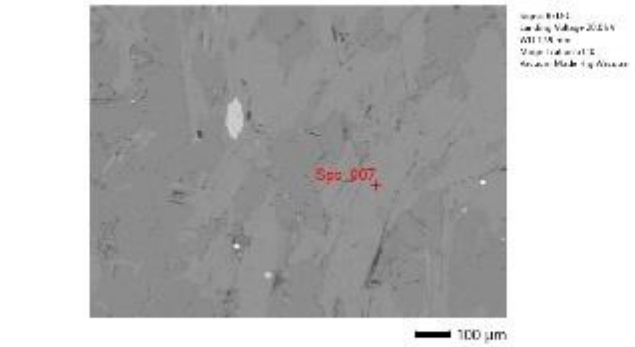

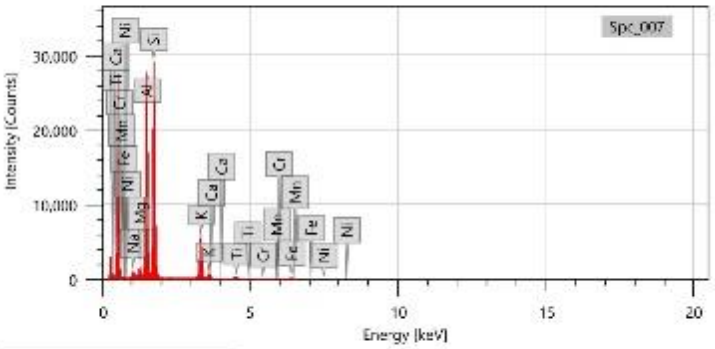

Items	Value
measurement conditions	
Acceleration voltage	20.00 kV
Probe current	
Magnification	x 110
Process time	13
Measurement detector	First
Live time	30.00 seconds
Real time	35.90 seconds
Dead time	16.00 %
Count rate	3451.20 CPS

Display name	Standard data	Quantification method	Result type
Spc 007	Standardless	ZAF	Oxide (Number of oxygen: 12)

Chemical formula	Line	Mass%	Mol%	Cation
O	K			
Na2O	K	1.17±0.02	1.36±0.03	0.12
MgO	K	1.24±0.02	2.24±0.04	0.19
Al2O3	K	20.79±0.11	23.75±0.13	1.96
SiO2	K	47.24±0.15	51.75±0.16	4.27
K2O	K	8.14±0.10	5.98±0.08	0.49
CaO	K	nd	nd	-
TiO2	K	0.62±0.02	0.51±0.02	0.03
Cr2O3	K	0.04±0.01	0.03±0.01	0.00
MnO	K	nd	nd	
FeO	K	0.68±0.02	0.61±0.02	0.04
NiO	K	0.07±0.01	0.05±0.01	0.00
Total		100.00	100.00	

Spc 007 Tilting adj: 0.3307

GK 7b
Garnet

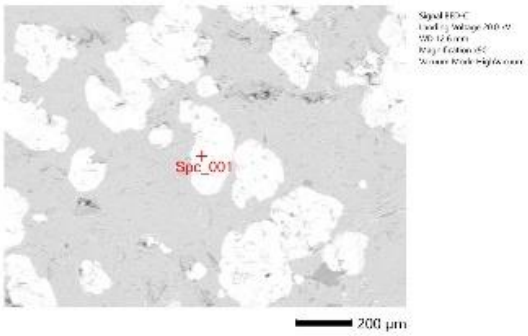

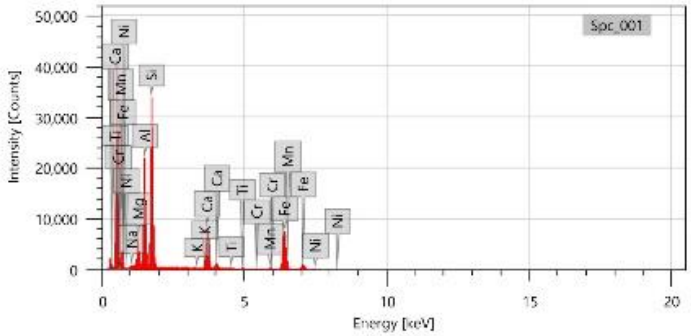

Items	Value
measurement conditions	
Acceleration voltage	20.00 kV
Probe current	-
Magnification	x 90
Process time	T3
Measurement detector	-irst
Live time	30.00 seconds
Real time	39.10 seconds
Dead time	23.00 %
Count rate	49798.00 CPS

Display name	Standard data	Quantification method	Result Type
Spc_001	Standardless	ZAF	Oxide (Number of oxygen 12)

Chemical formula	Line	Mass%	Mol%	Sigma
O	K			
Na_2O	K	0.26±0.07	0.33±0.09	0.04
MgO	K	5.23±0.14	6.82±0.18	0.12
Al_2O_3	K	22.24±0.28	16.87±0.21	2.00
SiO_2	K	40.04±0.31	48.57±0.37	3.07
K_2O	K	nd	nd	
CaO	K	10.01±0.15	11.91±0.18	0.62
TiO_2	K	0.38±0.11	0.35±0.10	0.02
Cr_2O_3	K	0.15±0.11	0.07±0.05	0.01
MnO	K	0.58±0.12	0.54±0.11	0.04
FeO	K	20.70±0.28	19.11±0.26	1.32
NiO	K	0.06±0.11	0.05±0.09	0.00
Total		100.00	100.00	

Spc_001 *Fitting ratio 0.1845

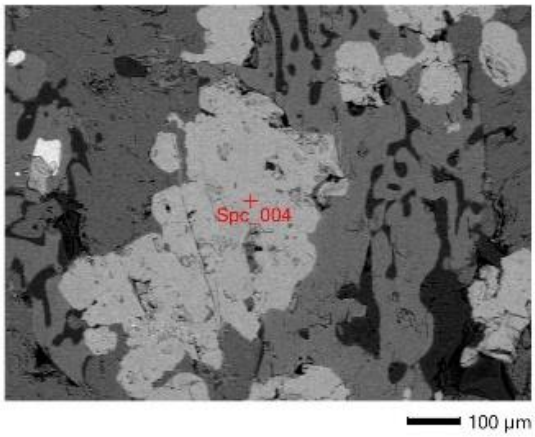

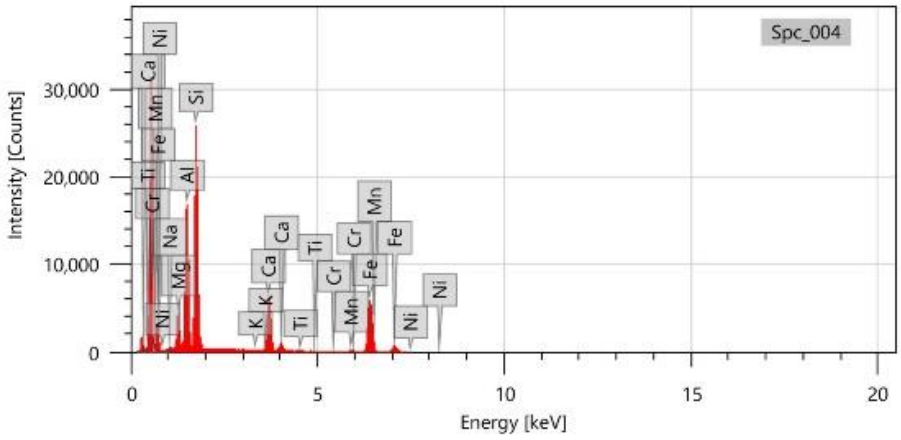

Items	Value
measurement conditions	
Acceleration voltage	20.00 kV
Probe current	-
Magnification	x 130
Process time	T3
Measurement detector	First
Live time	30.00 seconds
Real time	36.76 seconds
Dead time	18.00 %
Count rate	37844.00 CPS

Display name	Standard data	Quantification method	Result Type
Spc_004	Standardless	ZAF	Oxide (Number of oxygen 12)

Chemical formula	Line	Mass%	Mol%	Cations
O	K			
Na2O	K	0.22±0.02	0.28±0.03	0.03
MgO	K	5.08±0.04	8.37±0.07	0.58
Al2O3	K	22.25±0.09	14.49±0.06	2.00
SiO2	K	40.17±0.13	44.41±0.14	3.07
K2O	K	nd	nd	-
CaO	K	10.29±0.05	12.19±0.06	0.84
TiO2	K	0.19±0.01	0.16±0.01	0.01
Cr2O3	K	0.03±0.01	0.01±0.01	0.00
MnO	K	0.49±0.02	0.48±0.02	0.03
FeO	K	21.23±0.10	19.63±0.09	1.36
NiO	K	0.05±0.02	0.05±0.01	0.00
Total		100.00	100.00	
Spc_004				Fitting ratio 0.3211

Figure 82. SEM-EDS analysis data of garnet

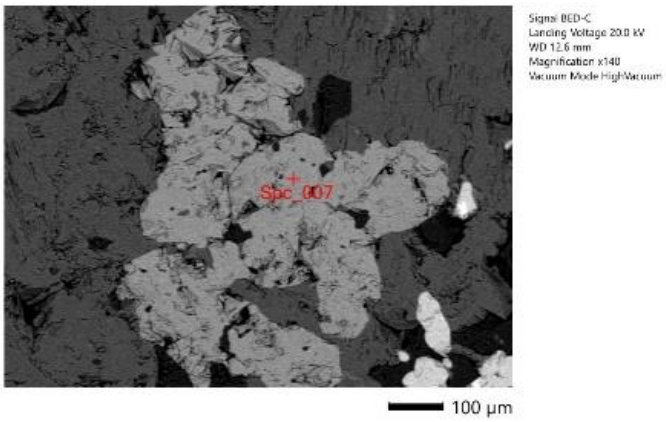

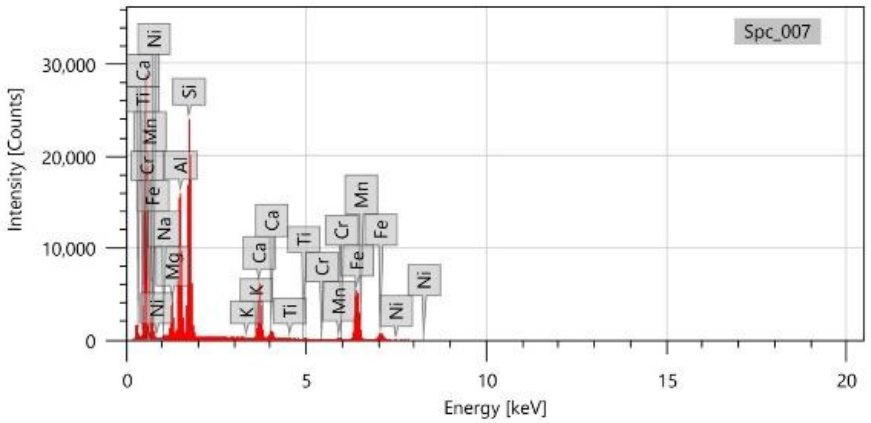

Items	Value
measurement conditions	
Acceleration voltage	20.00 kV
Probe current	-
Magnification	x 140
Process time	T3
Measurement detector	First
Live time	30.00 seconds
Real time	36.36 seconds
Dead time	17.00 %
Count rate	35650.00 CPS

Display name	Standard data	Quantification method	Result Type
Spc_007	Standardless	ZAF	Oxide (Number of oxygen 12)

Chemical formula	Line	Mass%	Mol%	Cations
O	K			
Na2O	K	0.22±0.02	0.23±0.02	0.03
MgO	K	5.08±0.04	9.37±0.07	0.58
Al2O3	K	22.16±0.09	14.43±0.06	2.00
SiO2	K	39.88±0.13	44.06±0.14	3.05
K2O	K	nd	nd	-
CaO	K	10.76±0.06	12.74±0.07	0.88
TiO2	K	0.34±0.02	0.28±0.01	0.02
Cr2O3	K	0.08±0.01	0.03±0.01	0.00
MnO	K	0.50±0.02	0.47±0.02	0.03
FeO	K	20.97±0.10	19.37±0.09	1.34
NiO	K	0.01±0.02	0.01±0.01	0.00
Total		100.00	100.00	
Spc_007				Fitting ratio 0.3145

Figure 83 SEM-EDS analysis data of garnet

Omphacite

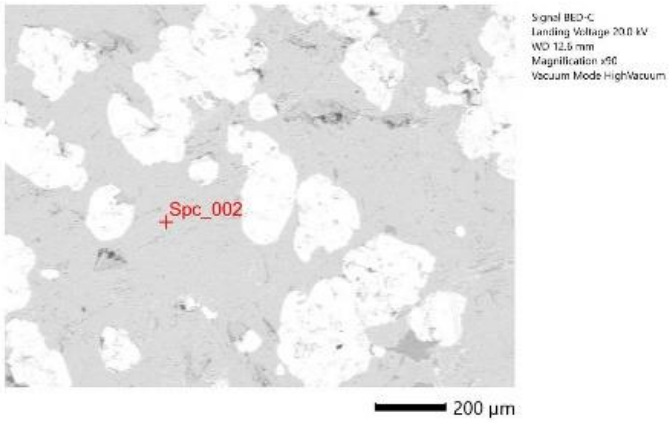

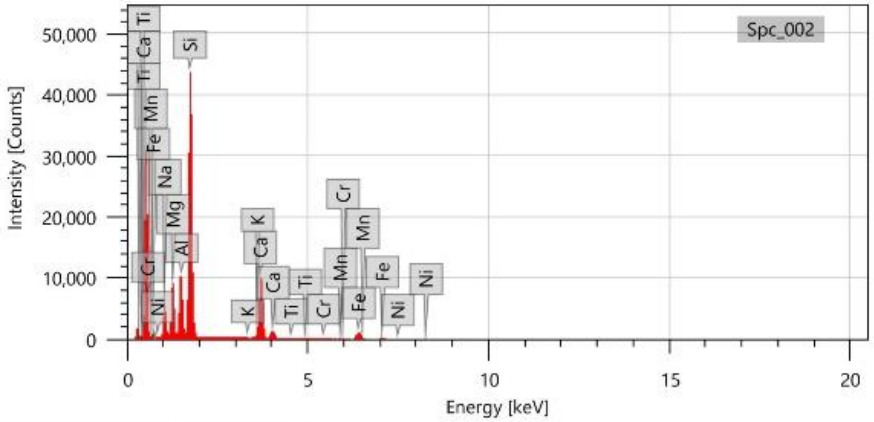

Items	Value
measurement conditions	
Acceleration voltage	20.00 kV
Probe current	-
Magnification	x 90
Process time	T3
Measurement detector	First
Live time	30.00 seconds
Real time	37.43 seconds
Dead time	20.00 %
Count rate	42378.00 CPS

Display name	Standard data	Quantification method	Result Type
Spc_002	Standardless	ZAF	Oxide (Number of oxygen 6)

Chemical formula	Line	Mass%	Mol%	Cations
O	K			
Na2O	K	6.11±0.04	5.93±0.04	0.42
MgO	K	9.05±0.05	13.54±0.07	0.48
Al2O3	K	11.15±0.06	6.57±0.03	0.47
SiO2	K	55.20±0.13	55.21±0.13	1.96
K2O	K	nd	nd	-
CaO	K	14.39±0.06	15.42±0.06	0.55
TiO2	K	0.23±0.01	0.17±0.01	0.01
Cr2O3	K	0.12±0.01	0.05±0.01	0.00
MnO	K	0.05±0.01	0.04±0.01	0.00
FeO	K	3.63±0.04	3.04±0.03	0.11
NiO	K	0.04±0.01	0.03±0.01	0.00
Total		100.00	100.00	
Spc_002				Fitting ratio 0.3189

Figure 84. SEM-EDS analysis data of omphacite

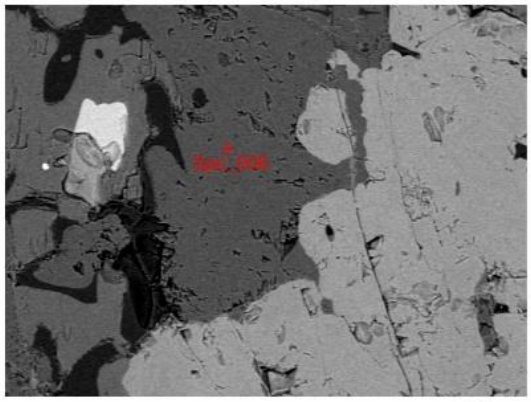

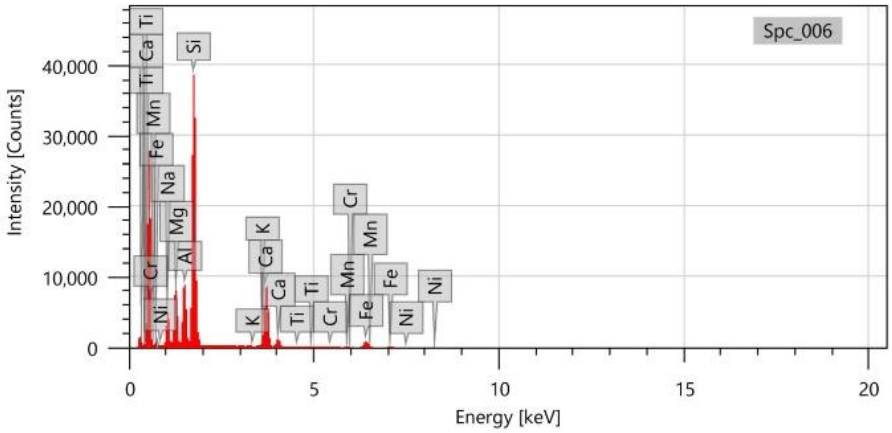

Items	Value
measurement conditions	
Acceleration voltage	20.00 kV
Probe current	-
Magnification	x 250
Process time	T3
Measurement detector	First
Live time	30.00 seconds
Real time	36.50 seconds
Dead time	18.00 %
Count rate	37118.00 CPS

Display name	Standard data	Quantification method	Result Type
Spc_006	Standardless	ZAF	Oxide (Number of oxygen 6)

Chemical formula	Line	Mass%	Mol%	Cations
O	K			
Na2O	K	6.30±0.05	6.10±0.04	0.43
MgO	K	9.23±0.05	13.72±0.08	0.49
Al2O3	K	10.67±0.06	6.28±0.04	0.45
SiO2	K	55.74±0.14	55.62±0.14	1.98
K2O	K	0.00±0.01	0.00±0.01	0.00
CaO	K	14.08±0.06	15.05±0.07	0.54
TiO2	K	0.21±0.01	0.16±0.01	0.01
Cr2O3	K	0.16±0.02	0.06±0.01	0.00
MnO	K	0.06±0.01	0.05±0.01	0.00
FeO	K	3.51±0.04	2.92±0.03	0.10
NiO	K	0.03±0.01	0.03±0.01	0.00
Total		100.00	100.00	
Spc_006				Fitting ratio 0.3235

Figure 85. SEM-EDS analysis data of omphacite

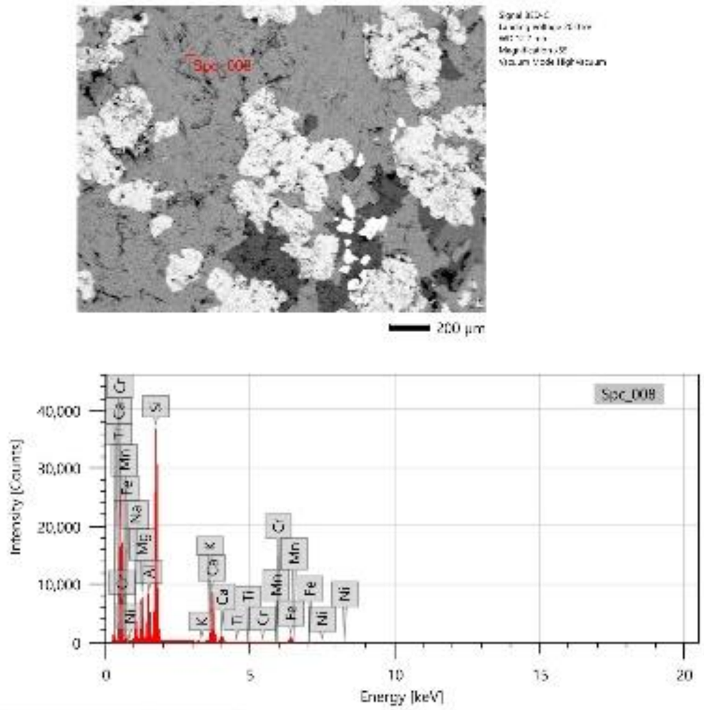

Items	Value
measurement conditions	
Acceleration voltage	20.00 kV
Probe current	-
Magnification	x 63
Process time	T3
Measurement detector	First
Live time	30.00 seconds
Real time	36.21 seconds
Dead time	17.00 %
Count rate	35623.00 CPS

Display name	Standard data	Quantification method	Result Type
Spc_008	Standardless	ZAF	Oxide (Number of oxygen 6)

Chemical formula	Line	Mass%	Mol%	Cation
O	K			
Na2O	K	[illegible]	[illegible]	[illegible]
MgO	K	[illegible]	[illegible]	[illegible]
Al2O3	K	[illegible]	[illegible]	[illegible]
SiO2	K	[illegible]	[illegible]	[illegible]
K2O	K	nd	nd	-
CaO	K	[illegible]	[illegible]	[illegible]
TiO2	K	[illegible]	[illegible]	[illegible]
Cr2O3	K	[illegible]	[illegible]	[illegible]
MnO	K	[illegible]	[illegible]	[illegible]
FeO	K	[illegible]	[illegible]	[illegible]
NiO	K	[illegible]	[illegible]	[illegible]
Total		[illegible]	[illegible]	
Spc_008				Fitting ratio [illegible]

Figure 86. SEM-EDS analysis data of omphacite

Amphibole

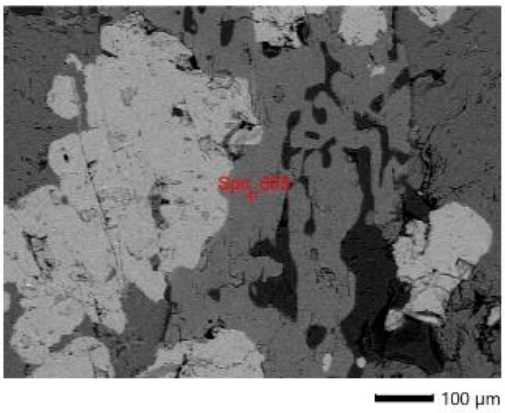

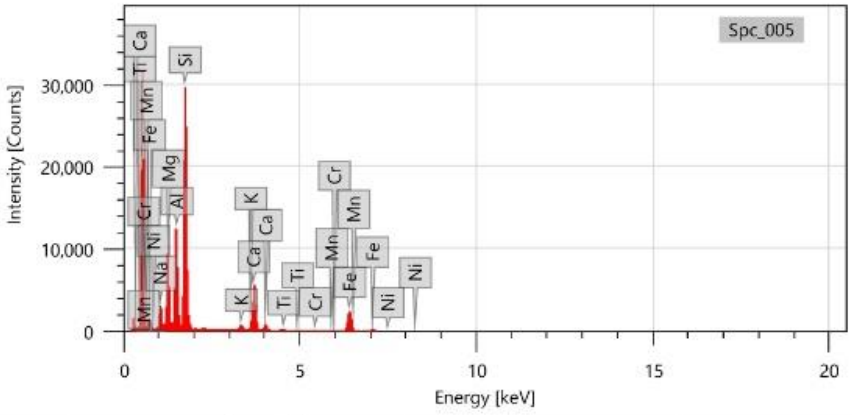

Items	Value
measurement conditions	
Acceleration voltage	20.00 kV
Probe current	-
Magnification	x 150
Process time	T3
Measurement detector	First
Live time	30.00 seconds
Real time	36.40 seconds
Dead time	17.00 %
Count rate	36607.00 CPS

Display name	Standard data	Quantification method	Result Type
Spc_005	Standardless	ZAF	Oxide (Number of oxygen 22)

Chemical formula	Line	Mass%	Mol%	Cations
O	K			
Na2O	K	4.13±0.04	4.10±0.04	1.07
MgO	K	12.36±0.06	18.86±0.10	2.46
Al2O3	K	16.90±0.08	10.19±0.05	2.66
SiO2	K	46.77±0.14	47.87±0.14	6.24
K2O	K	0.71±0.02	0.46±0.01	0.12
CaO	K	9.35±0.05	10.26±0.06	1.34
TiO2	K	0.66±0.02	0.51±0.02	0.07
Cr2O3	K	0.11±0.01	0.04±0.01	0.01
MnO	K	0.01±0.01	0.01±0.01	0.00
FeO	K	8.99±0.06	7.69±0.05	1.00
NiO	K	0.01±0.02	0.01±0.01	0.00
Total		100.00	100.00	
Spc_005				Fitting ratio 0.3545

Figure 87. SEM-EDS analysis data of amphibole

GK 8a
Garnet

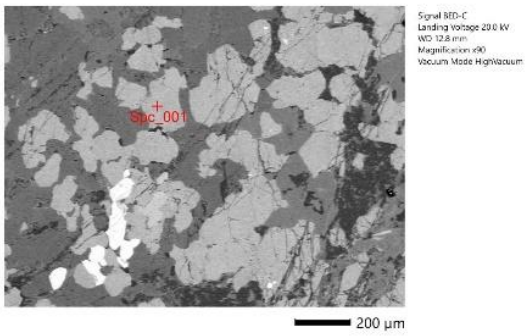

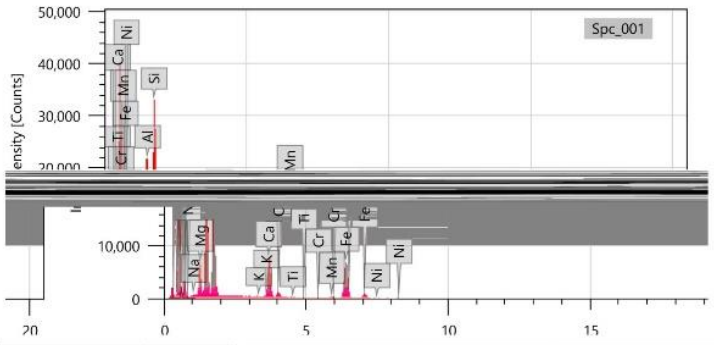

Items	Value
measurement conditions	
Acceleration voltage	20.00 kV
Probe current	-
Magnification	x 90
Process time	T3
Measurement detector	First
Live time	30.00 seconds
Real time	38.75 seconds
Dead time	23.00 %
Count rate	48183.00 CPS

Display name	Standard data	Quantification method	Result Type
Spc_001	Standardless	ZAF	Oxide (Number of oxygen 12)

Chemical formula	Line	Mass%	Mol%	Cations
O	K			
Na2O	K	0.25±0.02	0.26±0.02	0.04
MgO	K	5.85±0.04	9.60±0.07	0.66
Al2O3	K	22.69±0.08	14.72±0.05	2.03
SiO2	K	40.56±0.11	44.67±0.12	3.08
K2O	K	nd	nd	-
CaO	K	10.01±0.05	11.81±0.06	0.81
TiO2	K	0.04±0.01	0.03±0.01	0.00
Cr2O3	K	0.15±0.01	0.07±0.01	0.01
MnO	K	0.53±0.02	0.48±0.02	0.03
FeO	K	19.99±0.08	18.36±0.08	1.26
NiO	K	nd	nd	-
Total		100.00	100.00	
Spc_001				Fitting ratio 0.9249

Figure 88. SEM-EDS analysis data of garnet

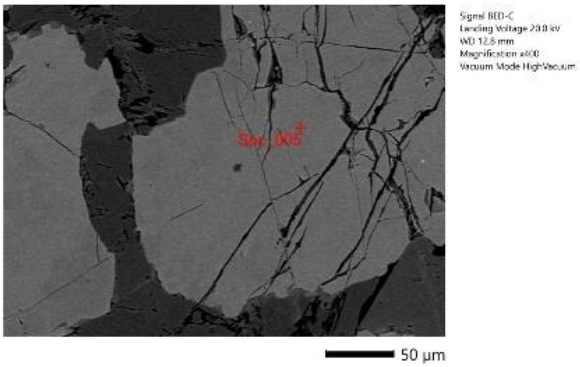

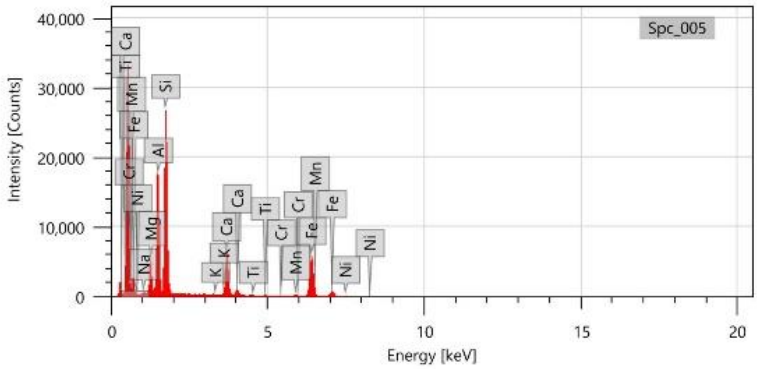

Items	Value
measurement conditions	
Acceleration voltage	20.00 kV
Probe current	-
Magnification	x 400
Process time	T3
Measurement detector	First
Live time	30.00 seconds
Real time	37.01 seconds
Dead time	19.00 %
Count rate	39264.00 CPS

Display name	Standard data	Quantification method	Result Type
Spc_005	Standardless	ZAF	Oxide (Number of oxygen 12)

Chemical formula	Line	Mass%	Mol%	Cations
O	K			
Na2O	K	0.11±0.02	0.12±0.02	0.02
MgO	K	5.77±0.04	9.48±0.07	0.65
Al2O3	K	22.57±0.09	14.66±0.06	2.02
SiO2	K	40.45±0.13	44.58±0.14	3.07
K2O	K	nd	nd	-
CaO	K	9.91±0.06	11.70±0.06	0.81
TiO2	K	0.09±0.01	0.08±0.01	0.01
Cr2O3	K	0.11±0.01	0.06±0.01	0.01
MnO	K	0.61±0.02	0.57±0.02	0.04
FeO	K	20.32±0.09	18.72±0.09	1.29
NiO	K	0.05±0.02	0.04±0.01	0.00
Total		100.00	100.00	
Spc_005				Fitting ratio 0.8283

Figure 89. SEM-EDS analysis data of garnet

Omphacite

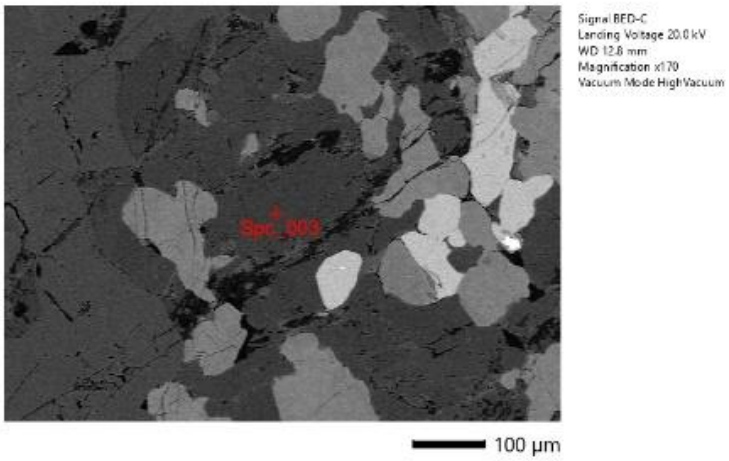

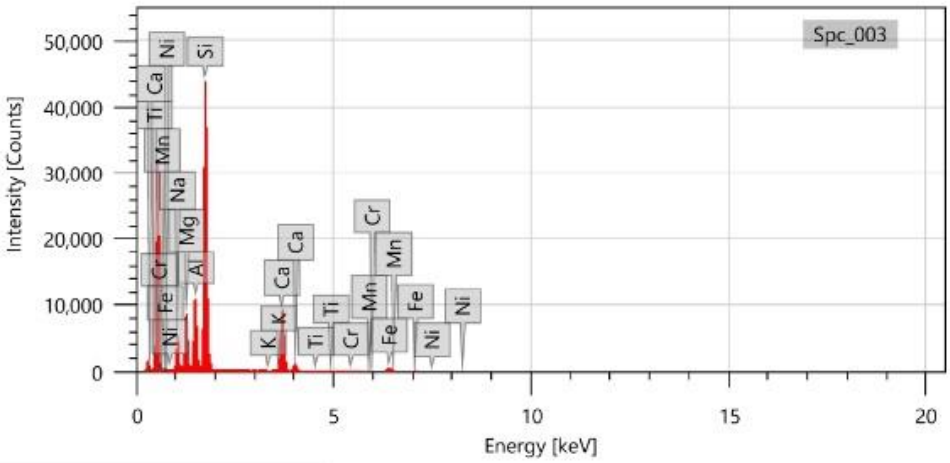

Items	Value
measurement conditions	
Acceleration voltage	20.00 kV
Probe current	-
Magnification	x 170
Process time	T3
Measurement detector	First
Live time	30.00 seconds
Real time	37.33 seconds
Dead time	20.00 %
Count rate	41652.00 CPS

Display name	Standard data	Quantification method	Result Type
Spc_003	Standardless	ZAF	Oxide (Number of oxygen 6)

Chemical formula	Line	Mass%	Mol%	Cations
O	K			
Na2O	K	5.96±0.04	5.80±0.04	0.41
MgO	K	8.89±0.05	13.31±0.07	0.47
Al2O3	K	12.20±0.06	7.22±0.04	0.51
SiO2	K	56.33±0.13	56.56±0.14	1.98
K2O	K	0.00±0.01	0.00±0.01	0.00
CaO	K	13.74±0.06	14.78±0.06	0.52
TiO2	K	0.23±0.01	0.17±0.01	0.01
Cr2O3	K	0.16±0.01	0.06±0.01	0.00
MnO	K	0.03±0.01	0.02±0.01	0.00
FeO	K	2.47±0.03	2.08±0.03	0.07
NiO	K	nd	nd	-
Total		100.00	100.00	
Spc_003				Fitting ratio 0.3258

Figure 90. SEM-EDS analysis data of omphacite

Rutile

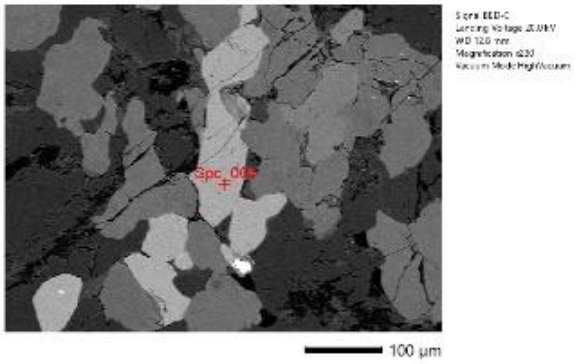

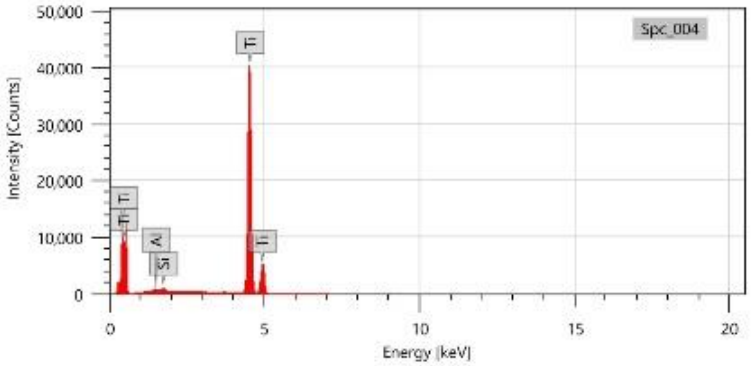

Items	Value
measurement conditions	
Acceleration voltage	20.00 kV
Probe current	-
Magnification	x 250
Process time	T3
Measurement detector	First
Live time	30.00 seconds
Real time	37.46 seconds
Dead time	20.00 %
Count rate	39155.00 CPS

Display name	Standard data	Quantification method	Result Type
Spc_004	Standardless	ZAF	Oxide (Number of oxygen 2)

Chemical formula	Line	Mass%	Mol%	Cations
O	K			
Al2O3	K	0.25±0.02	0.20±0.02	0.00
SiO2	K	0.51±0.02	0.67±0.03	0.01
TiO2	K	99.24±0.18	99.13±0.18	0.99
Total		100.00	100.00	
Spc_004				Fitting ratio 0.0816

Figure 91. SEM-EDS analysis data of rutile